

1. Report No. FHWA/TX-81/15+242-1	2. Government Accession No.	3. Recipient's Catalog No.	
4. Title and Subtitle THE INFLUENCE OF CASTING POSITION ON DEVELOPMENT AND SPLICE LENGTH OF REINFORCING BARS		5. Report Date June 1981	6. Performing Organization Code
7. Author(s) J. J. Luke, B. S. Hamad, J. O. Jirsa, and J. E. Breen		8. Performing Organization Report No. Research Report 242-1	
9. Performing Organization Name and Address Center for Transportation Research The University of Texas at Austin Austin, Texas 78712		10. Work Unit No.	11. Contract or Grant No. Research Study 3-5-78-242
12. Sponsoring Agency Name and Address Texas State Department of Highways and Public Transportation; Transportation Planning Division P. O. Box 5051 Austin, Texas 78763		13. Type of Report and Period Covered Interim	
15. Supplementary Notes Study conducted in cooperation with the U. S. Department of Transportation, Federal Highway Administration. Research Study Title: "Influence of Casting Position and of Shear on the Strength of Lapped Splices"		14. Sponsoring Agency Code	
16. Abstract The objective of this study was to reexamine the development and splice length requirements for top cast bars based on a comparison of stresses developed at ultimate rather than at a specified value of loaded end slip. To understand the historical development of design provisions for the influence of casting position, an extensive survey of the literature was undertaken. An experimental investigation of the magnitude of bond strength reduction as a function of (1) the location and orientation of the reinforcement and (2) the properties (slump) of the fresh concrete was undertaken. Specimens were designed and constructed with bars cast at different heights above the bottom of the form and oriented horizontally or vertically. The bond strength of each of these bars was compared to that of a bottom bar at ultimate. The specimens consisted of large blocks of concrete with a number of bars or splices cast in each block. The spacing of adjacent bars along the specimen height was varied to minimize the interaction of splitting cracks. Four trial specimens were designed and tested to define the dimensions of the primary test specimens. A total of six specimens containing from 8 to 16 anchored or spliced bars was tested. Slip of the bar relative to the concrete was measured and comparisons between bars were made using load-slip curves. Based on the test results, suggestions are made for revising specifications for "top reinforcement" development and splice length as a function of casting position and concrete slump characteristics. The tests discussed in this report are part of a larger project which includes tests to investigate the effect of casting position and shear on the bond strength of lapped splices.			
17. Key Words splice length, reinforcing bars, casting position, development, stresses, specifications, concrete slump		18. Distribution Statement No restrictions. This document is available to the public through the National Technical Information Service, Springfield, Virginia 22161.	
19. Security Classif. (of this report) Unclassified	20. Security Classif. (of this page) Unclassified	21. No. of Pages 174	22. Price

THE INFLUENCE OF CASTING POSITION ON DEVELOPMENT AND  
SPLICE LENGTH OF REINFORCING BARS

by

J. J. Luke, B. S. Hamad, J. O. Jirsa, and J. E. Breen

Research Report No. 242-1

Research Project No. 3-5-78-242

Influence of Casting Position and of Shear on the  
Strength of Lapped Splices

Conducted for

Texas

State Department of Highways and Public Transportation

In Cooperation with the  
U. S. Department of Transportation  
Federal Highway Administration

by

CENTER FOR TRANSPORTATION RESEARCH  
BUREAU OF ENGINEERING RESEARCH  
THE UNIVERSITY OF TEXAS AT AUSTIN

June 1981

The contents of this report reflect the views of the authors who are responsible for the facts and accuracy of the data presented herein. The contents do not necessarily reflect the views or policies of the Federal Highway Administration. This report does not constitute a standard, specification, or regulation.

## P R E F A C E

In this report, the first phase of a study on "The Influence of Casting Position and of Shear on Strength of Lapped Splices" is presented. The objective of the project was to review existing data and to conduct an experimental program for determining the effect of casting position and shear on anchorage strength and to suggest modification, if needed, for design codes. In this report the influence of casting position on development and splice length of reinforcing bars is described. A subsequent report will describe the influence of shear on splices in reinforcing bars and in the final report suggestions for changes in design specifications will be presented.

The work was sponsored by the Texas State Department of Highways and Public Transportation and the Federal Highway Administration and administered by the Center for Transportation Research at The University of Texas at Austin. Close liaison with the State Department of Highways and Public Transportation has been maintained through Mr. Melvin C. Jackson, James C. Wall, and Warren K. Sandbert, who served as contact representatives during the project, and with Mr. William Dallas of the Federal Highway Administration.

The project was conducted in the Phil M. Ferguson Structural Engineering Laboratory located at the Balcones Research Center of The University of Texas at Austin.

This page replaces an intentionally blank page in the original.

-- CTR Library Digitization Team

## S U M M A R Y

The objective of this study was to reexamine the development and splice length requirements for top cast bars based on a comparison of stresses developed at ultimate rather than at a specified value of loaded end slip. To understand the historical development of design provisions for the influence of casting position, an extensive survey of the literature was undertaken.

An experimental investigation of the magnitude of bond strength reduction as a function of (1) the location and orientation of the reinforcement and (2) the properties (slump) of the fresh concrete was undertaken. Specimens were designed and constructed with bars cast at different heights above the bottom of the form and oriented horizontally or vertically. The bond strength of each of these bars was compared to that of a bottom bar at ultimate. The specimens consisted of large blocks of concrete with a number of bars or splices cast in each block. The spacing of adjacent bars along the specimen height was varied to minimize the interaction of splitting cracks. Four trial specimens were designed and tested to define the dimensions of the primary test specimens. A total of six specimens containing from 8 to 16 anchored or spliced bars was tested. Slip of the bar relative to the concrete was measured and comparisons between bars were made using load-slip curves.

Based on the test results, suggestions are made for revising specifications for "top reinforcement" development and splice length as a function of casting position and concrete slump characteristics. The tests discussed in this report are part of a larger project which includes tests to investigate the effect of casting position and shear on the bond strength of lapped splices.

This page replaces an intentionally blank page in the original.

-- CTR Library Digitization Team

## I M P L E M E N T A T I O N

The results of this study will permit further refinement of recommendations resulting from Project 3-5-72-154. The recommendations included in that study have been the subject of considerable discussion in appropriate committees of the American Concrete Institute. The Committee on Bond and Development (ACI 408) has made a recommendation to the Building Code Committee of the American Concrete Institute (ACI 318) for changes in the provisions for development length and splices. The proposed changes are based largely on the work carried out under Project 154. Because AASHTO provisions are based primarily on ACI design recommendations, it is likely that the changes in ACI 318 will eventually appear in AASHTO Specifications. To provide a design recommendation which handles all aspects of development and splice length of reinforcement, including the effect of casting position and shear, the research conducted under Project 242 will further improve design recommendations.

Current design specifications contain confusing, often anomalous, statements which are difficult for designers to apply in design situations. The implementation of the results from this program should help to clarify the role of casting position, shear, and properties of fresh concrete on the strength of anchored bars.

This page replaces an intentionally blank page in the original.

-- CTR Library Digitization Team

## C O N T E N T S

Chapter		Page
1	INTRODUCTION . . . . .	1
	1.1 Definition of Bond . . . . .	1
	1.2 Influence of Casting Position . . . . .	2
	1.3 Current Specifications . . . . .	5
	1.4 Objectives and Scope . . . . .	7
2	REVIEW OF PREVIOUS RESEARCH . . . . .	9
	2.1 Introduction . . . . .	9
	2.2 Abrams, 1913 . . . . .	11
	2.3 Menzel, 1939 . . . . .	12
	2.4 Clark, 1946 . . . . .	16
	2.5 Clark, 1949 . . . . .	19
	2.6 Collier, 1947 . . . . .	22
	2.7 C.U.R., 1963 . . . . .	24
	2.8 Ferguson and Thompson, 1965 . . . . .	28
	2.9 Welch and Patten . . . . .	30
	2.10 Summary . . . . .	31
3	A REVIEW OF DESIGN PROCEDURES FOR ANCHORED DEFORMED BARS . . . . .	33
	3.1 Regulatory Approach . . . . .	33
	3.2 Development Lengths of the Anchored Bars . . . . .	37
4	EXPERIMENTAL PROGRAM . . . . .	41
	4.1 Outline of Test Specimens . . . . .	41
	4.2 Development Length Tests (D Series) . . . . .	41
	4.3 Splice Tests (S Series) . . . . .	44
	4.4 Materials . . . . .	44
	4.4.1 Concrete . . . . .	44
	4.4.2 Reinforcing Steel . . . . .	47
	4.5 Formwork . . . . .	48
	4.6 Transverse Reinforcement . . . . .	51
	4.7 Test Frame . . . . .	51
	4.8 Measurement of Slip . . . . .	58
	4.9 Test Procedure . . . . .	67

Chapter	Page
5	BEHAVIOR--DEVELOPMENT TESTS . . . . . 71
5.1	Introduction . . . . . 71
5.2	Variation of Concrete Strength . . . . . 71
5.3	General Characteristics of Behavior . . . . . 72
5.3.1	Specimens D1 and D2 . . . . . 74
5.3.2	Specimen D3 (High Slump Concrete) . . . . . 74
5.3.3	Specimen D4 (Horizontal/Vertical Bars) . . . . . 80
5.4	Effect of Casting Position . . . . . 84
5.5	Effect of Slump . . . . . 84
5.6	Horizontal vs. Vertical Bars . . . . . 99
5.7	The Influence of Slip Level . . . . . 102
6	BEHAVIOR--SPLICE TESTS . . . . . 103
6.1	Introduction . . . . . 103
6.2	Influence of Splice Orientation . . . . . 103
6.3	Crack Patterns . . . . . 107
6.4	Stress-Slip Curves . . . . . 107
6.5	Splice Tests vs. Development Length Tests . . . . . 115
7	SUMMARY AND CONCLUSIONS . . . . . 119
7.1	Summary . . . . . 119
7.2	Conclusions . . . . . 119
	REFERENCES . . . . . 121
	APPENDIX A DIMENSIONING THE TEST SPECIMENS . . . . . 125
	APPENDIX B MATERIALS . . . . . 143

## F I G U R E S

Figure		Page
1.1	Top bar definition, ACI 318 . . . . .	3
1.2	Definition of casting position . . . . .	4
2.1	Bond pullout test with bond stress distribution, Ferguson . . . . .	10
2.2	Pullout tests investigating the effect of concrete settlement, Abrams . . . . .	13
2.3	Casting positions, Menzel . . . . .	15
2.4	Test specimens, Clark . . . . .	17
2.5	Beam tests, Clark . . . . .	20
2.6	Cross sections of Collier's specimens, Collier . . . .	23
2.7	Effect of slump on stress-slump relationship, Collier	25
2.8	Details of test specimens, C.U.R. . . . .	26
2.9	Typical beam specimen, Ferguson and Thompson . . . .	29
2.10	Test results showing the top bar effect, Ferguson and Thompson . . . . .	29
2.11	The effect of settlement on the bond strength of top and bottom bars (Welch and Patten) . . . . .	32
3.1	Calculation of bond stress, $u$ . . . . .	34
4.1	Schematic presentation of Specimens D1, D2, and D3 . .	42
4.2	Schematic representation of Specimen D4 . . . . .	43
4.3	Schematic representation of Specimen S1 . . . . .	45
4.4	Schematic representation of Specimen S2 . . . . .	46

Figure	Page
4.5 Additional side form to hold the bar in place . . . . .	49
4.6 Form of Specimen D3 prior to casting . . . . .	49
4.7 Positioning details for bars in Specimen D4 . . . . .	50
4.8 Stacked splice on side of splice specimen . . . . .	52
4.9 Typical transverse reinforcement pattern for D Series specimens . . . . .	53
4.10 Transverse reinforcement details--Specimens D1 and D3	54
4.11 Transverse reinforcement pattern for Specimen S2 . . . . .	55
4.12 Transverse reinforcement pattern for test bars in Specimen D4 . . . . .	56
4.13 Transverse reinforcement in place in horizontal/vertical test specimen . . . . .	57
4.14 Test frame A for side bars, side view . . . . .	59
4.15 Test frame A for side bars, top view . . . . .	60
4.16 Test frame B for middle top and bottom bars, elevation view . . . . .	61
4.17 Test frame B for middle top and bottom bars, top view . . . . .	62
4.18 Test frame A used to test the side bars . . . . .	63
4.19 Test frame B used to test the middle top and bottom bars . . . . .	63
4.20 Wedge grip assembly mounted in the test frame of the middle top and bottom bars . . . . .	64
4.21 Location of slip wires . . . . .	65
4.22 Slip wires extending from a middle top bar to the specimen face . . . . .	66

Figure	Page
4.23 Slip potentiometer mounting . . . . .	66
4.24 Slip correction method . . . . .	68
5.1 Comparison of stress-slip curves at the loaded end and the free end of #7 bars in Specimen D2 . . . . .	73
5.2 V-notch splitting mode of failure of side bars of test Specimens D1 and D2 . . . . .	75
5.3 Interaction of the crack patterns of adjacent side bars in test Specimen D2 . . . . .	76
5.4 V-notch splitting mode of failure of the #7 bar at z = 12 in. in test Specimen D2 . . . . .	77
5.5 Corner-splitting mode of failure of the #9 bar at z = 12 in. in test Specimen D2 . . . . .	77
5.6 Typical crack pattern of the middle top and bottom bars . . . . .	78
5.7 Shrinkage cracks formed around top middle #9 bars on face of high slump specimen . . . . .	79
5.8 Longitudinal shrinkage cracks formed along cover of top middle #7 bar in high slump specimen . . . . .	79
5.9 Crack patterns after testing of top middle #9 (on right) and #7 bars of high slump specimen . . . . .	81
5.10 Position of test bars in formwork of horizontal/ vertical specimen . . . . .	81
5.11 Crack patterns of test bars of horizontal/vertical specimen . . . . .	82
5.12 Crack patterns of test bars of horizontal/vertical specimen . . . . .	82
5.13 Crack pattern of test bar along the end of horizontal/ vertical specimen . . . . .	83
5.14 Stress-slip relationship for #11 bars (Specimen D1, Side A) . . . . .	85

Figure	Page
5.15 Stress-slip relationship for #11 bars (Specimen D1, Side B) . . . . .	86
5.16 Stress-slip relationship for #7 bars (Specimen D2) . . . . .	87
5.17 Stress-slip relationship for #9 bars (Specimen D2) . . . . .	88
5.18 Bond strength reduction--casting position relationship, normal slump specimens . . . . .	92
5.19 Stress-slip relationship for #9 bars, Specimen D3, high slump . . . . .	93
5.20 Stress-slip curves for #7 bars, Specimen D3, high slump . . . . .	94
5.21 Bar stress at ultimates vs. bar height for high slump (9-1/2 in.) and low slump (3 in.) specimens . . . . .	96
5.22 Ultimate bond efficiency ratio vs. bar height, influence of slump . . . . .	97
5.23 Bond efficiency ratio at 0.01 in. slip, influence of slump . . . . .	98
5.24 Stress-slip curves for bars at z = 18 in., Specimen D4 . . . . .	100
5.25 Stress-slip curves for bars at z = 48 in., Specimen D4 . . . . .	101
6.1 Load-slip curves for stacked splices (S1) . . . . .	104
6.2 Load-slip curves for side-by-side test (S2) . . . . .	105
6.3 The effect of splice orientation on accumulation of inferior concrete . . . . .	106
6.4 Crack patterns for stacked splices along specimen side . . . . .	108
6.5 Crack patterns for side-by-side splices . . . . .	108
6.6 Bar stress vs. height for stacked and side-by-side splices . . . . .	110

Figure	Page
6.7 Comparison of stress-slip curves for face-parallel and face-perpendicular splices at $z = 30$ in. . . . .	113
6.8 Stress-slip curves for top and bottom splices in S1 and S2 . . . . .	114
6.9 Bar stress vs. height for splice and development tests	116
6.10 Bond efficiency ratio vs. height for splice and development tests . . . . .	117
A.1 Splitting cracks for a single tension bar, ACI Committee 408 . . . . .	125
A.2 Bar arrangement in Specimen T0 . . . . .	127
A.3 Specimen T0 prior to casting . . . . .	128
A.4 Splitting cracks radiating out from one test bar intersecting adjacent untested bar in Specimen T0 . .	128
A.5 Bar arrangement on one side of Specimen T1 . . . . .	131
A.6 Bar arrangement on one side of trial Specimen T3 . . .	132
A.7 Cracks from bar at $z = 12$ in. spreading into the test zone of the middle bottom bar, Specimen T1 . . . . .	133
A.8 Cracks from bar at $z = 57$ in. spreading into the test zone of the middle top bar, Specimen T1 . . . . .	133
A.9 V-notch splitting mode of failure for side bars of Specimen T3 . . . . .	134
A.10 Specimen T2 with the additional #3 reinforcement in place . . . . .	135
A.11 Additional #3 reinforcement on one side of Specimen T3 . . . . .	135
A.12 Corner-splitting mode of failure of bar at $z = 12$ in., Specimen T3 . . . . .	137
A.13 Typical crack pattern of the middle top and bottom bars of trial Specimen T2 . . . . .	137

Figure		Page
A.14	Test results of Specimen T1 . . . . .	138
A.15	Test results of Specimen T2 . . . . .	139
A.16	Test results of Specimen T3 . . . . .	140
B.1	Variation of concrete compression strength with age-- Specimen T1 . . . . .	146
B.2	Variation of concrete compression strength with age-- Specimen T2 . . . . .	147
B.3	Variation of concrete compression strength with age-- Specimen T3 . . . . .	148
B.4	Variation of concrete compression strength with age-- Specimen D1 . . . . .	149
B.5	Variation of concrete compression strength with age-- Specimen D2 . . . . .	150
B.6	Concrete data--Specimen D3 . . . . .	151
B.7	Concrete data--Specimen D4 . . . . .	152
B.8	Concrete data--Specimens S1 and S2 . . . . .	153
B.9	Deformation patterns of bars used in the investigation . . . . .	154
B.10	Stress-strain relationship for bars used in the study	154

T A B L E S

Table		Page
2.1	Summary of Test Results on Beams and Pullout Tests . .	21
2.2	Test Results, C.U.R. . . . .	27
3.1	Computation of Development Length of Anchored Bars . .	39
5.1	Ultimate Bar Stress, Specimen D1, #11 Bars . . . . .	89
5.2	Ultimate Bar Stress, Specimen D2 . . . . .	90
5.3	Comparison of Bond Efficiency Ratios, Specimens D1 and D2 . . . . .	91
6.1	Summary of Stresses at Failure - Splice Tests - S1 and S2 . . . . .	109
6.2	Summary of Stress at Failure - Influence of Splice Orientation . . . . .	112
A.1	Test Results of Specimen T1 . . . . .	138
A.2	Test Results of Middle Top and Bottom Bars of Specimen T2 . . . . .	139
A.3	Test Results of Side Bars of Specimen T2 . . . . .	139
A.4	Test Results of Middle Top and Bottom Bars of Specimen T3 . . . . .	140
A.5	Test Results of Side Bars of Specimen T3 . . . . .	140
B.1	Concrete Mix Design for Specimen T1 . . . . .	146
B.2	Concrete Mix Design for Specimen T2 . . . . .	147
B.3	Concrete Mix Design for Specimen T3 . . . . .	148
B.4	Concrete Mix Design for Specimen D1 . . . . .	149
B.5	Concrete Mix Design for Specimen D2 . . . . .	150
B.6	Deformed Bar Designation Numbers, Nominal Weights, Nominal Dimensions and Deformation Characteristics . .	155

# C H A P T E R 1

## INTRODUCTION

### 1.1 Definition of Bond

Reinforced concrete consists of a relatively small amount of steel embedded in concrete. The resulting composite material takes advantage of the high tensile strength and ductility of the steel and the high compressive strength and low cost of the concrete. A clear understanding of the interaction of the two materials is necessary to ensure that the resulting design is both safe and economical.

External loads are typically applied to the concrete. The transfer of load from the concrete to the steel is made possible by the shear stresses acting at the concrete-steel interface. The shear stresses provide resistance to slip between the concrete and the embedded steel. The term bond stress has generally been used to describe the stress transfer phenomena. Bond stresses exist whenever there is a change in bar force along the length of the bar. This situation can arise either through anchorage of the bar (anchorage bond) or through the existence of a moment gradient along the member (flexural bond). Bond stresses also occur in lapped splices, where stress is transferred from one bar to another through the medium of the concrete.

Bond, or resistance to slip, is the result of several mechanisms. For plain bars, bond is principally due to chemical adhesion and friction [30,20,33]. Bond due to chemical adhesion between the bar and the mortar paste is very weak and slip can result at even very low stresses. After the onset of slip, bond is produced by friction due to the wedging action of small sand particles between the steel and the concrete mass. For deformed bars, adhesion and friction play only a minor role and bond is produced mainly by bearing of the bar deformations (lugs) against the concrete. This results in axial bearing forces which may lead to the crushing of the concrete in front of the lugs and axial shearing forces which may shear the

concrete between the lugs to produce failure. Bearing between the lugs and the concrete produces radial components of stress which leads to splitting of the concrete surrounding the bar.

### 1.2 Influence of Casting Position

Many factors including bar cover, concrete strength, bar spacing, transverse reinforcement, and bar deformation patterns have been investigated to determine their influence on bond strength. One of the most influential but least precisely defined variables influencing bond is the position of the embedded bar during casting. Casting position is defined as the location of the bar within the fresh concrete and the orientation of the bar relative to the direction the concrete is cast.

The location of the bar is generally determined by the height of the bar above the bottom of the formwork or the concrete joint during casting (see Fig. 1.1). Investigators very early recognized that when the depth of fresh concrete below a bar was large, the bond strength was adversely influenced [10,31]. In the 1951 American Concrete Institute (ACI) "Building Code Requirements for Reinforced Concrete" the term "top bar" was first used to describe a horizontal bar with more than 12 in. of concrete cast below. The "top bars" were assigned a reduced bond strength relative to bottom cast bars.

The bar may be positioned horizontally or vertically during casting and, if oriented vertically, the bar may be loaded in the direction of or opposite to that of concrete placement and settlement (see Fig. 1.2).

The importance of casting position is the result of two processes [1,9,24,11,20,31,34,38,39,41,29,35,25,5] that take place during the concrete placement:

(a) Sedimentation. After initial placement and prior to settling, a segregation of the components of the mixture takes place. The heavier cement and aggregates tend to settle, while the air, particles of low specific gravity, and excess water tend to rise. As the air and particles rise they become trapped under horizontal bars, under the lugs of vertical

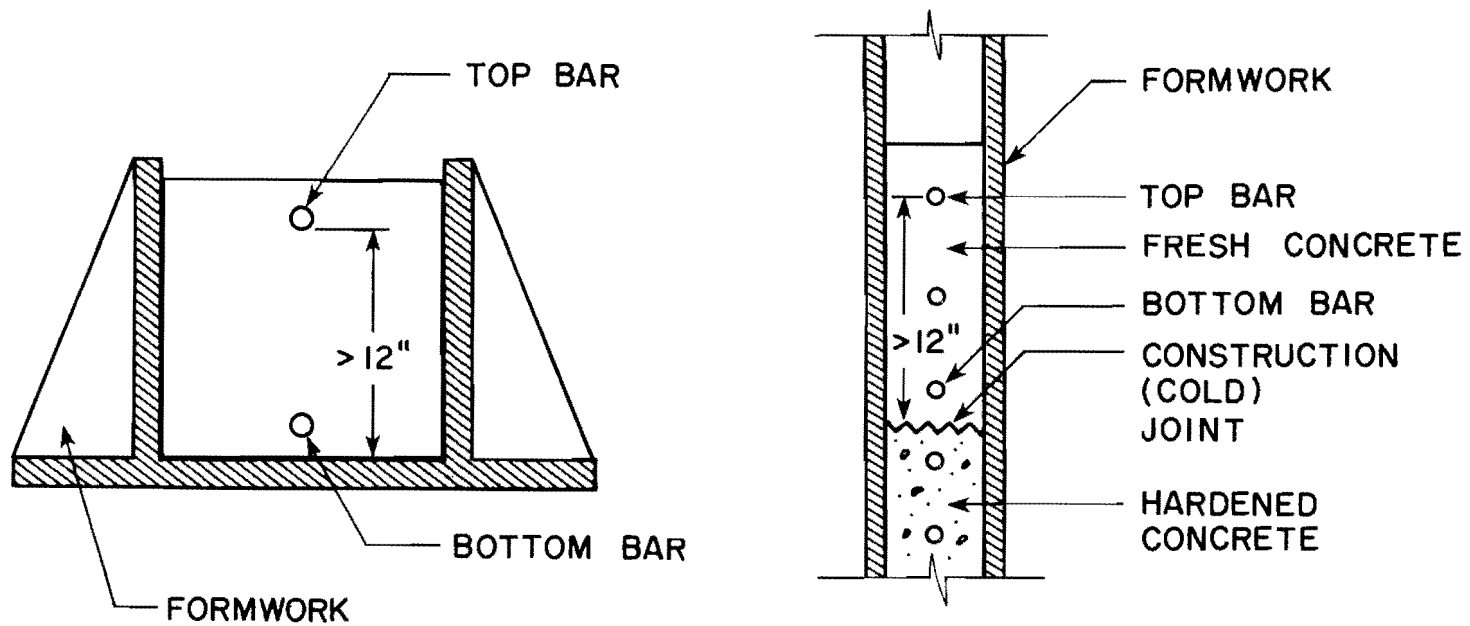


Fig. 1.1 Top bar definition, ACI 318

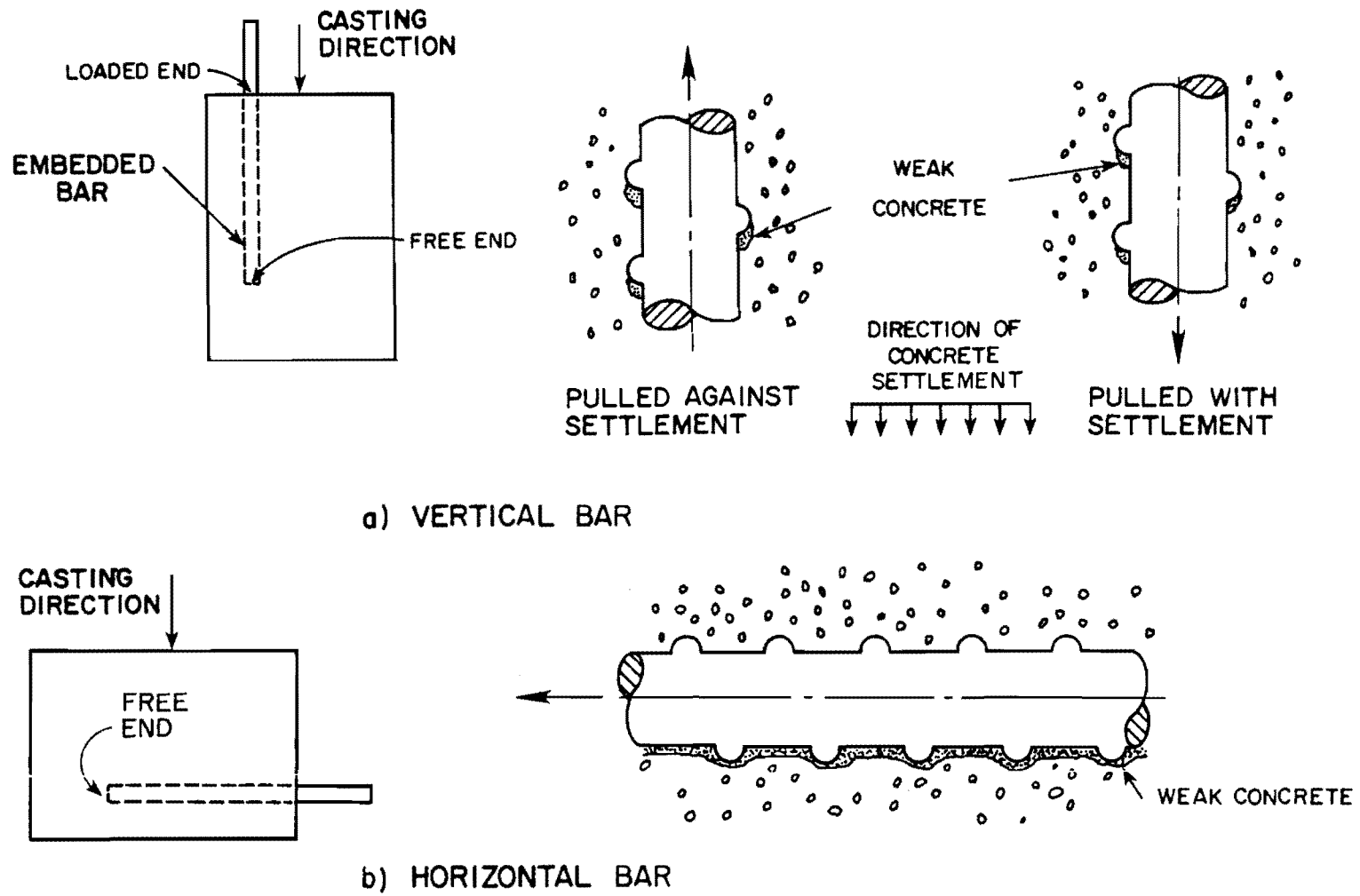


Fig. 1.2 Definition of casting position

bars, and under the coarse aggregate in the upper portion of the fresh concrete mass. Sedimentation produces weaker concrete in the upper portion of a concrete mass relative to the lower portion. The reduction in strength can be attributed to increased porosity and increased water content. Air and lightweight particles trapped under the bars or lugs form soft, spongy pockets of very weak concrete (see Fig. 1.2). The air pockets reduce the area of bearing between the concrete and the lugs with a resulting loss of bond strength. The "soft" concrete under the lugs is easily crushed and the bar may slip before full bearing (and strength) is developed. Mechanical vibration tends to eliminate the shear stresses between particles in the mix and to increase sedimentation. An increase in water-cement ratio and even more importantly an increase in the slump of the concrete also produces an increase in sedimentation.

(b) Settlement. As free water leaves the concrete during consolidation, the cement-paste and the aggregate settle. During settlement or consolidation, concrete at any level is compressed by the concrete above and becomes more dense. The greater the depth of concrete, the greater will be the effect. When the embedded bars are held rigidly in place while the concrete is settling, the concrete recedes from the bar or the lugs. This leads to the formation of voids under the bars or lugs that have much the same effect as the air pockets formed by sedimentation. Settlement is related to the water-tightness of the formwork [30] and is greater with leaky forms.

### 1.3 Current Specifications

The only aspect of casting position covered by the current AASHTO Bridge Specification or ACI Building Code is the influence of height of casting on the bond strength of horizontal bars. No difference in bond behavior is indicated for vertical bars compared to horizontal bars and the implication is given that the "top bar" effect is only relevant for horizontal bars. In the 1951 ACI Code, "top bars" were defined as "horizontal bars so placed that more than 12 in. of concrete is cast in the member below the bar." The allowable unit bond stress of top bars was limited to 0.7 of bottom bars.

The 1951 ACI Code provision for top bars was heavily influenced by work done by Clark [9,10]. Clark assumed that the loaded end slip of a bar in a pullout test corresponded to one-half the crack width that would develop in a beam at the same bar stress. A crack width of 0.02 in. would then correspond to a loaded end slip of 0.01 in. Based on serviceability requirements, the 0.02 in. crack width was taken as an upper limit on the permissible crack widths in beams at working loads. Clark's studies provided the basis on which ACI Committee 208, Bond Stress, proposed a set of allowable unit stresses for bond which were later adopted by Committee 318 for the 1951 ACI Code [3].

The ACI Code specifications concerning allowable unit bond stress of a top bar remained unchanged in the 1957 and 1963 ACI Codes [4]. With the introduction of ultimate strength design requirements in the 1971 ACI Code [4], the limitation on unit bond stress was dropped in favor of development length,  $l_d$ , requirements.

$$u_{\text{top}} = 0.7 u_{\text{bottom}} \quad \begin{array}{l} \text{(ACI 318-51)} \\ \text{(ACI 318-57)} \\ \text{(ACI 318-63)} \end{array}$$

and  $l_d \propto 1/u$

therefore 
$$l_{d\text{top}} = (1/0.7) \times l_{d\text{bottom}}$$

$$= 1.4 l_{d\text{bottom}} \quad \begin{array}{l} \text{(ACI 318-71)} \\ \text{(ACI 318-77)} \end{array}$$

Even though the ACI Code switched to ultimate strength from working stress design criteria, the limitations on development length were still tied to values of unit stress that were based on serviceability requirements. The development length specifications of the 1971 ACI Code (ACI 318-71) were adopted by the 1975 AASHTO (American Association of State Highway and Transportation Officials) Interim Specifications for Bridges and more recently the 1977 ACI Code (ACI 318-77) [4] has accepted this specification unchanged. It is of interest to note that the ACI Code

defines a top bar -- "12 in. of concrete cast in member below the bar." The 1975 AASHTO Specifications include the same definition, however, subsequent versions omit the definition so that a "top" bar is not specified.

In 1978, ACI-ASME Technical Committee on Concrete Pressure Components for Nuclear Service [6] proposed that the 1.4 factor for "top bars" not be applied to horizontal or diagonal wall bars. The committee suggested that in walls the effect of rising water and air is lessened by the depth of the member and by the multiple runs of horizontal bars, which tend to distribute any excess air and water. The committee also suggested that the higher hydrostatic head of the wet concrete in walls would minimize the bond degradation under bars. No experimental evidence was given to support the proposal.

It is evident that provisions for top reinforcement based on a serviceability limitation for the crack width (.02 in.) in beams were retained in the current AASHTO Specification and ACI Code even though ultimate strength design is specified. However, tests show that reinforcement tends to show increasing resistance to slip at higher levels of loading before failure [13].

#### 1.4 Objectives and Scope

The main objective of this study was to reexamine the development and splice length requirements for top cast bars based on a comparison of stresses developed at ultimate rather than at a specified value of loaded end slip. To understand the historical development of design provisions for the influence of casting position, an extensive survey of the literature was undertaken.

The second objective of this study was to investigate the magnitude of bond strength reduction as a function of the location and orientation of the reinforcement and the properties (**slump**) of the fresh concrete. This was accomplished by designing specimens with bars cast at different heights above the bottom of the form and oriented horizontally or vertically.

The bond strength of each of these bars was compared to that of a bottom bar at ultimate.

Specimens consisted of large blocks of concrete with a number of bars or splices cast in each block. The spacing of adjacent bars along the specimen height was varied to minimize the interaction of splitting cracks. Four trial specimens were designed and tested to define the dimensions of the primary test specimens. A total of six specimens containing from 8 to 16 anchored or spliced bars was tested. Slip of the bar relative to the concrete was measured and comparisons between bars were made using load-slip curves.

Based on the test results, suggestions are made for revising specifications for "top reinforcement" development and splice length as a function of casting position and concrete slump characteristics. The tests discussed in this report are part of a larger project which includes tests to investigate the effect of casting position and shear on the bond strength of lapped splices.

## C H A P T E R 2

### REVIEW OF PREVIOUS RESEARCH

#### 2.1 Introduction

Permissible bond stresses for various reinforcing bars embedded in concrete of different strengths were established primarily from the results of pullout tests. In the pullout test, a bar is embedded in a cylinder or rectangular block of concrete and the force required to pull it out or to produce a given slip is measured. In most pullout tests as the bar is pulled from the surrounding concrete, transverse compression against the bar is induced.

The concrete confinement induced by the pullout test procedure was first demonstrated by Abrams [1]. He tested two identical specimens, one with a rubber cushion between the test specimen and the test bearing surface and one with the test specimen resting directly on the bearing surface. As a result of the reduced confinement the test specimen with the rubber cushion developed only 80 per cent of the maximum bond resistance developed by the more typical pullout test specimen.

To overcome what were seen as very basic weaknesses of concentric pullout tests, several types of beam tests were designed to more closely simulate the actual behavior of reinforced concrete members. Comparisons of results of beam tests to pullout tests have not helped to clarify the reliability of pullout tests as a measure of bond efficiency. Clark's [10] tests in 1949 seemed to indicate that pullout tests give an accurate estimate of the bonding efficiency of deformed bars. However, later tests by Mathey and Watstein [29] showed that for #8 bars, bond strengths in pullout tests were significantly greater than values obtained in beam tests. The type of beam tests used in both studies were the same.

Figure 2.1 [20] shows the pullout test schematically. The bond stress distribution in such a specimen is nonuniform. Even a very small load causes some slip and develops a high bond stress in the vicinity of the

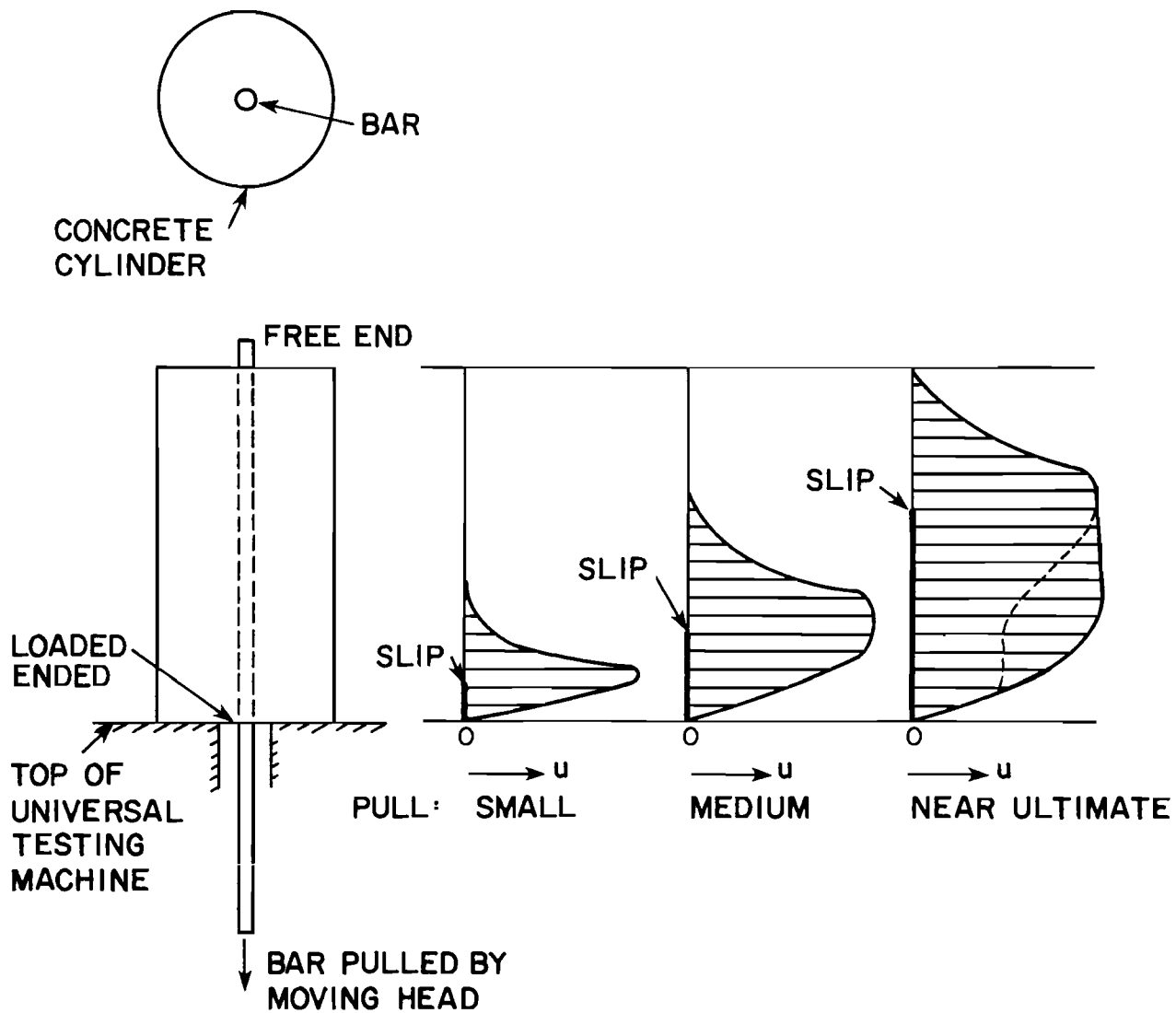


Fig. 2.1 Bond pullout test with bond stress distribution, Ferguson [20]

loaded end leaving the upper part of the bar totally unstressed as shown in Fig. 2.1. Additional loading will increase the loaded end slip and will cause an extension of the high bond stress along the bar and an increase in the length of the bar which develops slip. When the slip reaches the unloaded end, the maximum resistance is generally achieved. Failure will usually occur by longitudinal splitting of the concrete in the case of deformed bars or by breaking the bar if the embedment is long enough [20]. It is very important to note that in the pullout test procedure, no attempt is made to measure maximum unit bond resistance.

The major drawbacks of pullout tests include:

(1) The average bond stress is always calculated just as though it were uniform over the bar embedment length. Actually, the bond stress distribution varies greatly as slip develops. At any load, the average bond stress masks the wide variation between maximum and minimum stresses.

(2) Factors affecting bond in reinforced concrete beams such as splitting cracks initiated by dowel action, concrete cover, and shear forces and consequent diagonal cracks cannot be easily included in the pullout test. Most present-day investigators of bond efficiency seem to agree with Ferguson [20] that pullout tests are useful chiefly where relative rather than actual bond resistance values are desired.

## 2.2 Abrams, 1913 [1]

In 1913, Abrams reported a series of pullout tests on plain round bars to investigate the effect of settlement and shrinkage of concrete during setting and hardening. In one set of tests, the horizontal bar was supported by the form in such a way that settlement with the concrete was prevented, while in another set the horizontal bar was free to settle with the concrete. Specimens were also made in which the end of the bar to be loaded was oriented upward as the specimen was cast. Figure 2.2 shows the test specimens and a summary of the test results. Abrams defined the maximum bond resistance as the bond stress measured at a free end slip of 0.01 in.

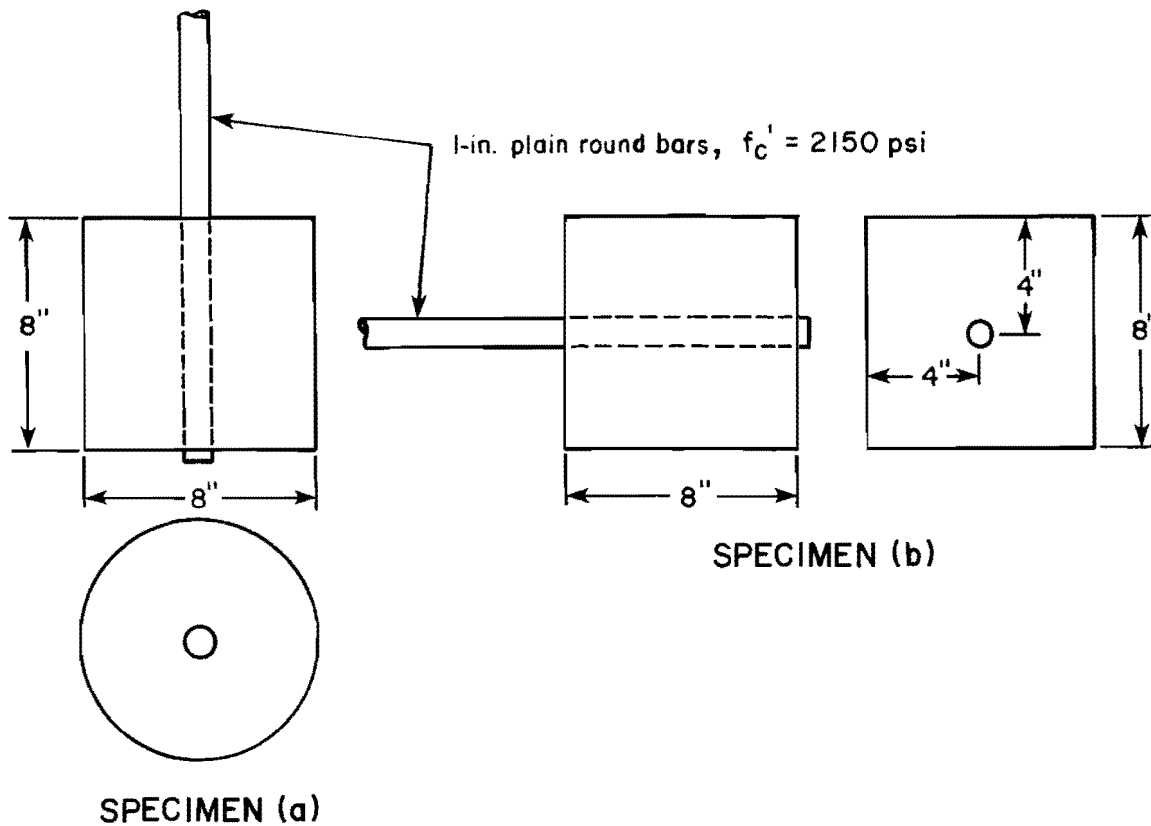
Bars cast in a horizontal position exhibited lower bond resistance than vertical bars. When the settlement of the horizontal bar was prevented, the maximum bond resistance was reduced to about 60 per cent of that for pullout specimens from the same concrete with the bar oriented in a vertical position during casting. Abrams emphasized the inferior bond properties of horizontal plain bars held rigidly in place during concreting. The effects of various concrete depths under the bar were not studied. It is difficult to assess the "fixity" of a bar and to evaluate the importance of settlement in practical situations.

In 1928, Richart [37] reported cavities under the negative reinforcement in some test beams. These cavities reduced the bond between concrete and steel, and thus were believed to have been the cause of serious slip observed at low loads. Edwards and Greenleaf [12] published some tests in 1928 in which pullout prisms 8 x 8 x 12 in. were cast with the bar held in a horizontal position. In discussing that paper, Richart emphasized the effects of settlement of the fresh concrete under the bars and stated that a good type of test piece for bond tests would be one with horizontal bars near the top of a beam section.

### 2.3 Menzel, 1939 [30]

The fundamental importance of the effect of depth of concrete under a horizontal bar was first discussed by Menzel [30]. Tests were designed to determine the factors influencing the results of pullout bond tests.

One set of pullout tests was run to determine the influence of cover or thickness of concrete below and alongside #8 deformed bars. Three covers were considered, 1 in., 1-1/2 in., and 2 in. For low slip values, the specimen with 2 in. cover developed the lowest steel stress of the covers considered. However, tests with 2 in. cover consistently showed a greater increase in stress as the slip increased. This difference became more marked as the length of embedment and richness of mix were increased. These differences in behavior were referred by Menzel to the opposing effects of two factors. As the amount of concrete under and at the sides of the bar



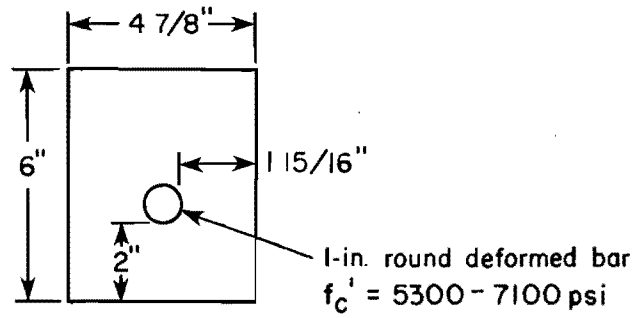
NUMBER OF TESTS	CHARACTERISTICS	UNIT BOND STRESS (psi) AT FREE END SLIP OF		MAXIMUM BOND RESISTANCE psi
		0.005"	0.001"	
4	SPECIMEN (b) BARS FREE TO SETTLE WITH CONCRETE	234	248	288
4	SPECIMEN (b) BARS HELD RIGIDLY IN PLACE	191	...	211
4	SPECIMEN (a)	278	315	372

Fig. 2.2 Pullout tests investigating the effect of concrete settlement, Abrams [1]

increases, the bond resistance should increase. However, as the depth of concrete under the bar increases, the settlement of the concrete under the bar during placing also increases, thereby weakening the bond resistance.

In another set of tests, Menzel investigated the influence of horizontal and vertical casting positions on the resistance developed by #8 deformed bars with transverse lugs or deformations. Three casting positions, shown in Fig. 2.3, were considered. The reported load-slip curves, based on slip at the free end, showed that the highest steel stress for a given slip was developed for position (c) and the lowest steel stress for position (a). In explaining this, Menzel argued that in position (c) the concrete settled in a direction opposite to the pull on the bar and against the lugs whereas in position (a) the concrete settled in the same direction as the pull on the bar and away from the lugs. Thus in position (c) sound concrete was in contact with the lugs improving the bearing between steel and concrete. In position (a), the bar had to slip appreciably before the lugs were brought into bearing with the concrete. At a given free end slip, bond resistance developed by specimens cast with the bars horizontal, position (b), were intermediate between those developed by bars in the vertical positions (a) and (c). Although the concrete settled under the horizontal bars, the settlement was less unfavorable with respect to bearing under the lugs than for vertical bars in position (a) where the concrete settled under each lug on both sides of the bar. Upon varying the slump of the concrete mix from 6 in. to 2 in., there was no substantial effect on the bond resistance of vertical bars in either position (a) or (c). On the other hand, horizontal bars in position (b) showed higher resistances with the 2 in. slump concrete.

In a very interesting set of tests, Menzel investigated the effect of water leakage from the mold on resistance developed with 1 in. plain round bars cast in a horizontal position, for two different slumps, 2 in. and 6 in. Test specimens with 6 in. slump concrete showed a higher bond resistance when cast in leaky molds than when cast in watertight molds. This increase averaged about 24 per cent at various free and slip values. On the other hand,



END VIEW OF a, b, & c

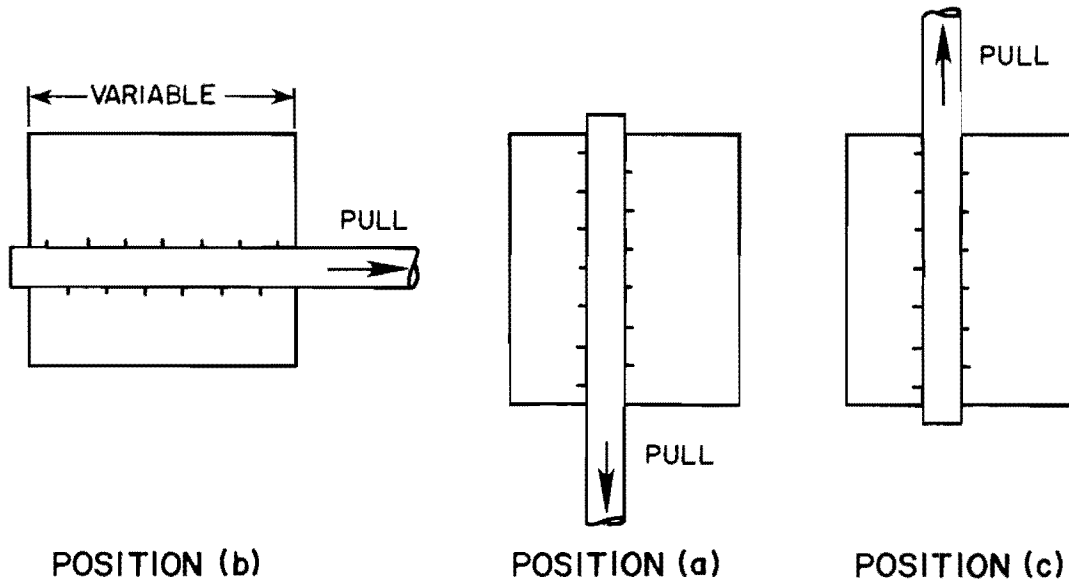
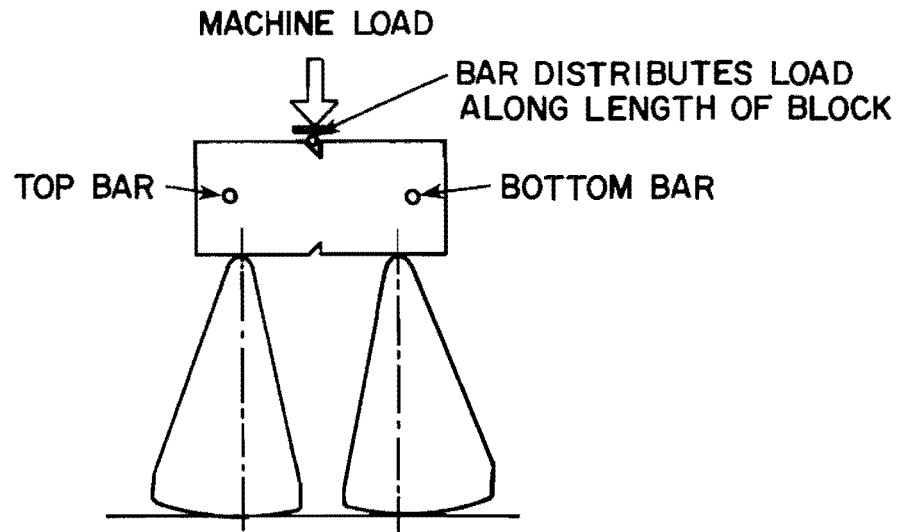


Fig. 2.3 Casting positions, Menzel [30]

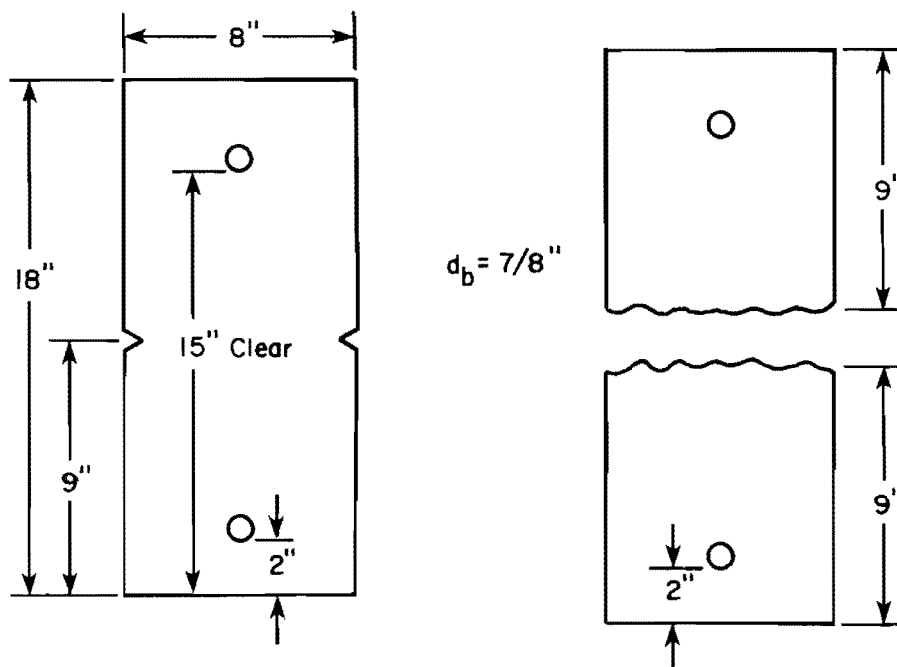
test specimens with 2 in. slump showed practically no difference in bond resistance for both leaky and watertight molds. Menzel reported that less water leakage occurred and the rate of leakage was lower from the 2 in. slump than from the 6 in. slump concrete. Finally, Menzel emphasized that the improved resistance using leaky molds required further investigation, with particular attention to the depth of concrete under the bar.

#### 2.4 Clark, 1946 [9]

The purpose of this study [9] which was part of a larger project was to determine the resistance to slip in concrete of bars with seventeen different deformation patterns. Embedment lengths of 8 in. and 12 in. were used with 7/8 in. diameter bars. Pullout specimens were cast with top and bottom bars, both in a horizontal position. The top bar had 15 in. and the bottom 2 in. of concrete cast below the bar. Specimens were then separated into two parts for testing by breaking them in flexure as shown in Fig. 2.4. Provision was made for measuring the slip of the bar at both the loaded and the free ends. Tests were continued until failure of the specimen occurred, either by splitting of the concrete or by the bar pulling through the concrete. The typical splitting was in a plane through the longitudinal ribs of the bar. Other specimens failed by splitting in a plane approximately at right angles to the plane through the longitudinal ribs. To evaluate the efficiency of the bars in bond resistance, a method for comparison was adopted to rate the bars on the basis of average performance through a wide range of slip values as measured at the loaded end and at the free end of the bar. The method selected was to record the stress developed at several values of slip from the smallest at which readings were reliable up to the maximum slip developed by the majority of the bars. Slip values at the loaded end were 0.0005, 0.001, 0.002, 0.004, 0.005, 0.0075, and 0.01 in. Slips of 0.00005, 0.0001, 0.0005, and 0.001 in. were used in a similar manner for free end comparison. The stresses for each bar were totaled and the sum divided by the number of readings to obtain a figure indicative of the rating or bond efficiency of the bar.



(a) METHOD OF BREAKING BLOCKS TO PRODUCE TWO PULLOUT SPECIMENS, CLARK



(b) SPECIMEN GEOMETRY, CLARK

Fig. 2.4 Test specimens, Clark [9,10]

Based on this method and considering the slip at both ends and for both embedments, the rating for all bars investigated in the top position was 56.8 per cent of the rating for the bars in the bottom position. In other words, in the top position bars were about two-thirds as effective in bond as in the bottom position. Height of bar deformations appeared as an important factor influencing the loss of bond strength due to the settlement of plastic concrete under the bar; the average stress rating of the bar seemed to increase with increases in heights of deformation. On the other hand, the data indicated that for bars cast in a horizontal position, the pattern of the deformations on the bar was not an important factor in determining the bond resistance. As far as the inclination of the face of the deformations is concerned, the tests indicated that it was an important factor in determining the bond resistance where an increase in the bearing area of the deformations increased the bond resistance.

In a discussion of Clark's paper, Zipprodt [41] argued that Clark's method of evaluating the effectiveness of the bond resistance of reinforcing bars provided a better method for comparing bond performance than other methods employed before. Zipprodt gave Clark credit for being the first to base his conclusions on determination of slip of the bar at the loaded end of the specimen. Zipprodt considered that slip at the free or unloaded end of the bar is meaningless. By the time measurable slip has occurred at the free end of embedded bars, bond between the reinforcing steel and the concrete has deteriorated to such an extent that, for many uses, the bars are no longer effective and should be considered as having failed. Finally, Zipprodt questioned the significance of pullout tests as a measure of bond resistance. He stated that the distribution of stresses in the concrete in pullout specimens was fundamentally different from that prevailing in the concrete in flexural members.

In a discussion of Clark's paper, Posey [41] pointed out that an ideal deformation should be the first subject for study. He argued that only small-scale deformations, of the order of large sand grains could ensure better bond efficiency. However, in his closure to the discussion, Clark disagreed with Posey's suggestion about small-scale deformations. He said

that, on the contrary, his tests and those of Menzel [30] and many others showed the need for deformations of substantial height where there might be water gain under the bar. Clark's closure stated that:

It is now recognized that one of the criteria of the bond efficiency of a bar is the resistance to slip, when cast in a horizontal position, with several inches of concrete under the bar.

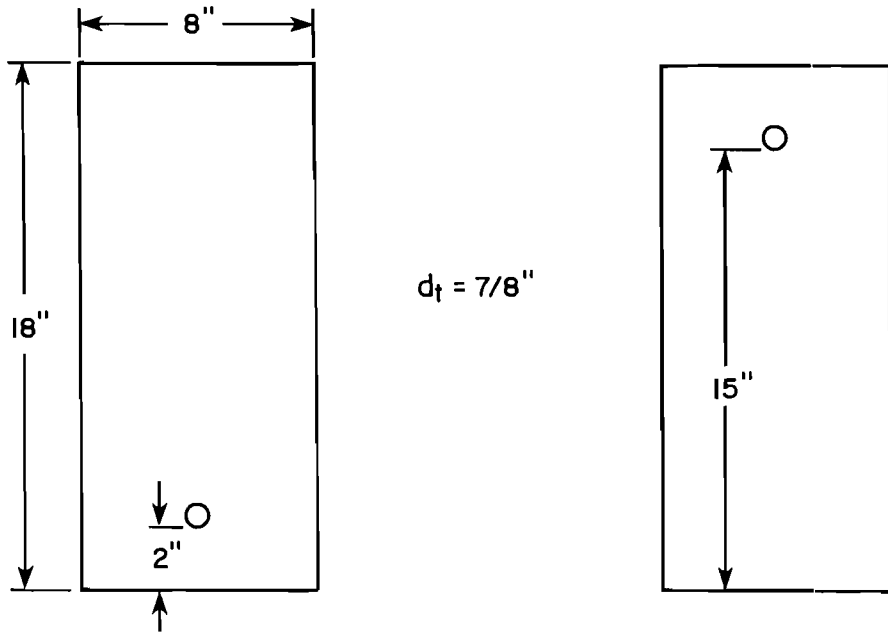
## 2.5 Clark, 1949 [10]

In 1949, further tests were reported by Clark [10]. The objective of this new series was to compare the bond resistance of deformed bars in beams and in pullout specimens made at the same time and under identical conditions. The bars were cast in a horizontal position in all test specimens.

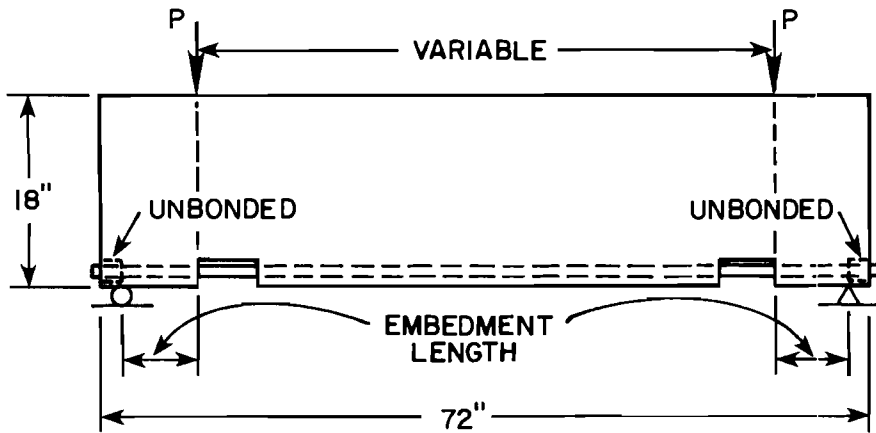
Apart from the different designs of deformed bars used, the variables were the depth of concrete under the bar, length of embedment of the bar in concrete, strength of concrete, and diameter of the bar. The beam specimens are shown in Fig. 2.5. Slip of the bar was measured at the loaded end and the free end. Pullout specimens were as shown in Fig. 2.4.

Beams generally failed in bond although with longer embedments, diagonal tension failure combined with bond failure occurred in some specimens. The pullout specimens failed by splitting of the concrete. The reported bond stress and slip values (Table 2.1) were based on the average results for all tests and all lengths of embedment. To obtain a comparison of bond developed in beam specimens with that in pullout specimens cast at the same time, Clark used the averaging technique discussed previously to rate the bond efficiency of bars.

From the results of the beam and the pullout tests, Clark concluded that the pullout test gave a fairly reliable estimate of the relative bond efficiency of deformed bars. It is important to note that not all the bars included in the study met ASTM A305-47T specifications for maximum spacing and minimum height of deformations. Taking into consideration all the #7 bars tested in pullout specimens, the average bond efficiency of top cast bars, as measured at the loaded end, was 65 percent of that of the



(a) BOTTOM BAR BEAM SPECIMEN (b) TOP BAR BEAM SPECIMEN



(c) BEAM TEST SET-UP

Fig. 2.5 Beam tests, Clark [10]

TABLE 2.1 SUMMARY OF TEST RESULTS ON BEAMS AND PULLOUT TESTS, CLARK [10]

7/8-in. Bar Design Reference Number	Bond Efficiency** Ratio Top/Bot. Loaded End		Bond Stress Ratio Top/Bot. at 0.01-Loaded End Slip	
	Pullout psi/psi	Beam psi/psi	Pullout psi/psi	Beam psi/psi
1	185/310 = 0.60	190/330 = 0.58	312/560 = 0.56	300/597 = 0.50
2	125/290 = 0.43	103/242 = 0.43	182/452 = 0.40	147/387 = 0.38
3	182/315 = 0.58	175/347 = 0.50	312/587 = 0.53	387/625 = 0.62
4	220/350 = 0.63	200/352 = 0.57	320/600 = 0.53	305/635 = 0.48
5*	225/355 = 0.63	102/370 = 0.28	360/625 = 0.58	325/670 = 0.49
6*	230/330 = 0.76	190/347 = 0.55	392/602 = 0.65	350/635 = 0.55
7	212/345 = 0.61	160/357 = 0.45	325/697 = 0.47	252/645 = 0.39
8*	310/405 = 0.77	265/420 = 0.63	547/730 = 0.75	442/800 = 0.55
9†	110/220 = 0.50	47/200 = 0.24	125/325 = 0.38	52/247 = 0.21
10*	230/390 = 0.59	--	400/722 = 0.55	--
11*	305/395 = 0.77	247/435 = 0.57	460/720 = 0.64	422/797 = 0.53
13	207/340 = 0.61	--	342/600 = 0.57	--
14*	355/370 = 0.96	--	592/645 = 0.92	--
17	245/318 = 0.77	--	410/570 = 0.72	--
Average ratio for all bars	65%	48%	59%	47%
Average ratio for bars meeting A.S.T.M. A305-47T	74%	51%	68%	53%

\* Bar meets A.S.T.M. A305-47T.

\*\* This refers to the average of bond stresses measured at loaded end slips of 0.00005, 0.001, 0.002, 0.003, 0.004, 0.005, 0.0075, and 0.01 in.

† Bar is plain with no deformations.

bottom cast bars (see Table 2.1). In beam specimens the ratio was 48 percent. If only bars meeting A.S.T.M. A305-47T are considered, the percentages would be 74 and 51, respectively.

Based on a loaded end slip of 0.01 in., the average bond stress of all tested designs of top cast #7 bars in pullout specimens was 59 percent of that of bottom cast bars (see Table 2.1). In beam specimens the ratio was 47 percent. If only bars meeting ASTM A305-47T are considered, the percentages would be 68 and 53, respectively.

The two projects reported by Clark provided the basis on which ACI Committee 208, Bond Stress, proposed a set of allowable unit stresses for bond. The unit stresses were adopted by Committee 318. Later the recommended bond stresses appeared in the ACI Code 318-51 [3] in which the term "top bar" was described as a bar near the top of beams and girders having more than 12 in. of concrete under the bar. Top bars were assigned an allowable unit stress 0.7 of that assigned to bottom cast bars. In terms of development, the assigned top bar factor resulted in a 43 percent increase in length.

## 2.6 Collier, 1947 [11]

Collier reported a series of tests which revealed problems and relationships that were new at the time. The purpose of the tests was to study bond of deformed reinforcing bars as affected by type of deformation, position of anchorage, and consistency of the concrete. Pullout tests were carried out for bars cast in three positions. The specimens cast vertically were placed in standard 6 x 12 in. concrete cylinder molds. Horizontal bars were cast in upper and lower positions in 6 x 10-1/2 x 18 in. prisms with 3 or 15 in. of concrete below the center of the bar (see Fig. 2.6). After the prisms had cured for fourteen days, the bars and surrounding concrete were separated by sawing the prisms on two planes, designated as "A" and "B" in Fig. 2.6. By this procedure, separate 6 x 6 x 10.5 in. prisms with centered bars were provided. Specimens were assumed to have failed when the slip at the loaded end reached 0.02 in.

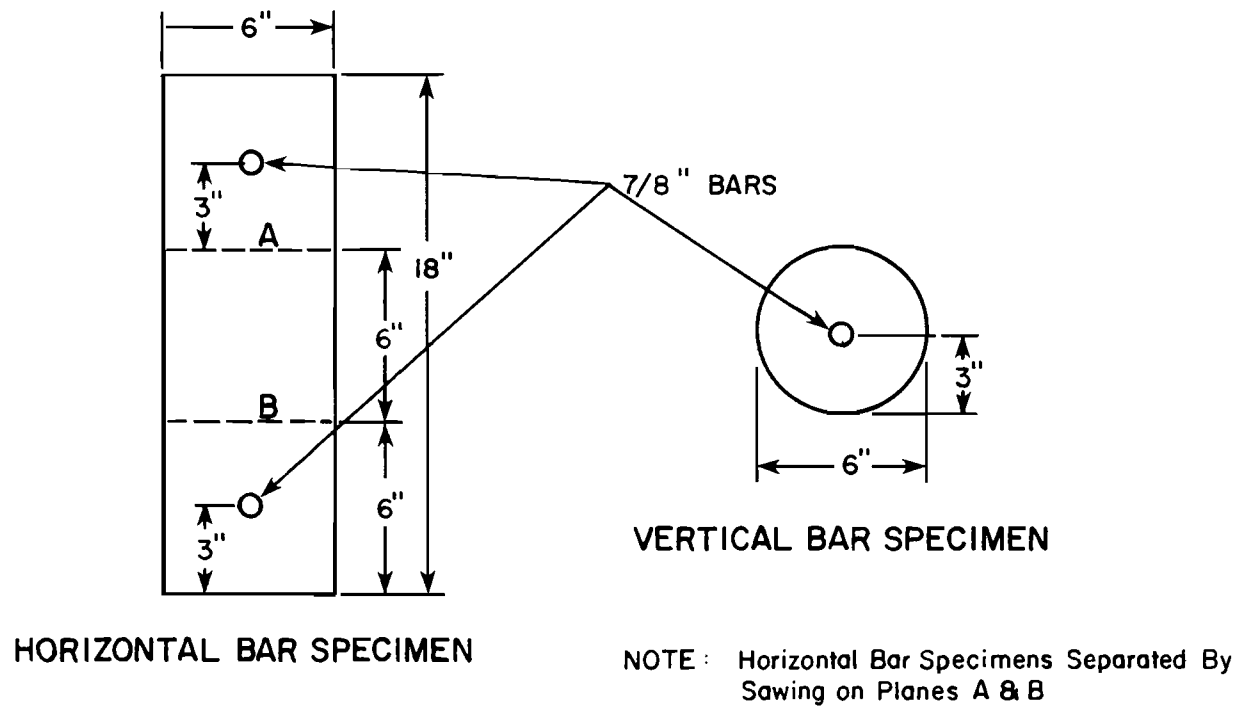


Fig. 2.6 Cross sections of Collier's specimens, Collier [11]

Test results indicated that the stress-slip relationship was primarily affected by position of casting and to a lesser extent by slump as shown in Fig. 2.7. The stresses reached by bars cast in the upper horizontal position were always less than about 60 percent of the stresses of bars cast in other positions. The performance of bars cast vertically was very similar to that of bars cast in the lower horizontal position.

## 2.7 C.U.R., 1963 [24]

In 1963, the Commissie voor Uitvoering van Research in The Netherlands [24] reported an extensive study of the various aspects of the bond of deformed steel bars with concrete. The effect of casting position was examined in that project. Figure 2.8 shows the details of test specimens used, and Table 2.2 lists the results of two series of tests dealing with the effect of casting position. The variables were the bar size, the casting height represented by the specimen height, the anchorage length, the bottom and side cover, the transverse reinforcement, and the concrete compression strength.

In series I the concrete strength was kept constant. Three bar sizes, each with a different casting height, a different anchorage length, and different transverse reinforcement, were considered. For the same bar size, a few tests were done varying the bottom and side cover. In series II, the bar size, casting height, and side and bottom cover were kept constant. The anchorage length was varied and for each anchorage length a few tests were done varying the concrete strength. It is important to note that in both series, there was no set of tests in which the depth of concrete cast below the bar was varied while all other factors were kept constant.

After studying the test results, the following conclusions were made:

(a) Test results of series I show that for the same concrete strength, the bond efficiency ratio of a top cast reinforcing bar relative to a bottom cast bar decreased as the casting height increased. The average ratios were 0.91 for a 10-mm (0.4 in.) top bar in a 25-cm (10 in.) deep beam, 0.82

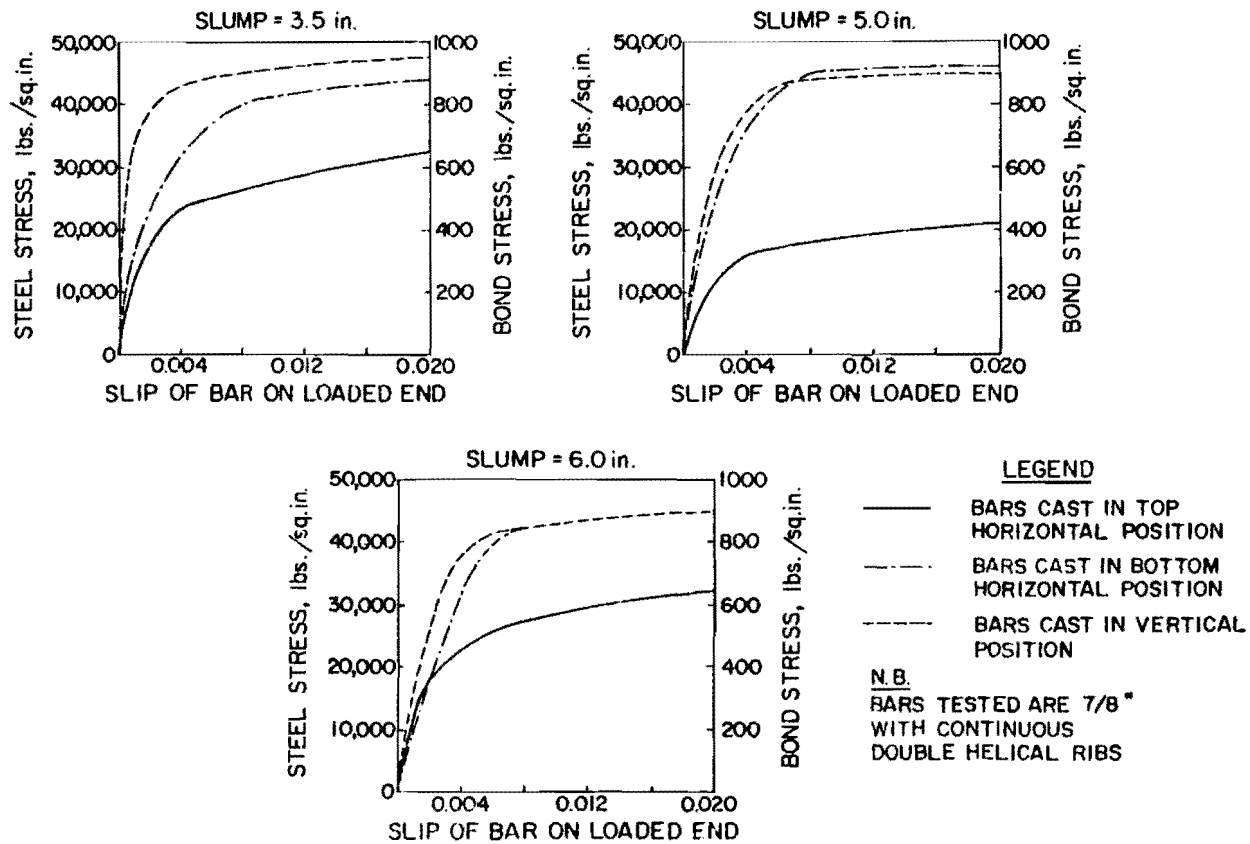
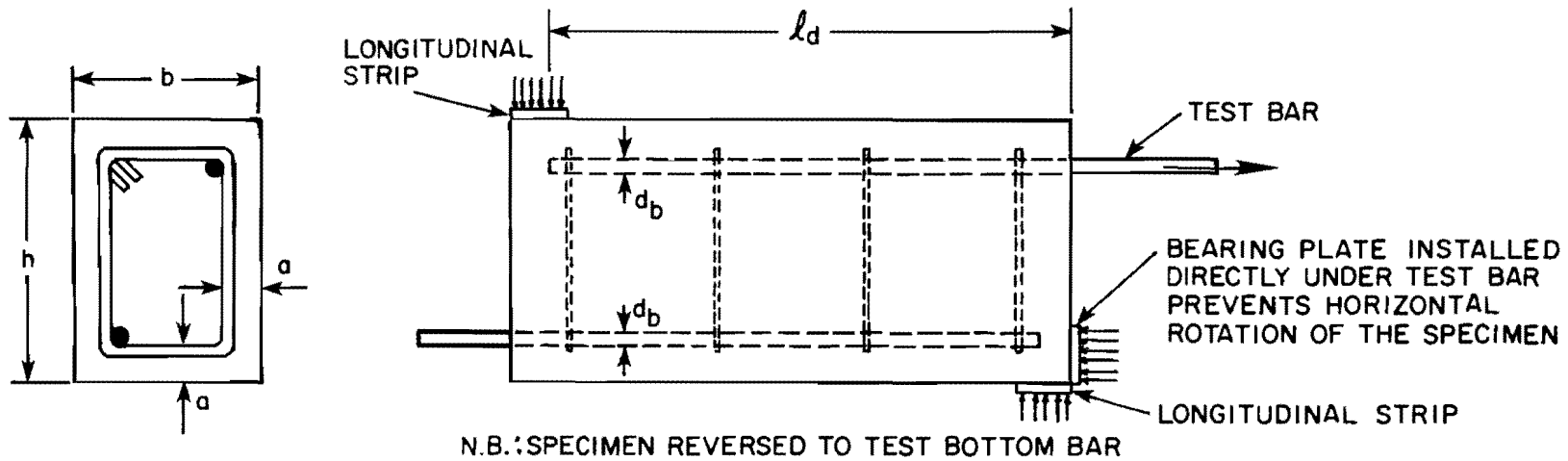


Fig. 2.7 Effect of slump on stress-slip relationship, Collier [11]



	$d_b$ , mm	$l_d$ , cm	$b$ , cm	$h$ , cm	$a$ , cm
SERIES I	10	14	20	25	2.3-5.4
	18	26.5	34	42.3	3.2-9.0
	26	35	40	50	2.5-10.4
SERIES II	10	14-35	20	25	1.5

N. B. ONLY TESTS WITH "HI-BOND" STEEL CONSIDERED

Fig. 2.8 Details of test specimens, C.U.R. [24]

TABLE 2.2 TEST RESULTS, C.U.R. [24]

Test	$l_d$ cm	$d_b$ mm	$h$ cm	$c_b$ cm	$c_s$ cm	$\frac{A_{tr} f_{yt}}{s d_b}$	$f'_c$ psi	$u_t$ psi	$\frac{(u_t)_{top}}{(u_t)_{bottom}}$
Series I	14.0	10	25.0	2.3	2.3	3050	2820	670*	0.81
	14.0	10	25.0	2.4	2.4	3050	2820	832	
	14.0	10	25.0	3.7	3.7	3050	2820	920*	
	14.0	10	25.0	5.3	5.3	3050	2820	1110*	1.01
	14.0	10	25.0	5.4	5.4	3050	2820	1100	
	26.5	18	42.3	3.2	3.2	1410	2820	548*	
	26.5	18	42.3	3.2	3.2	1410	2820	711	0.77
	26.5	18	42.3	6.3	6.3	1410	2820	639*	
	26.5	18	42.3	6.1	6.1	1410	2820	875	
	26.5	18	42.3	9.0	9.0	1410	2820	976*	0.97
	26.5	18	42.3	9.0	9.0	1410	2920	1011	
	35.0	26	50.0	2.5	2.5	1060	2820	336*	
	35.0	26	50.0	2.5	2.5	1060	2820	552	0.61
	35.0	26	50.0	6.4	6.4	1060	2820	579*	
	35.0	26	50.0	6.4	6.4	1060	2820	804	
35.0	26	50.0	10.4	10.4	1060	2820	696*	0.85	
35.0	26	50.0	10.1	10.1	1060	2820	819		
Series II	14.0	10	25.0	1.5	1.5	3050	2840		549*
	14.0	10	25.0	1.5	1.5	3050	2840	727	
	14.0	10	25.0	1.5	1.5	3050	3510	667*	0.77
	14.0	10	25.0	1.5	1.5	3050	3510	862	
	14.0	10	25.0	1.5	1.5	3050	3680	616*	
	14.0	10	25.0	1.5	1.5	3050	3680	797	0.77
	14.0	10	25.0	1.5	1.5	3050	4960	897*	
	14.0	10	25.0	1.5	1.5	3050	4960	852	
	14.0	10	25.0	1.5	1.5	3050	4960	852	1.05
	21.0	10	25.0	1.5	1.5	3050	2570	414*	
	21.0	10	25.0	1.5	1.5	3050	2570	686	
	21.0	10	25.0	1.5	1.5	3050	3820	744*	0.85
	21.0	10	25.0	1.5	1.5	3050	3820	875	
	21.0	10	25.0	1.5	1.5	3050	4040	513*	
	21.0	10	25.0	1.5	1.5	3050	4040	785	0.69
	21.0	10	25.0	1.5	1.5	3050	4960	927*	
	21.0	10	25.0	1.5	1.5	3050	4960	934	
	21.0	10	25.0	1.5	1.5	3050	4960	934	0.99
	28.0	10	25.0	1.5	1.5	3050	2480	306*	
	28.0	10	25.0	1.5	1.5	3050	2480	613	
	28.0	10	25.0	1.5	1.5	3050	4320	755*	0.83
	28.0	10	25.0	1.5	1.5	3050	4520	777	
	28.0	10	25.0	1.5	1.5	3050	4520	777	
	28.0	10	25.0	1.5	1.5	3050	4600	569*	0.97
	28.0	10	25.0	1.5	1.5	3050	4600	715	
	28.0	10	25.0	1.5	1.5	3050	4600	715	
	28.0	10	25.0	1.5	1.5	3050	4910	690*	0.80
28.0	10	25.0	1.5	1.5	3050	4910	789		
28.0	10	25.0	1.5	1.5	3050	4910	789		
35.0	10	25.0	1.5	1.5	3050	2930	478*	0.87	
35.0	10	25.0	1.5	1.5	3050	2930	580		
35.0	10	25.0	1.5	1.5	3050	3070	553*		
35.0	10	25.0	1.5	1.5	3050	3070	626	0.88	

\* Top cast bars

for an 18-mm (0.7 in.) top bar in a 42.3-cm (16-1/2 in.) deep beam, and 0.73 for a 26-mm (1 in.) top bar in a 50-cm (20 in.) deep beam.

(b) An increase in the side and bottom cover improved the relative bond efficiency of the top bar.

(c) The relative bond efficiency of the top bar did not seem to be seriously affected by variation of the concrete strength.

(d) An increase in anchorage length did not produce a pronounced change in the relative bond efficiency of the top bar.

(e) Considering all tests in both series, the average  $u_{\text{top}}/u_{\text{bottom}}$  was 0.82.

## 2.8 Ferguson and Thompson, 1965 [19]

Ferguson and Thompson reported a series of beam tests with ASTM A431 steel with  $f_y$  above 75 ksi. The primary variables were bar cover, beam width, stirrup ratio, development length, and depth of concrete cast below the bar. The test specimen was a simple beam with a cantilever overhang which permitted the test bar to be in the negative moment region, as shown in Fig. 2.9. Ferguson and Thompson argued that since this arrangement removed the test bar from reactions and load points, the simplest attainable bond conditions along the development length  $l_d$  were produced.

Beams were loaded to failure. In most test beams a combination of splitting and diagonal cracking appeared prior to failure. Although splitting was a factor in all failures, diagonal tension failures were observed in some tests. Ferguson and Thompson argued that the unit shear in such cases was quite low suggesting that splitting possibly contributed to the diagonal tension weakness.

The set of test specimens in which the effect of depth of concrete placed below the bar was considered were all 24-in. wide beams with #11 bars. Concrete slump varied between 1 in. and 3 in. Test results are shown in Fig. 2.10. It was intended to use 1-in. slump concrete, but the stiff mix obviously minimized the top bar effect. In three cases, a comparison of

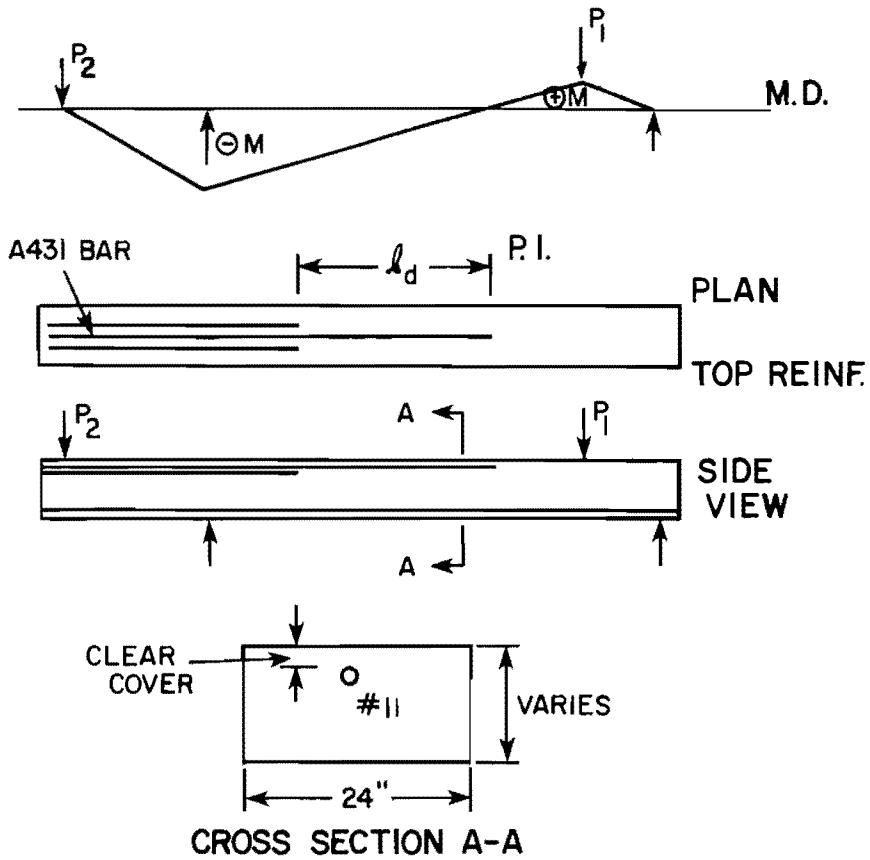


Fig. 2.9 Typical beam specimen, Ferguson and Thompson [13,14]

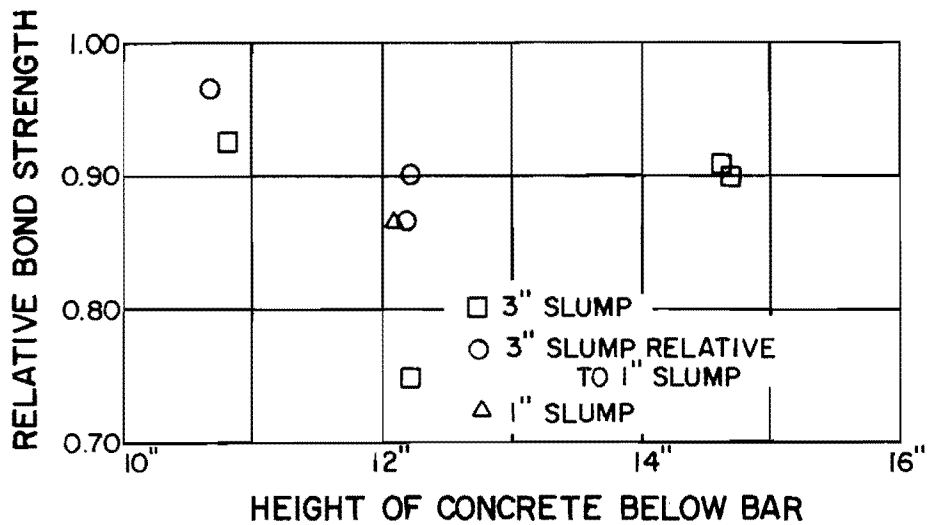


Fig. 2.10 Test results showing the top bar effect, Ferguson and Thompson [19]

companion beams cast with 3-in. slump concrete was available and these are plotted in Fig. 2.10 as open circles. With about 12 in. of concrete below the bar, the strength dropped 3 to 13 percent with the increase in slump.

Four comparisons between bottom cast bars and top cast bars in 3-in. slump concrete are shown by squares in Fig. 2.10. Two of these cases with about 15 in. of concrete below the bar gave bond strength reductions of 9 and 10 percent. Another with only 10.8 in. of concrete below the bar showed a 7.5 percent reduction. The fourth with 12.2 in. of concrete below the bar indicated nearly a 25 percent loss. The authors argued that the latter possibly indicated scatter which might be expected in this case. Ferguson and Thompson concluded from the above data that for the small beam depths and low or moderate slumps, the 0.7 reduction factor, which was present in the ACI Code (ACI 318-63) [4] at the time, was conservative on a strength basis.

#### 2.9 Welch and Patten, 1965 [40]

Welch and Patten investigated the effect of concrete sedimentation on pullout bond resistance of plain round, twisted square, and deformed reinforcing bars. The two specific characteristics studied were settlement and bleeding of fresh concrete.

The bleeding characteristics of the specimens were determined by collecting water from the top surface of the specimen at 15-minute intervals following casting. Bleeding was expressed as the ratio of the water collected relative to the amount of water in the freshly cast concrete.

Settlement was expressed as the ratio of the amount of settlement to the original height of the specimen. Both bleeding and settlement leveled off after approximately 90 minutes following casting.

Specimens were cast with both horizontal and vertical bars. The specimens with the horizontal bars were cast in molds with a design similar to the ones used by Clark except that in this case the top bar had 8-1/2 in. of concrete cast below it and the bottom bar had 2-1/2 in. of concrete cast

below it. All specimens with vertical bars were cast so that the bar was pulled in the direction opposite to that of concrete settlement.

Measurements of settlement and bleeding for each specimen did not agree closely with bond strength results. Some trends, however, were discernible. The bond strengths of top bars were definitely lower than those of bottom bars. On the average, the top bars developed only 60 percent of the bond stress of the bottom bars at 0.01 in. slip. Also, bond strengths of both bottom and top bars tended to be reduced with greater settlement. Figure 2.11 shows the bond stress values at 0.01 in. loaded end slip for various amounts of settlement. The authors stated that the separation of the two bands (top bar vs. bottom bar) increased when bar stresses at higher values of slip were recorded and that both top and bottom bars were equally affected by an increase in concrete settlement.

#### 2.10 Summary

The review of research indicates that while a considerable number of test results are available regarding the influence of casting position on bond performance, no systematic investigation has been undertaken to develop definitive relationships between bond strength and the variables shown to be important, e.g., height of bar in form, orientation, and concrete consistency (slump).

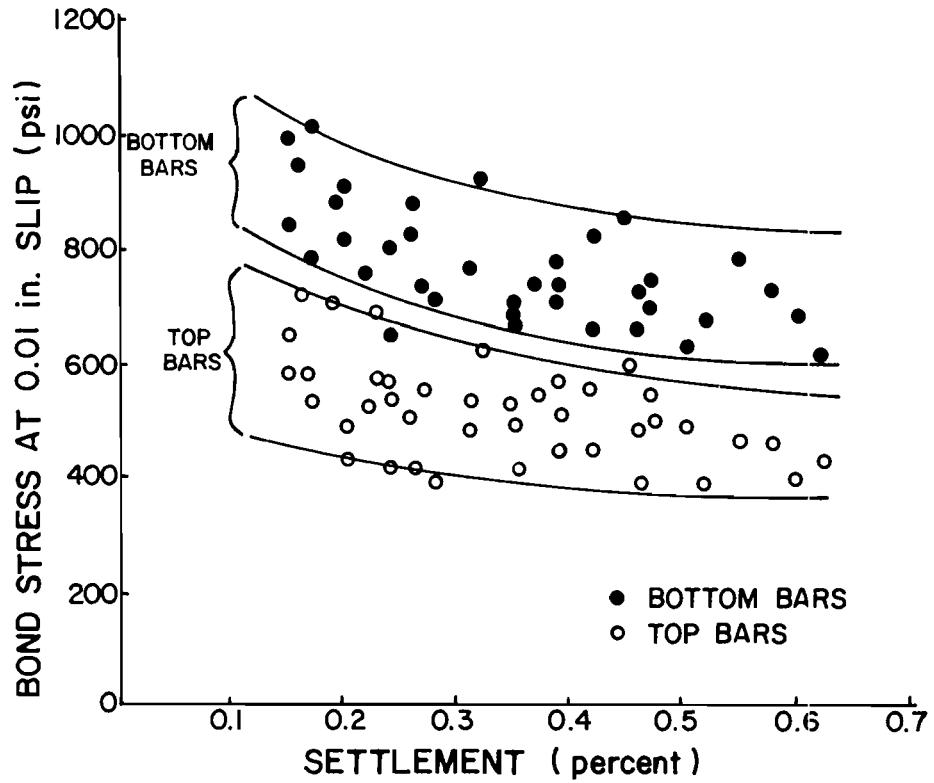


Fig. 2.11 The effect of settlement on the bond strength of top and bottom bars (Welch and Patten [40])

## CHAPTER 3

### A REVIEW OF DESIGN PROCEDURES FOR ANCHORED DEFORMED BARS

#### 3.1 Regulatory Approach

The term bond stress,  $u$ , was defined in Chapter 1 as the shear stresses acting at the concrete-steel interface. The meaning of this term can be illustrated by considering a section of a beam subjected to a moment gradient as shown in Fig. 3.1. Summing forces acting on the bar yields

$$\Delta T = \sum_o \cdot u \cdot dx$$

where  $\Delta T$  is the change in bar tensile force,  $\sum_o$  is the sum of the perimeters of the bars in tension, and  $dx$  is the length of the incremental element under consideration. Also, for the section shown,

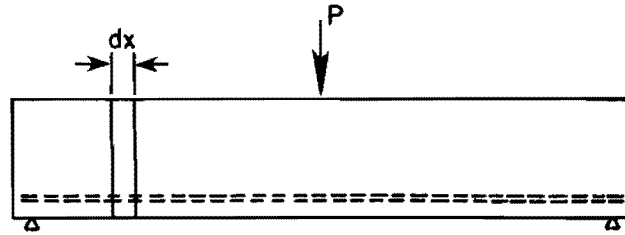
$$\Delta T = \frac{\Delta M}{jd} = \frac{Vdx}{jd}$$

where  $\Delta M$  is the change in bending moment at the section considered,  $j$  is the ratio of the distance between the centroid of compression and the centroid of tension to the depth  $d$  of a flexural member, and  $V$  is the shear force at the section considered. Then, combining these equations, the basic relationship for flexural bond was developed as

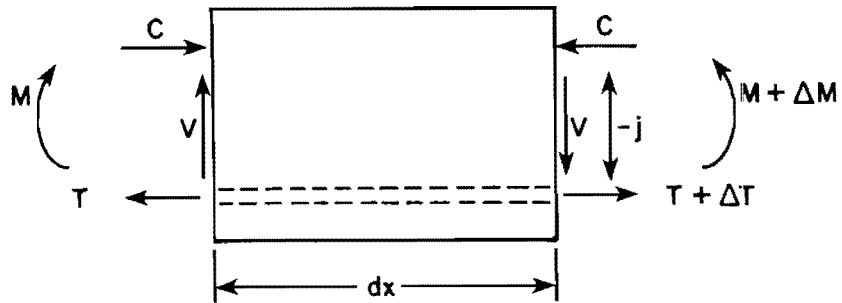
$$u = V/\sum_o \cdot j \cdot d$$

This expression for bond stresses was incorporated into ACI codes up to and including the 1963 ACI Code (ACI 318-63) [4]. It reflects an early concern with the flexural bond resistance of reinforcing bars, especially plain bars. AASHTO Specifications have generally followed the ACI Code pattern.

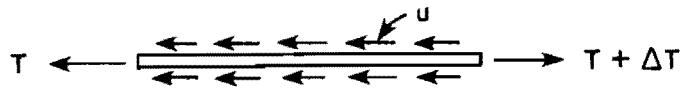
The monumental study by Abrams [1] in 1913 provided the foundation for most early specifications on bond. Abrams had concluded that for typical anchored bars, bond stresses could be considered to be uniformly distributed over the length of the bar and that bond resistance varied



(a) SIMPLY SUPPORTED SPAN WITH POINT LOAD



(b) FORCES ACTING ON SECTION OF BEAM WITH LENGTH  $dx$



(c) FORCES ACTING ON EMBEDDED BAR

Fig. 3.1 Calculation of bond stress,  $u$

directly with the compressive strength of the concrete. He also determined that the deformed bars then available performed only slightly better than plain bars. In accordance with Abrams' findings, the 1947 ACI Code (ACI 318-47) [2] set limiting values of bond stress at  $0.04 f'_c$  for plain bars and  $0.05 f'_c$  for deformed bars. Deformed bars were loosely defined in that code as "bars with closely spaced shoulders, lugs, or projections formed integrally with the bar during rolling."

In 1938, Gilkey, Chamberlain, and Beal [21] ran a series of tests to augment those of Abrams. They used higher strength concrete mixes and reinforcing bars then currently in use. The authors found that for concrete strengths above 2000 psi (roughly twice the value of concrete strengths used by Abrams), bond resistance was not directly proportional to concrete compressive strength and that with the higher strength bars, bond resistance did not increase directly with added length of embedment. They concluded that much more study was needed on the effectiveness of various types of deformed bars.

It was becoming increasingly evident to investigators that bar deformations were necessary to develop the bond resistance of large bars of high yield strength steel placed in high strength concrete and that these deformations resulted in longitudinal splitting becoming the predominant mode of failure for anchored bars.

Several investigators subsequently studied the effects of various deformation patterns, heights, and spacings on bond efficiency and since 1951 the ACI Code has specified minimum requirements for deformed bars corresponding to standards developed by the American Society for Testing and Materials (ASTM) [5].

The 1951 ACI Code doubled the allowable unit bond stresses (to  $0.10f'_c$ ) for bars meeting ASTM specifications. Plain bars were permitted only with hooked anchorages and the allowable unit stresses were set at  $0.45f'_c$ . The section on bond in the 1951 Code remained unchanged in the 1957 Code.

The recognition that the introduction of high strength deformed bars was changing the mode of failure for anchored bars led to some substantial

changes in the ACI Code in 1963 (ACI 318-63). The term flexural bond was introduced to identify the nominal bond stress induced by the transfer between concrete and steel of the change in bar tension. The equation for flexural bond was referred to as idealistic because it neglected complications due to flexural cracks and cut-off bars. More significant was the introduction of anchorage bond, defined as the average bond stress between the point of maximum tensile stress and the end of the bar where the tensile stresses are zero.

The code limited ultimate bond stress,  $u_u$ , for both flexural and anchorage bond to

$$u_u = \frac{9.5 \sqrt{f_c'}}{d_b} \leq 800 \text{ psi}$$

where  $d_b$  = bar diameter, for bottom cast bars. These limits were based on work at the Bureau of Standards [29] and The University of Texas [17] which indicated that ultimate bond stress varied as  $l/D$  and as  $\sqrt{f_c'}$ . The  $\sqrt{f_c'}$  term also indicated that the tensile capacity of the concrete was an important factor in bond resistance.

The current ACI Code and AASHTO Specifications are not based on bond stresses. Rather, development length,  $l_d$ , is computed directly. The provisions for development length, however, are based on the ultimate bond stresses specified in the 1963 Code. Assuming a uniform stress distribution along the bar, the length needed to develop 125 percent of the yield strength can be determined as follows:

$$l_d \cdot \pi \cdot d_b \cdot u_u = a_b (1.25f_y)$$

$$l_d = \frac{a_b (1.25f_y)}{\pi d_b (9.5 \sqrt{f_c'} / d_b)} \approx 0.04 a_b f_y / \sqrt{f_c'}$$

where  $a_b$  = bar area and  $f_y$  = bar yield strength. The basic problem with current provisions for bond is that a number of important parameters are

not considered. Variables which are known to influence the necessary development length of deformed bars such as bar cover and bar spacing are not even mentioned in the current sections on bond and anchorage.

### 3.2 Development Lengths of the Anchored Bars

Orangun, Jirsa, and Breen, in a research project conducted for the Texas Highway Department in 1974, developed an equation for the strength of an anchored deformed bar in terms of the average bond stress along the bar [33].

$$u = \left[ 1.2 + 3\frac{c}{d_b} + \frac{50d_b}{l_d} + \frac{A_{tr} f_{yt}}{500sd_b} \right] \sqrt{f'_c} \quad (3.1)$$

The equation includes the parameters of cover and spacing ( $c$ ), and transverse reinforcement ( $A_{tr}$ ) which are not included in ACI Code equations. Equating the tensile force on the bar with the total force on the surface of the bar and solving for  $l_d$

$$l_d = \frac{d_b \left( \frac{f_s}{4\sqrt{f'_c}} - 50 \right)}{1.2 + 3\frac{c}{d_b} + \frac{A_{tr} f_{yt}}{500sd_b}} \quad (3.2)$$

In Eq. (3.1) the strength of the anchored bar increases as the cover to bar diameter ratio increases. However, it is obvious that at some cover to diameter ratio the mode of failure will not involve splitting. For large  $c/d_b$  values, direct pullout could occur with the bar deformation shearing off the concrete between the lugs; therefore,  $c/d_b$  should be limited to 2.5 for computing  $l_d$ .

Orangun, et al. [33], in examining available test data, found that with increasing values of  $c_s/(c_b d_b)$ , the bond strength  $u$  increased. With large side or clear spacing, the concrete surrounding the bar tends to restrain splitting across the plane through the anchored bars. Evidence of this, as reported in Ref. 33, is the "V-notch" type of failure observed in tests with large bar spacings.

For the test specimens in this study, the ratio  $c_s / (c_b d_b)$  was very large and "V-notch" failure was expected.

Based on available data, Orangun, et al. [33], proposed for  $c_s / (c_b d_b)$  values exceeding 6 a reduction factor of 0.7 on the development length required by Eq. (3.2). This factor was used in evaluating the required development lengths of bars included in this study.

In Table 3.1 development lengths of the bars included in the study are tabulated. Computation was based on Eq. (3.2) using  $f'_c = 3000$  psi,  $f_s = 40$  ksi, and  $A_{tr} = 0$ . A steel stress of 40 ksi was chosen to provide specimens which would fail in anchorage prior to yielding of the reinforcement. For splices a length of 12 in. was selected for all tests. For purpose of comparison, the development lengths were computed using Section 12.2.2 of the ACI "Building Code Requirements for Reinforced Concrete," (ACI 318-77) [4].

$$l_d = 0.04 a_b f_y / \sqrt{f'_c} \quad (3.3)$$

$$l_d \geq 0.0004 d_b f_y \quad (3.4)$$

TABLE 3.1 COMPUTATION OF DEVELOPMENT LENGTH OF ANCHORED BARS\* ( $f'_c = 3000$  psi)

Bar Number	$d_b$ in.	$a_b$ sq. in.	$c_b$ in.	$c_b/d_b$ $\leq 2.5$ in.	$l_d$ (Eq. 3.2) in.	$k^{**}$	$l_d \times k$ in.	$l_d$ (ACI 318-77) in.	$l_d$ or $l_s$ used in tests in.
7	0.875	0.60	1.00	1.14	25.0	0.7	17.5	17.5	12.0
9	1.128	1.00	2.00	1.77	23.0	0.7	16.1	29.2	12.0
11	1.410	1.56	2.00	1.42	34.3	0.7	24.0	45.6	20.0

\*Without modifications for "top bar"

\*\*k = reduction factor for wide spacing

This page replaces an intentionally blank page in the original.

-- CTR Library Digitization Team

## C H A P T E R 4

### EXPERIMENTAL PROGRAM

#### 4.1 Outline of Test Specimens

The test specimens consisted of large blocks of concrete with anchored or spliced bars cast in the block. The test bars were arranged so that the depth of concrete placed in the form beneath the bar was varied. Other variables considered included concrete strength, concrete consistency (slump), concrete cover, and single bar or splice orientation. The length of the anchored bar or splice was chosen to ensure that failure would occur as a result of concrete splitting and not steel yielding (Table 3.1). A series of trial specimens was tested to determine the mode of failure and to investigate the interaction between adjacent bars in terms of splitting and V-notch cracking patterns. From the trial specimens changes were made in the dimensions of the final test specimens. Appendix A contains details of the trial specimens (T-Series).

#### 4.2 Development Length Tests (D Series)

Specimens D1, D2, and D3 included sixteen bars, as shown in Fig. 4.1. Bars on one side were the same diameter and had the same anchorage length and clear cover. The primary variable was the casting position. Specimens D1 and D2 were cast with concrete having a 3 in. slump and D3 purposely had an 8-1/2 in. slump.

Specimen D4 studied the behavior of horizontally positioned as opposed to vertically positioned anchored bars as shown in Fig. 4.2. The specimen was designed so that at two different heights in the concrete block ( $z = 18$  in. and  $z = 48$  in.) two #9 bars were cast for each of the following cases (see Fig. 1.2):

- (1) horizontally positioned;
- (2) vertically positioned, pulled against the direction of settlement; and
- (3) vertically positioned, pulled in the direction of settlement.

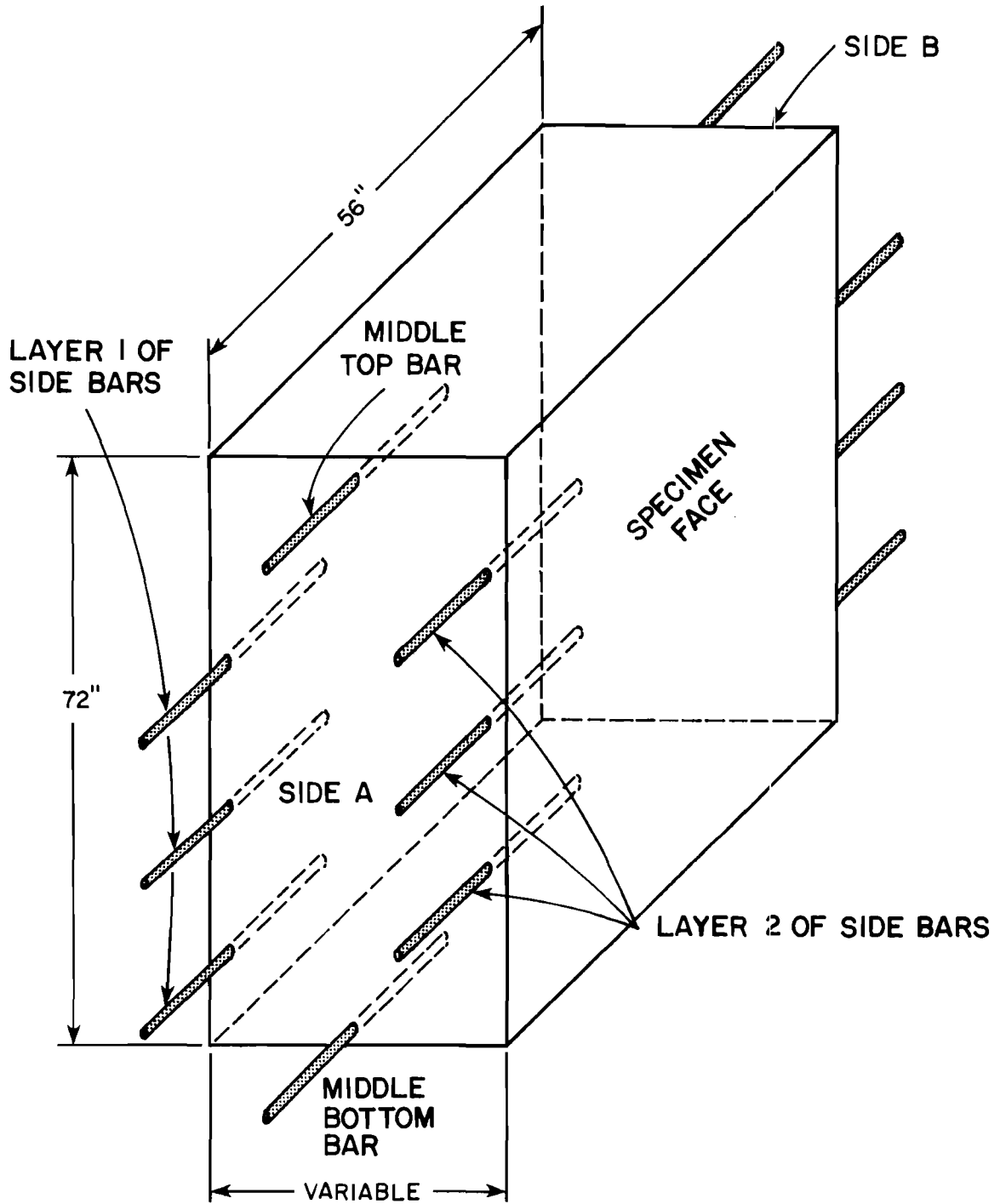


Fig. 4.1 Schematic presentation of Specimens D1, D2, and D3

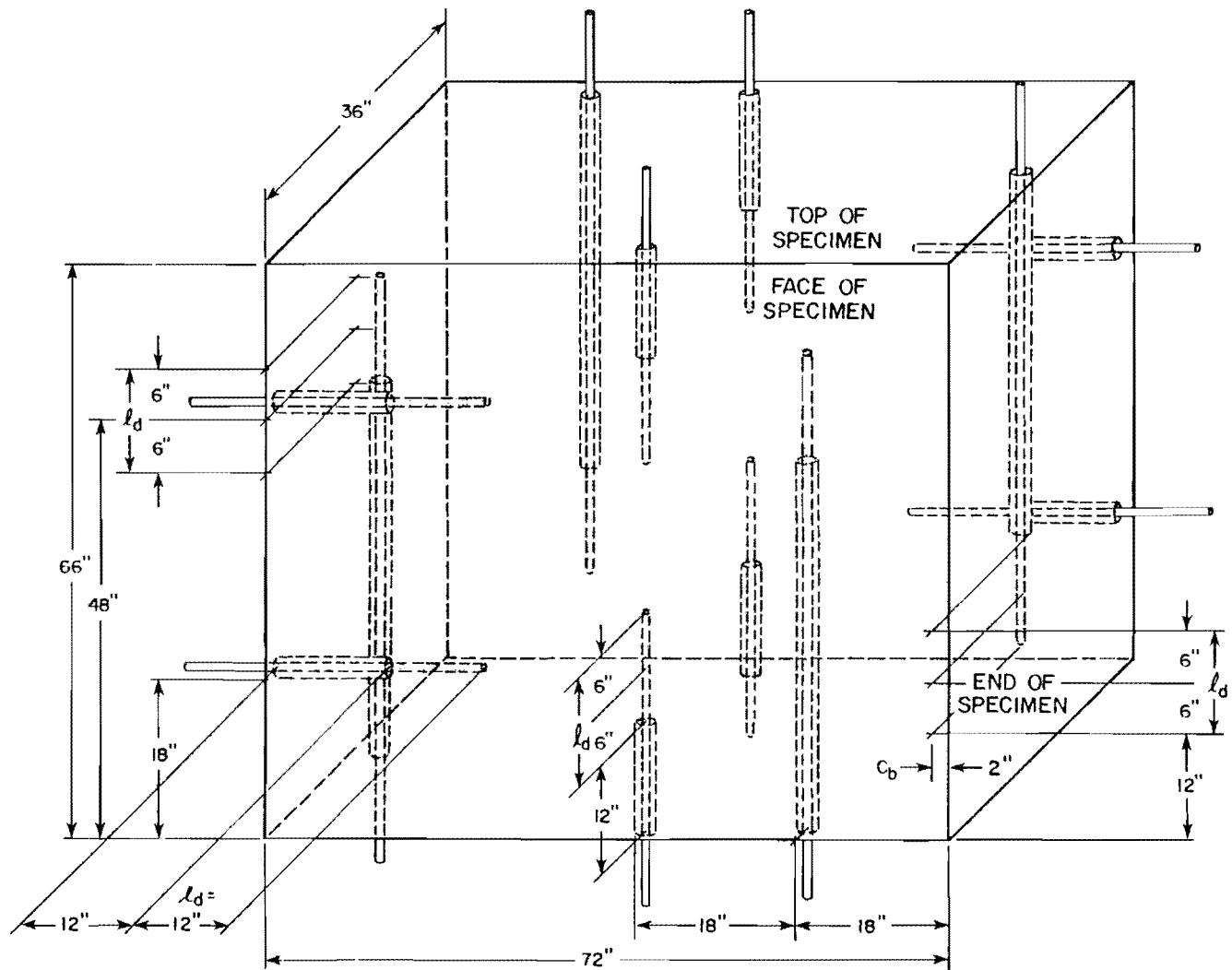


Fig. 4.2 Schematic representation of Specimen D4 (horizontal and vertical bars)

All bars had the same clear cover and development length. To ensure that the bars had the same development length, regardless of the direction of testing, a portion of the bar embedded in the concrete which was not to be developed was covered with a plastic tube.

### 4.3 Splice Tests (S Series)

Two specimens were tested to determine the influence of casting position on the behavior of horizontal (bar axes positioned horizontally) lapped splices (#9 bars). Figure 4.3 shows specimen S1 having splices oriented so that the plane of the splice (the plane containing the line of tangency and the axes of the two horizontal bars) is perpendicular relative to the bottom of the formwork. These splices will be referred to as stacked splices. Note that in this specimen the top and bottom splices are positioned so that the planes of the splices are perpendicular to the face of the concrete while the side splices are positioned so that their planes are parallel to the concrete face. The orientations will be referred to as face-perpendicular and face-parallel splices, respectively. It was not obvious from theoretical considerations whether the splice orientation relative to the concrete face or relative to the bottom of the formwork would dominate in determining the mode of failure for splices cast at different heights in the specimen. Therefore, a second specimen S2 contained all horizontal bars spliced side-by-side, with the top and bottom splices oriented face-parallel and the side splices face-perpendicular as shown in Fig. 4.4. The two specimens covered a range of possible splice orientations typical in construction with the exception of splices oriented vertically.

### 4.4 Materials

4.4.1 Concrete. The concrete mixes used in all test specimens were based on the Texas Department of Highways and Public Transportation Standard Specifications for Class A non-air-entrained concrete with a specified minimum compressive strength ( $f'_c$ ) of 3000 psi at 28 days after casting. These specifications require a slump of between 2 in. and 4 in. To investigate slump effects, the actual slumps used were 5.5 in. for the

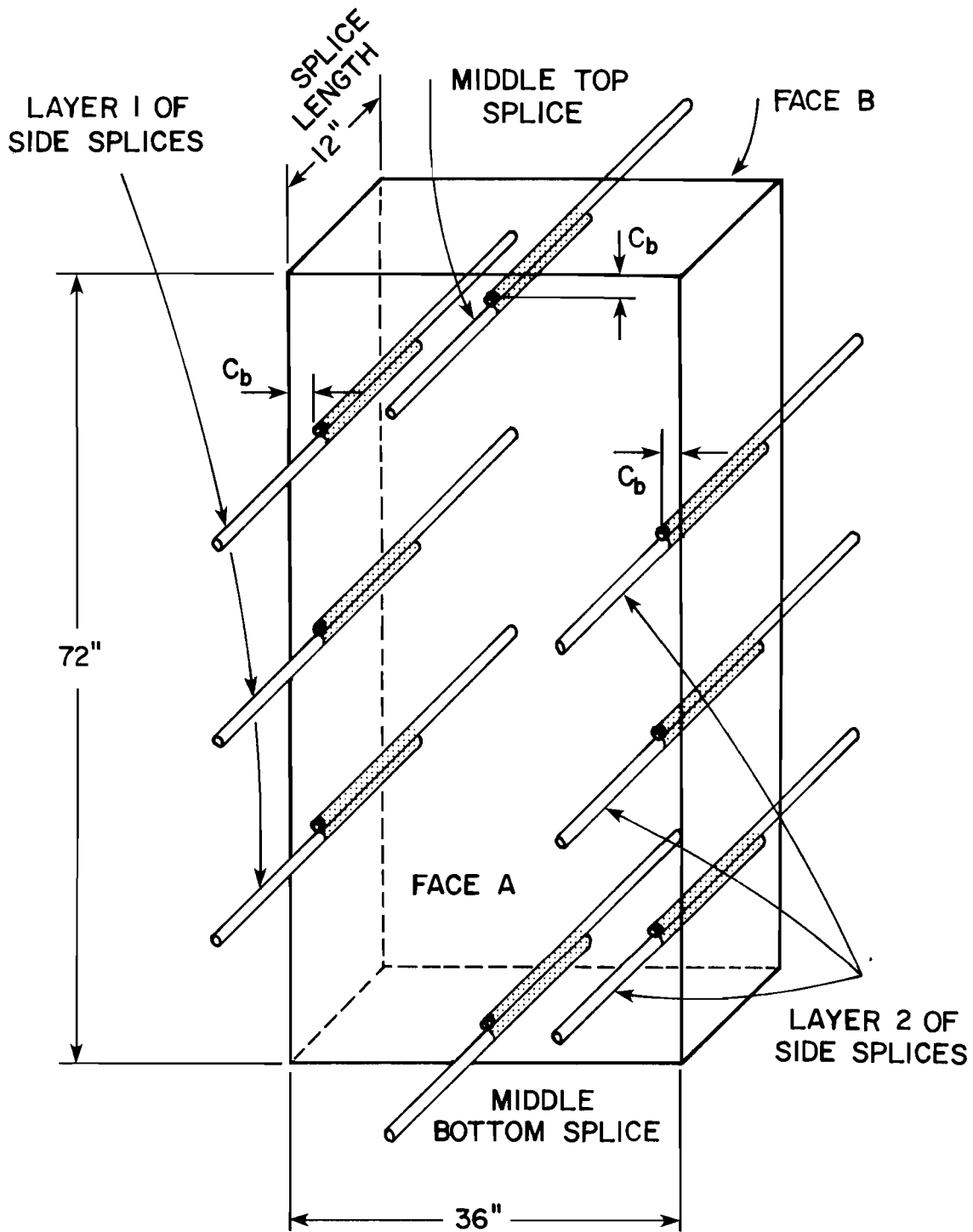


Fig. 4.3 Schematic representation of Specimen S1 (stacked splices)

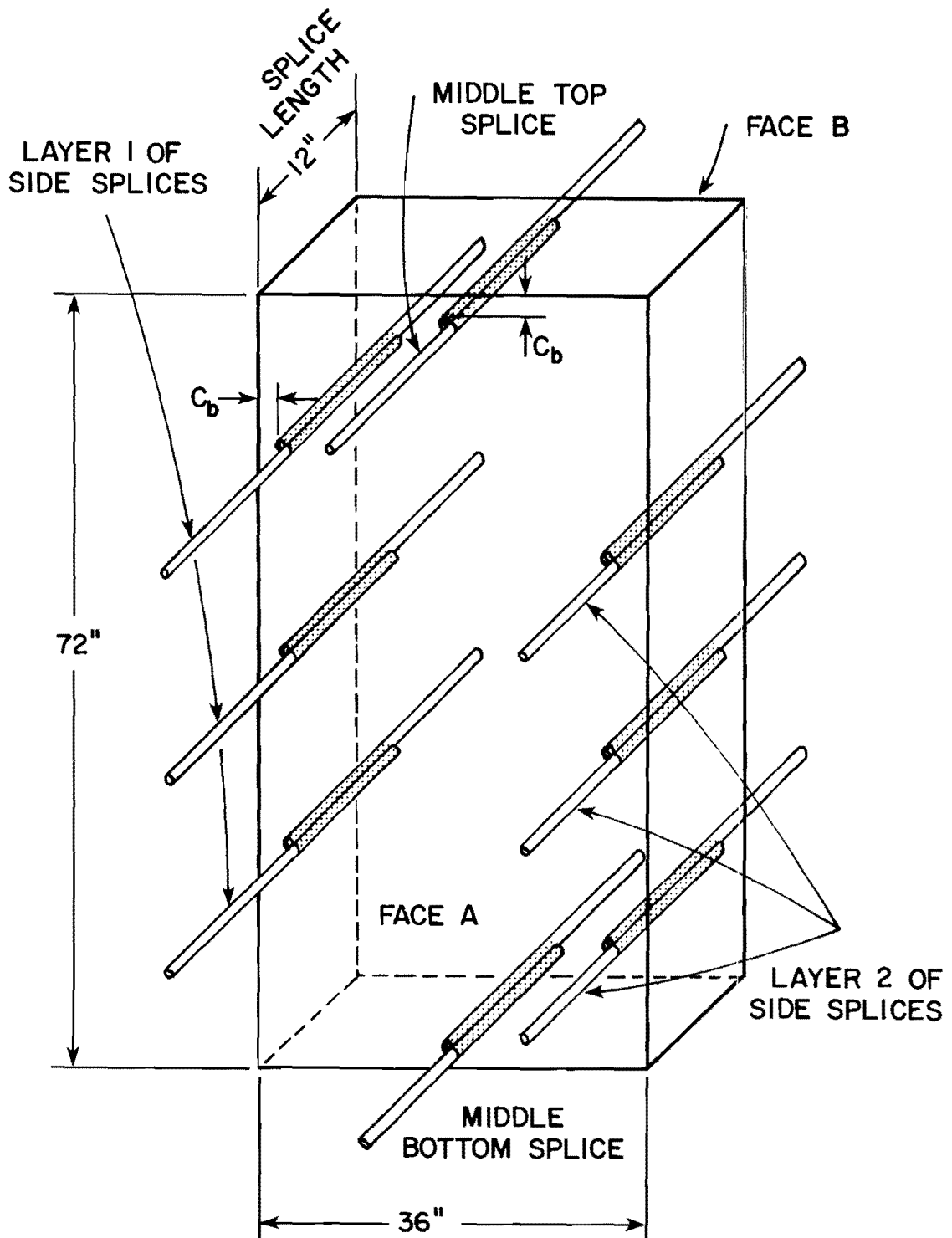


Fig. 4.4 Schematic representation of Specimen S2 (side-by-side splices)

splice specimens, 3.0 in. for the horizontal/vertical specimen, and 8.5 in. for the high slump specimen. Both the Highway Department's specifications and the actual mix designs used are given in Appendix B.

Type III Portland Cement was used for Specimens D1 and D2 and Type I for all other tests. The fine aggregate used was Colorado River sand, largely siliceous. The coarse aggregate was Colorado River gravel, largely hard limestone gravel with some quartz and siliceous particles, with a maximum size of 1 in.

As the concrete consistency was an important variable in the test program, the concrete was ordered from the readymix plant with approximately 10 percent less water than required by the mix design. Water was added at the laboratory until the desired slump was achieved.

The following casting procedure was the same for all specimens. The concrete was placed in the forms in one-foot lifts by means of a concrete bucket. Each layer of concrete was vibrated using mechanical vibrators to consolidate the concrete and to reduce the possibility of honey-combing in the vicinity of the test bars. The average rate of placement was approximately one lift every 8 minutes. Standard 6 x 12 in. cylinders were cast at the same time that the specimens were being cast.

Following casting the specimens and cylinders were screeded, troweled, and covered with a sheet of polyethylene. After five days the specimens and the cylinders were removed from their forms and stored until testing. The testing for each specimen did not begin until the concrete strength gain had leveled off so that no large changes in concrete characteristics were expected during the period of testing for each specimen.

4.4.2 Reinforcing Steel. Number 7, 9, and 11 deformed bars meeting ASTM A615-76a with a specified minimum yield strength of 60 ksi were used in the test specimens in this investigation. The transverse reinforcement was fabricated from #3 deformed bars. According to ASTM A615-76a [7], a deformed bar is defined as a bar that is intended for use as reinforcement in reinforced concrete construction. The surface of the bar

is to be provided with lugs or protrusions (deformations) which inhibit longitudinal movement of the bar relative to the concrete. Specifications for deformations are listed in Appendix B. The measured deformation characteristics for the bars are also provided in Appendix B. Stress-strain curves and photographs of the bars used are also given in Appendix B.

#### 4.5 Formwork

The formwork was constructed of 3/4-in. A/B fir plywood and construction grade fir 2 x 4 studs. For Specimens D1-D3 the form consisted of two side forms 84-in. wide and 72-in. high, two end forms 72-in. high and 36-in. wide, and a bottom base plate. Form-ties were utilized to ensure that the form was rigid and reasonably watertight. Four lifting inserts were located in each side of the form so that the specimen could be moved and rotated. The inside faces of the forms were given several coats of lacquer. Immediately prior to the placement of the test bars and the #3 reinforcing cages, the inside faces of the forms were coated with oil.

The end forms had holes of slightly larger diameter than the diameter of the test bars drilled at the desired bar positions. In addition to the end forms that served to contain the concrete, another set of end forms with exactly the same hole size and spacing was placed in a plane several inches from and parallel to the specimen end forms. The additional forms served to hold the test bars rigidly in place and to keep the cover and height of every bar constant along its length (see Fig. 4.5). Figure 4.6 shows the reinforcement in the form prior to closing the form.

The formwork for Specimen D4 was 66 in. high, 36 in. wide, and 72 in. long. As can be seen from Fig. 4.2, the formwork for this series of tests were considerably more complex than that for Specimens D1-D3. PVC tubing was used to hold the bars rigidly and to ensure that each bar had the same amount of clear cover and development length (see Fig. 4.7). At two points along the length of the portion of the bar covered by the tubing, tape was wrapped around the bar. This tape kept the bar snug within the tubing and eliminated any lateral movement of the bar. Both the tape and the bar

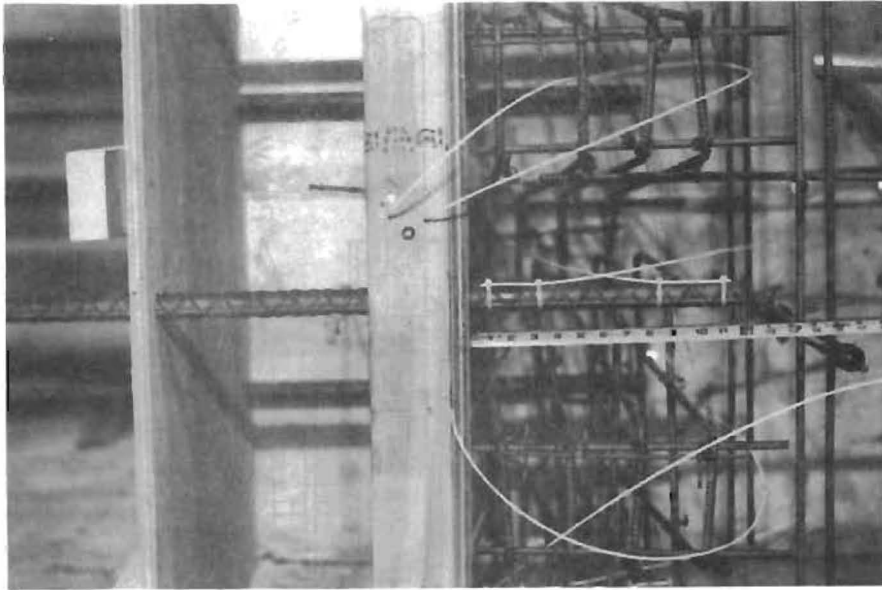


Fig. 4.5 Additional side form to hold the bar in place

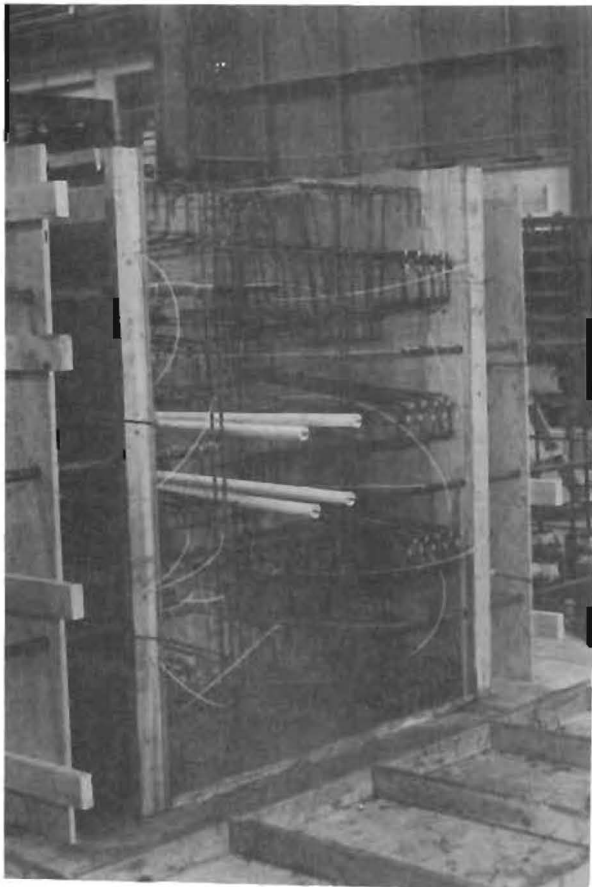


Fig. 4.6 Form of Specimen D1  
prior to casting

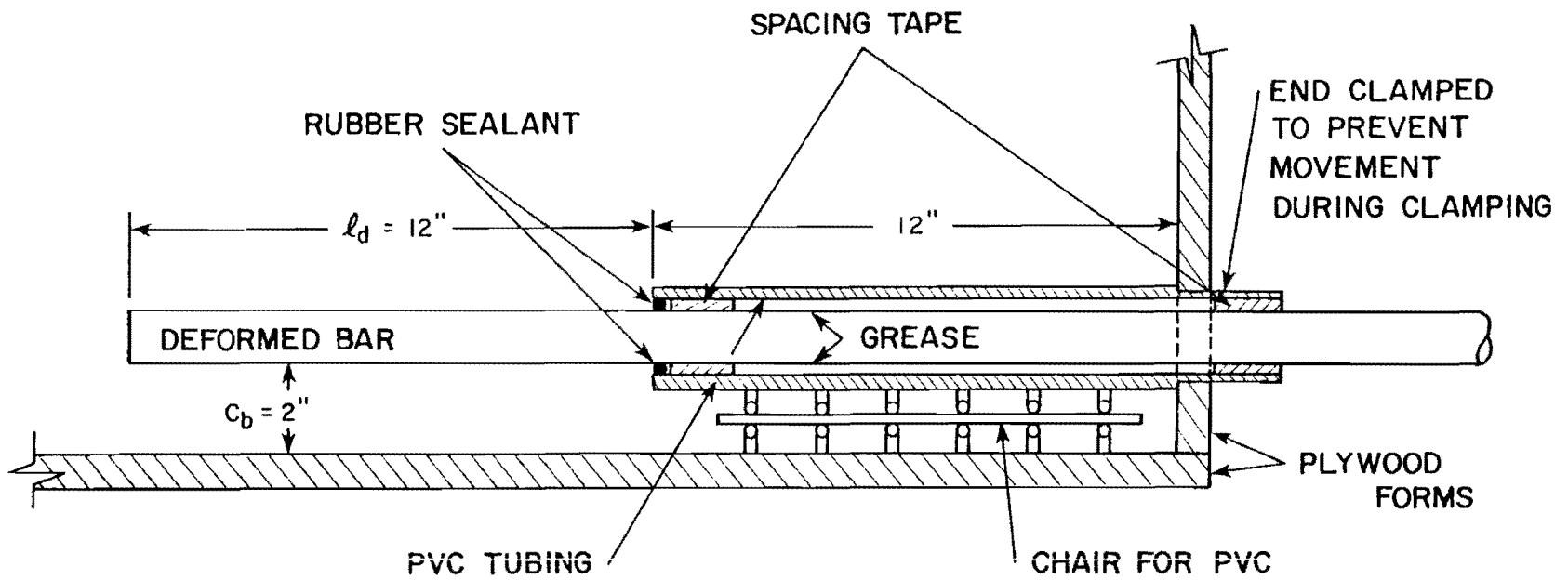


Fig. 4.7 Positioning details for bars in Specimen D4

within the tubing were coated with a layer of grease so that the bar was free to move axially. Rubber sealant placed at the end of the PVC embedded in the concrete prevented any cement paste from entering the tube. A clamp at the opposite end of the tube held the bar in place until after casting was complete.

The forms for the splice tests, S1 and S2, were 72 in. high, 36 in. wide, and 12 in. deep. The 12 in. depth of these specimens corresponded to the splice lengths. The lead end of each bar protruded through a hole in one of the faces of the forms while the free end was supported by a pin inserted in the end of the bar and the face of the formwork. Each splice was secured by two plastic ties to reduce the possibility of the relative movement of the spliced bars during the casting operation. Figure 4.8 shows stacked splice (S1) in position before casting.

#### 4.6 Transverse Reinforcement

The T-Series of tests (Appendix A) indicated that unless the spacing between the bars is very wide, cracks from the splitting produced by one bar tended to propagate into the anchorage zone of the adjacent bars. Since the spacing requirements would have necessitated either the use of two specimens or else a reduction in the number of test positions studied, a method for confining the cracks was devised. Specially built "cages" of #3 bars were placed in the specimens in a manner that ensured that each test bar or test splice was subjected to the same amount of confinement and that cracks from one test would not interfere with other bars.

The transverse reinforcement details for the development length Specimens D1-D3 are shown in Figs. 4.9 and 4.10. Details for the splice tests (S1, S2) are shown in Fig. 4.11. Individual cages were made for each bar. in the Specimen D4. The reinforcement pattern is shown in Fig. 4.12 and the actual positioning of one of the cages is shown in Fig. 4.13.

#### 4.7 Test Frame

The test frames used in this investigation were designed to simulate the forces acting on anchored and spliced bars in flexural members. The

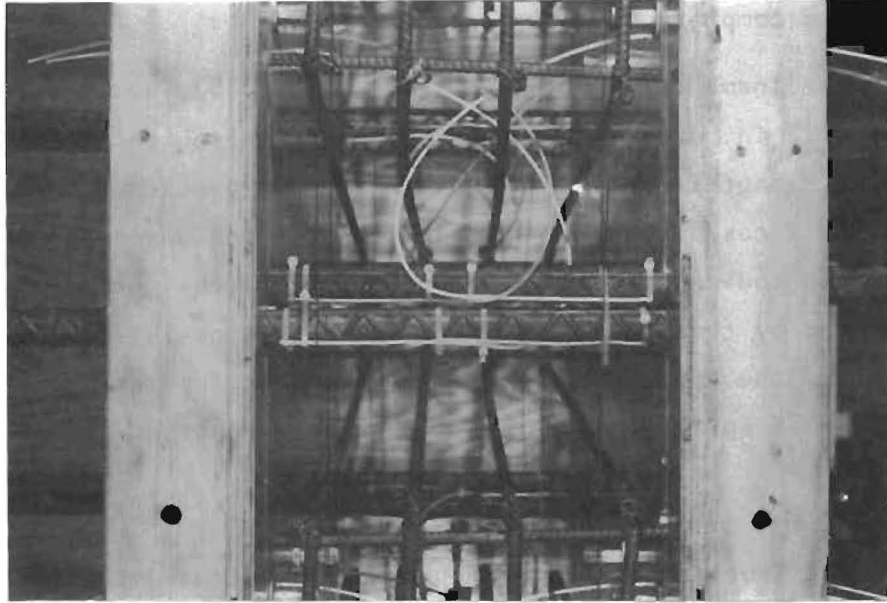


Fig. 4.8 Stacked splice on side of splice specimen

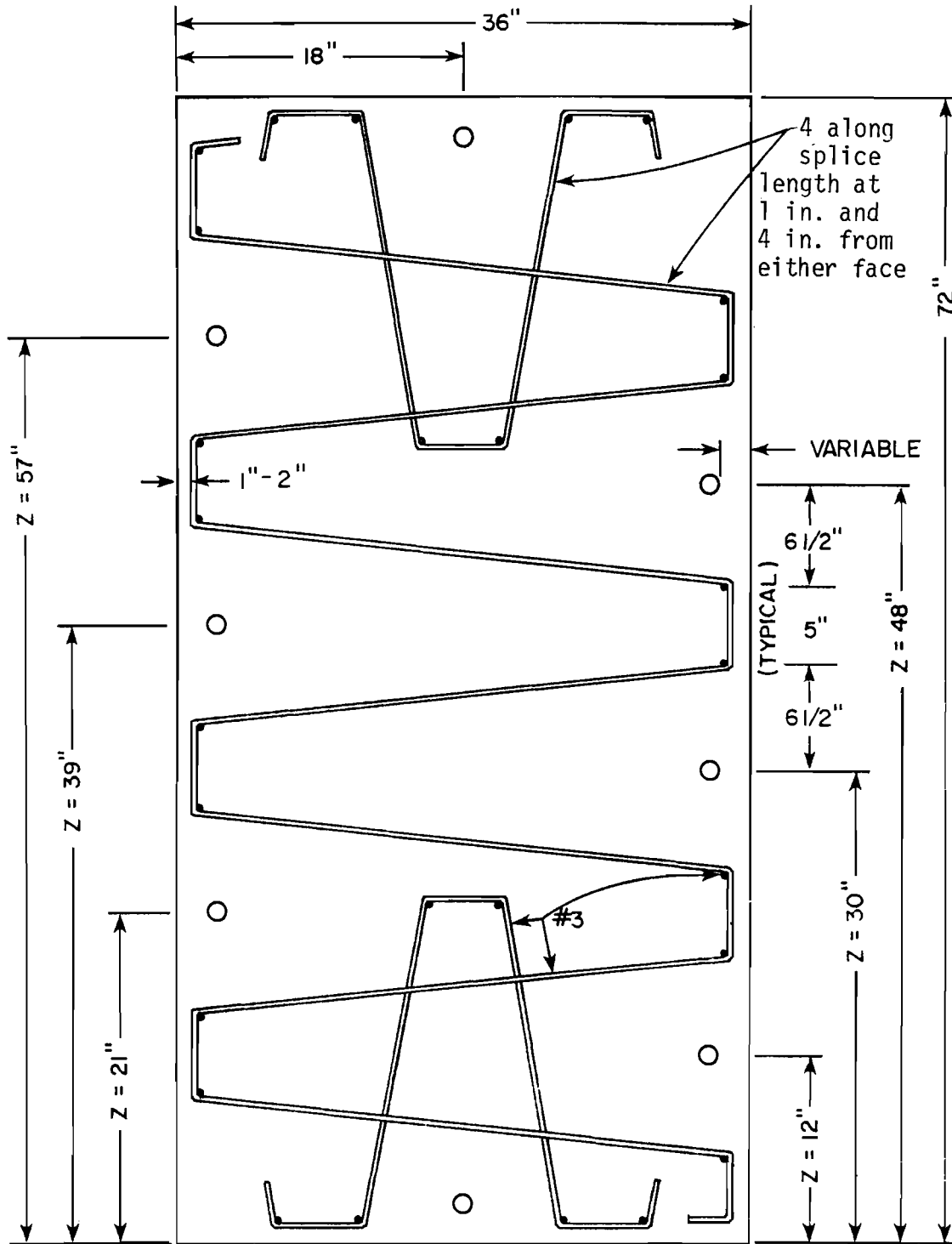


Fig. 4.9 Typical transverse reinforcement pattern for D Series specimens

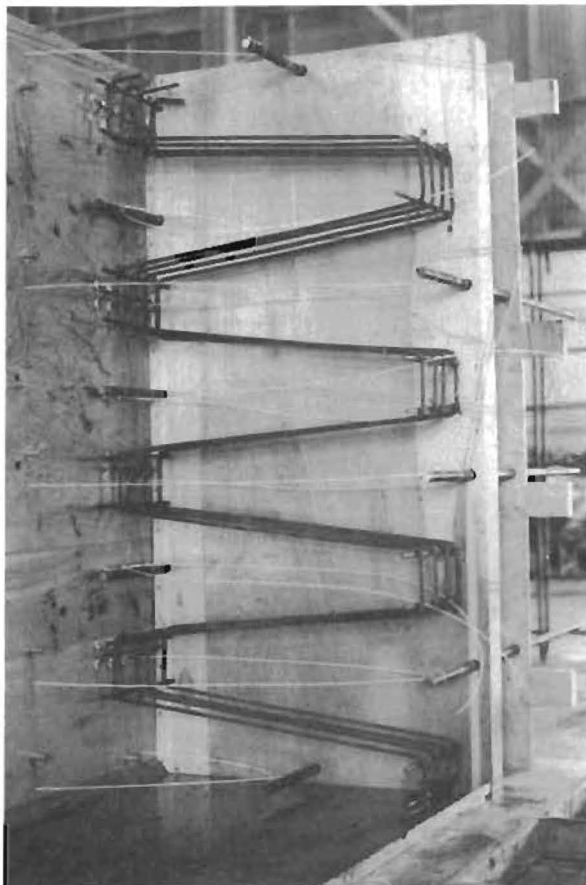
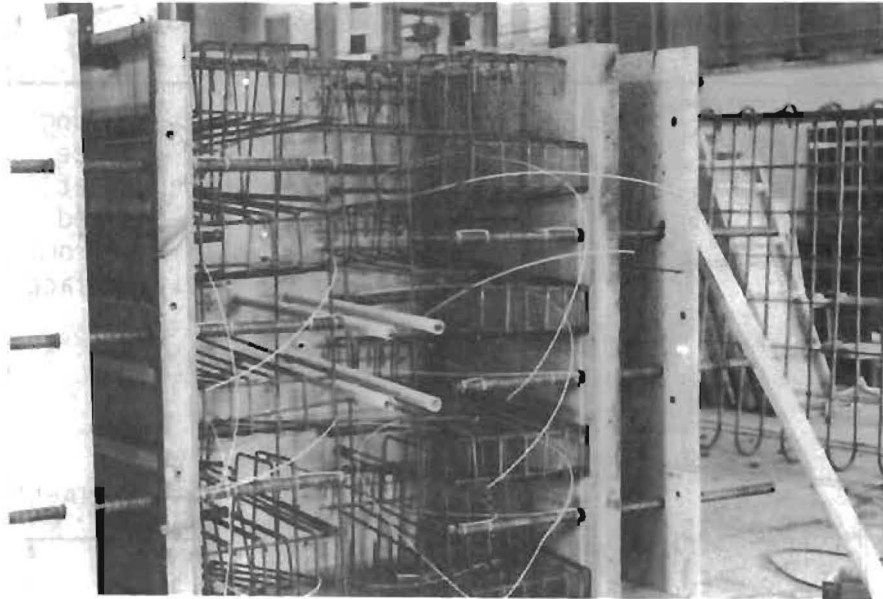


Fig. 4.10 Transverse reinforcement details--Specimens D1 and D3



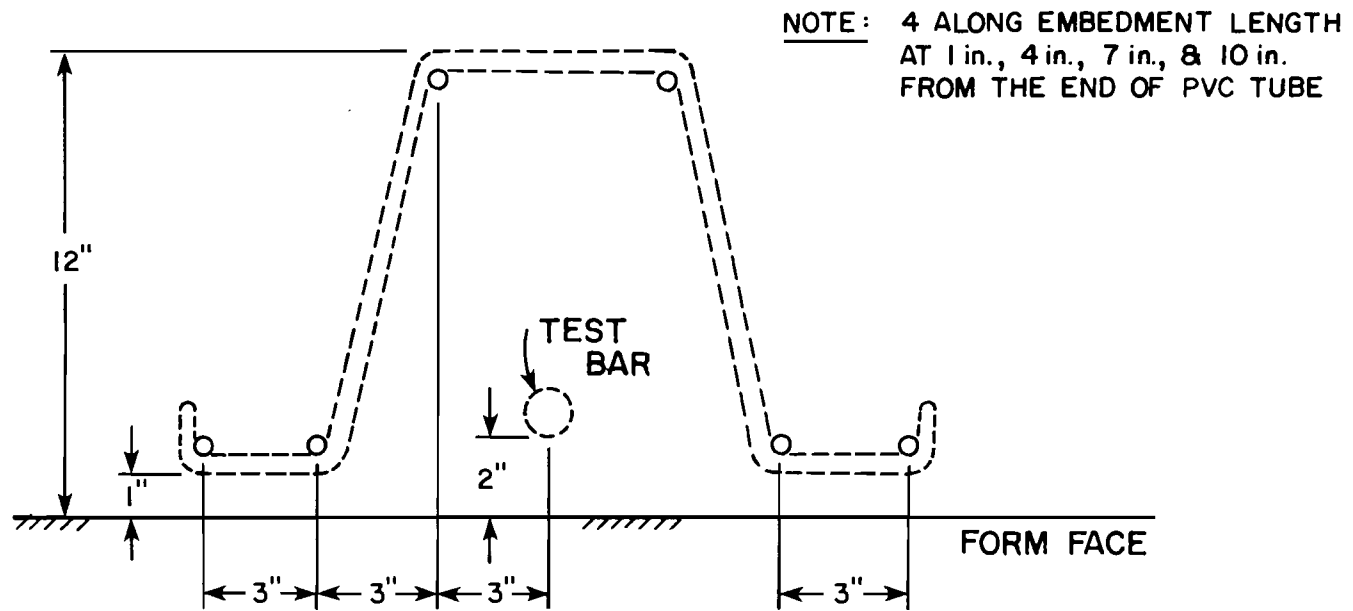


Fig. 4.12 Transverse reinforcement pattern for test bars in Specimen D4

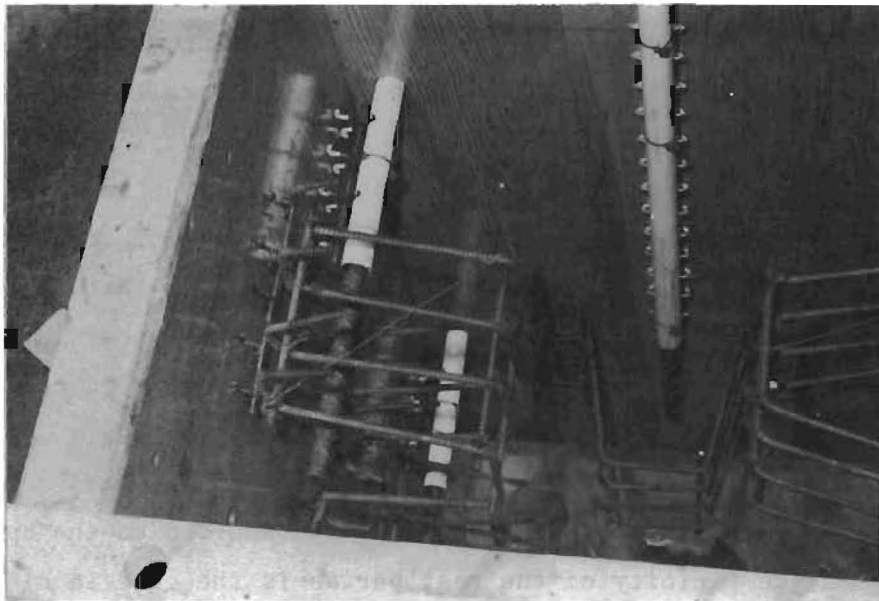


Fig. 4.13 Transverse reinforcement in place in horizontal/vertical test specimen

specimen faces represent large transverse flexural cracks which become points of high stress concentrations in actual members. The moment acting at the point of the flexural crack is introduced into the specimen by applying a tensile force to the protruding bar and a compressive force to the specimen face at some distance from the bar.

Because of the geometry of the specimens, two different types of reaction beams were necessary. Figures 4.14 and 4.15 show schematically the test setup for the bars positioned along the specimen sides, and Figs. 4.16 and 4.17 show the arrangement used for the bars placed at the middle top and middle bottom of the specimens. Overall views of both test frames are shown in Figs. 4.18 and 4.19. The basic method for applying loads to the specimen was the same in both cases. The test bar was passed through holes in the bearing plate and a center-hole 60-ton hydraulic ram. A wedge-grip assembly was then attached to the bar so that as the ram was extended between the bearing plate and the assembly a tensile force was applied to the bar. The compressive force was transferred to the specimen face from the bearing plate by means of a compression plate welded to the front of the bearing plate. The resulting force couple had a moment arm of 12 in. Note that no compressive force was applied to the specimen face in the immediate vicinity of the test bar as is the case in classical pullout tests. For uniform compression on the face of the test specimen, a layer of hydrostone was sometimes placed between the face of the specimen and the compression plate.

Figure 4.20 shows the assembly mounted in the test frame with wedges gripping the bar.

#### 4.8. Measurement of Slip

Slip of the anchored reinforcing bar relative to the concrete was measured to determine the performance of the bar during testing. The procedure used was originally developed by Minor [31].

A 0.059-in. diameter piano wire was attached to the anchored bar at selected locations by making a short 90° bend at the end of the wire and

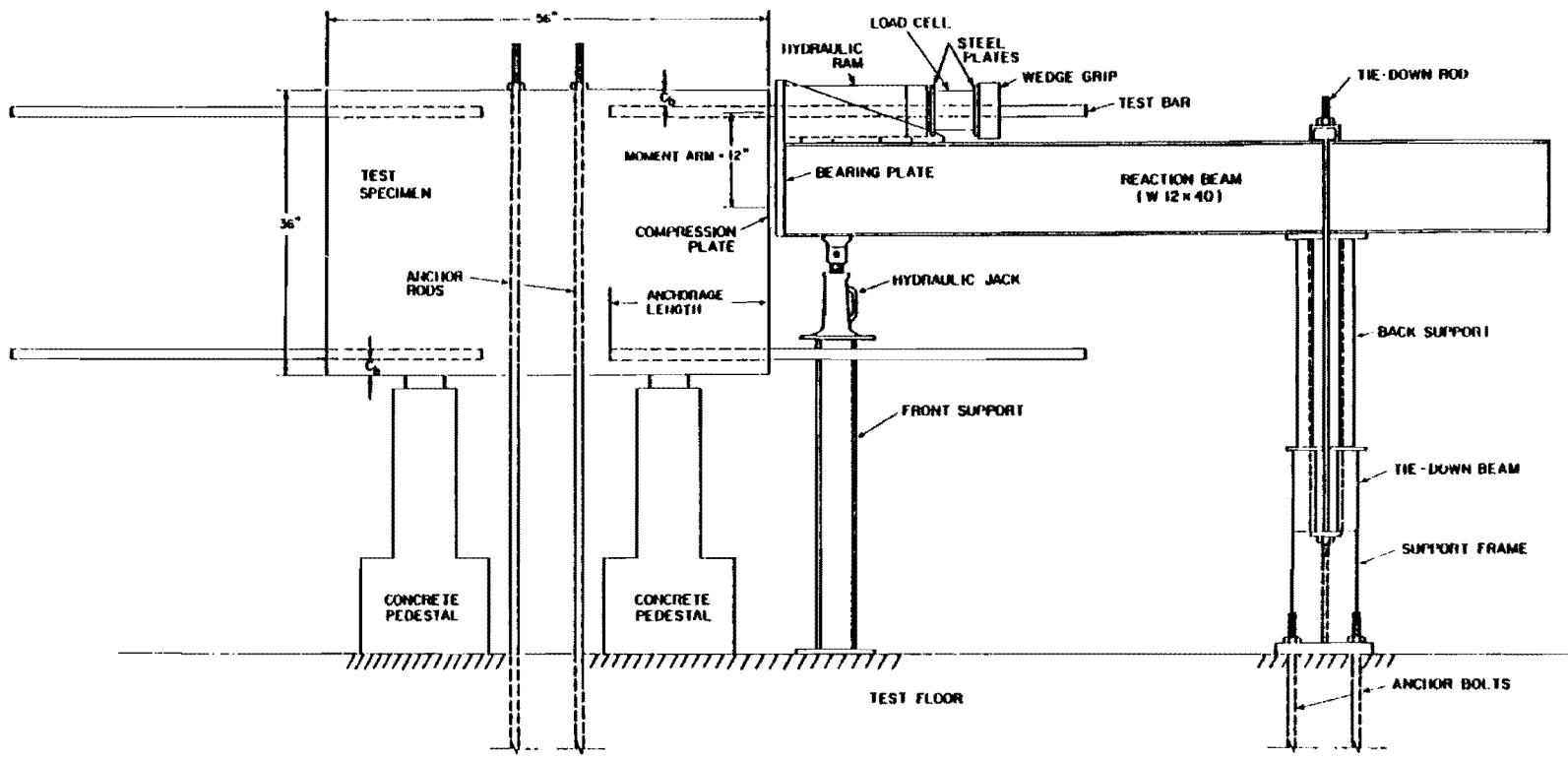


Fig. 4.14 Test frame A for side bars, side view

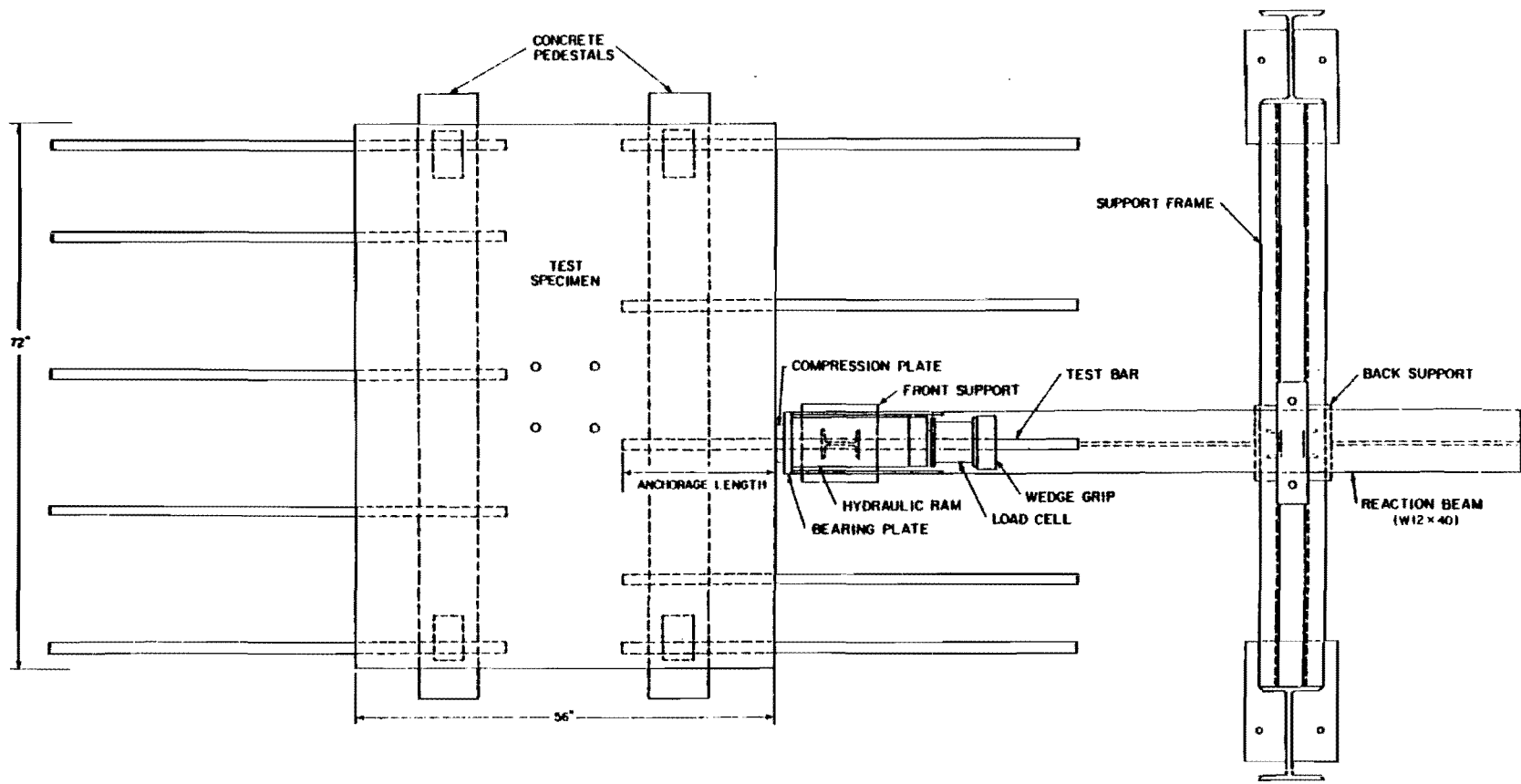


Fig. 4.15 Test frame A for side bars, top view

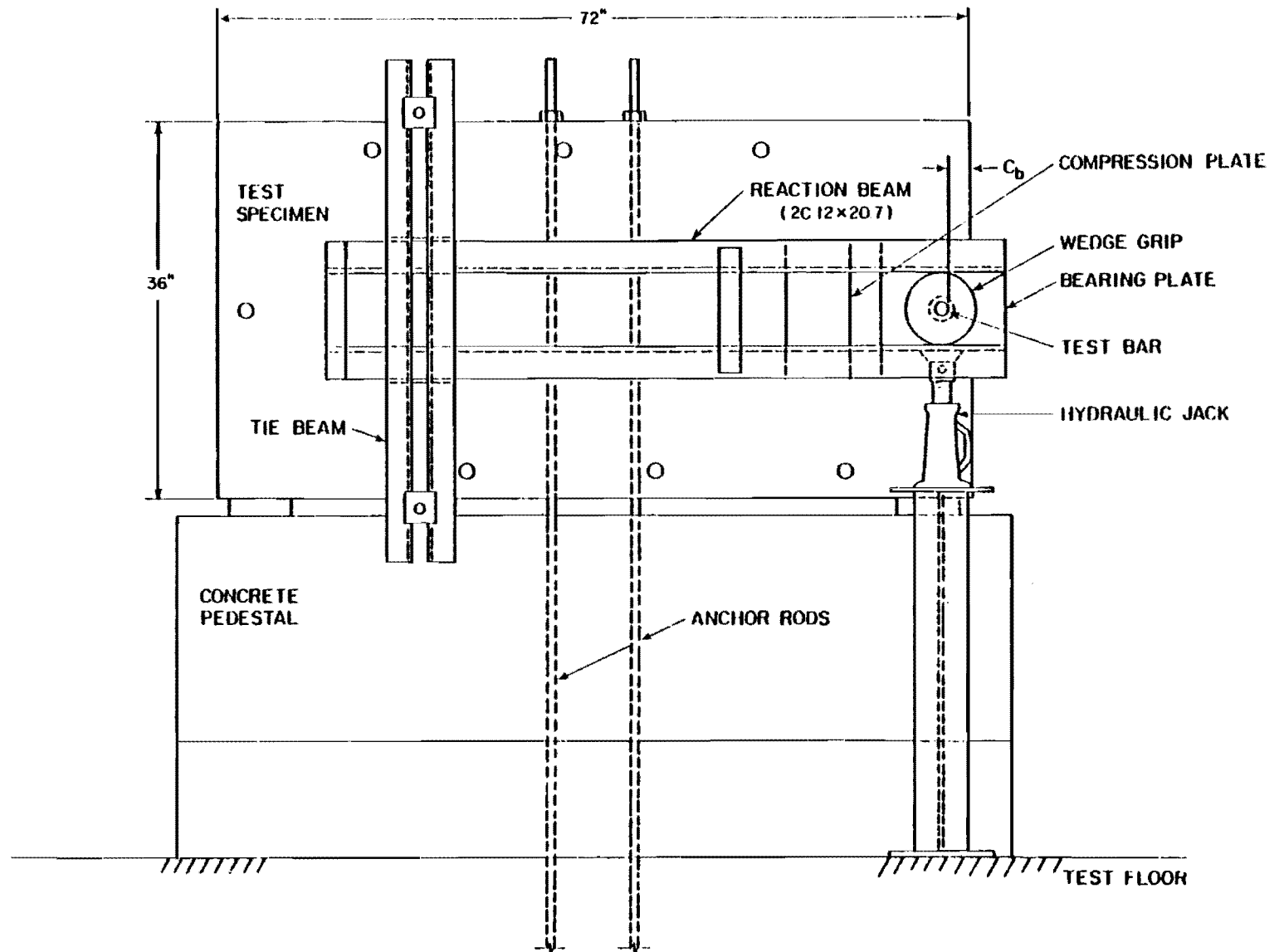


Fig. 4.16 Test frame B for middle top and bottom bars, elevation view

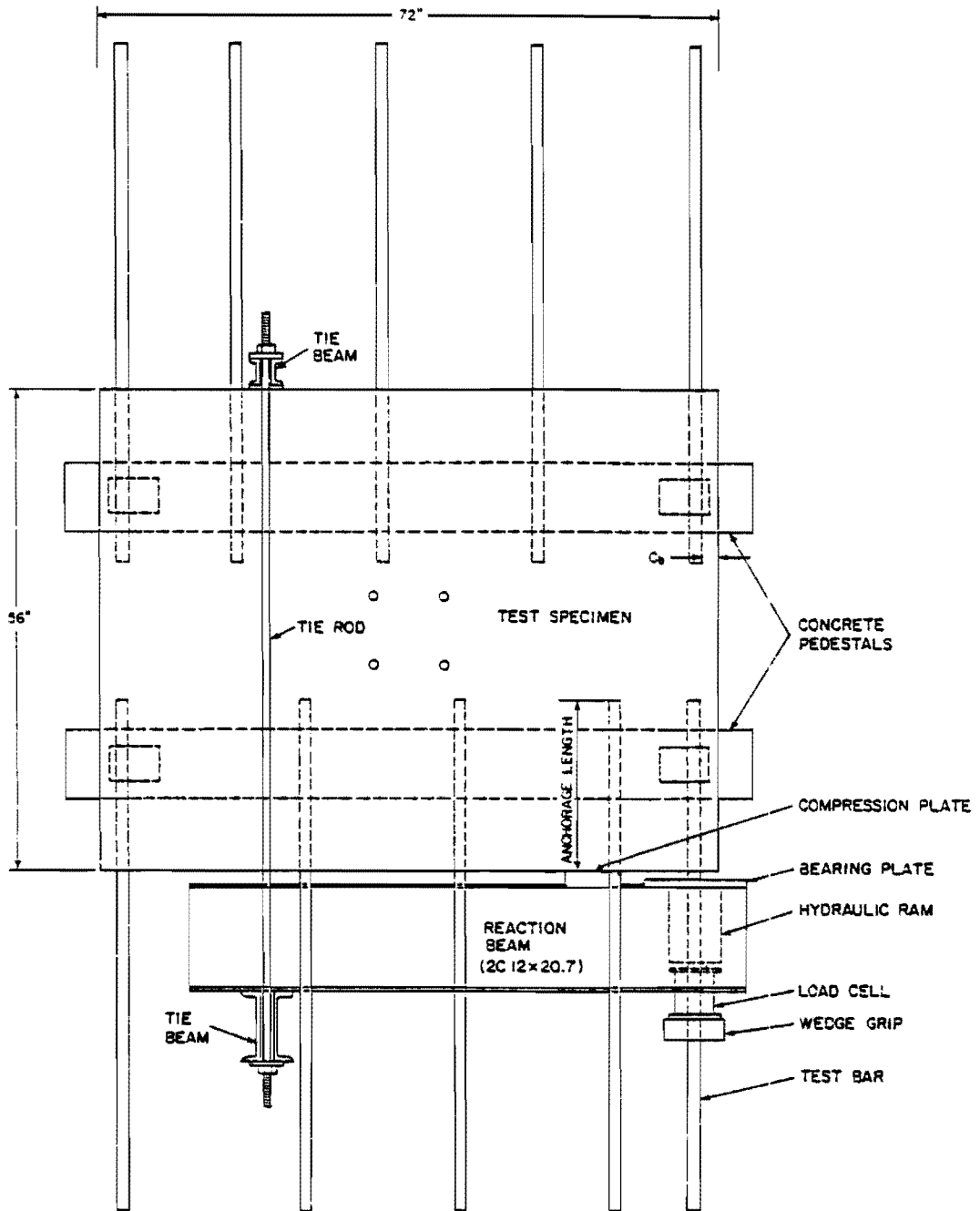


Fig. 4.17 Test frame B for middle top and bottom bars, top view

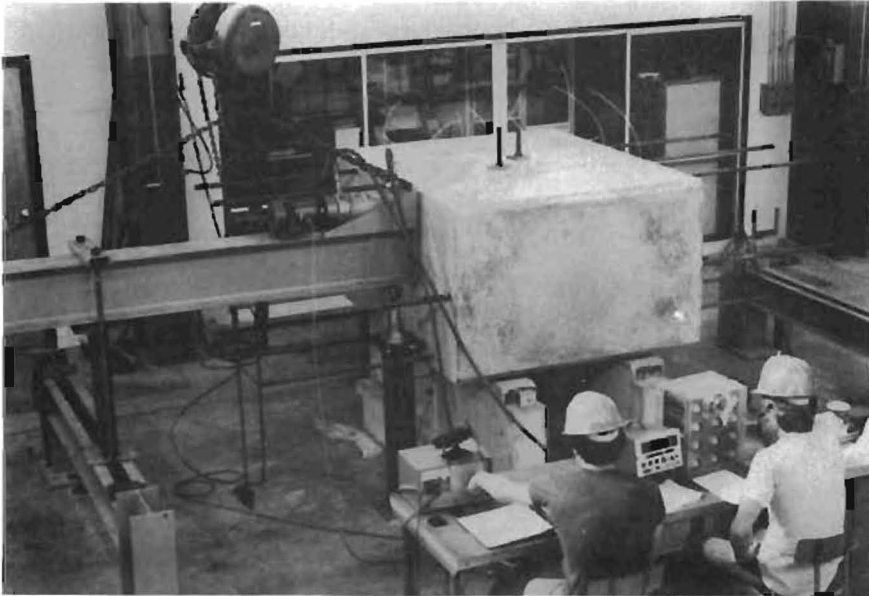


Fig. 4.18 Test frame A used to test the side bars

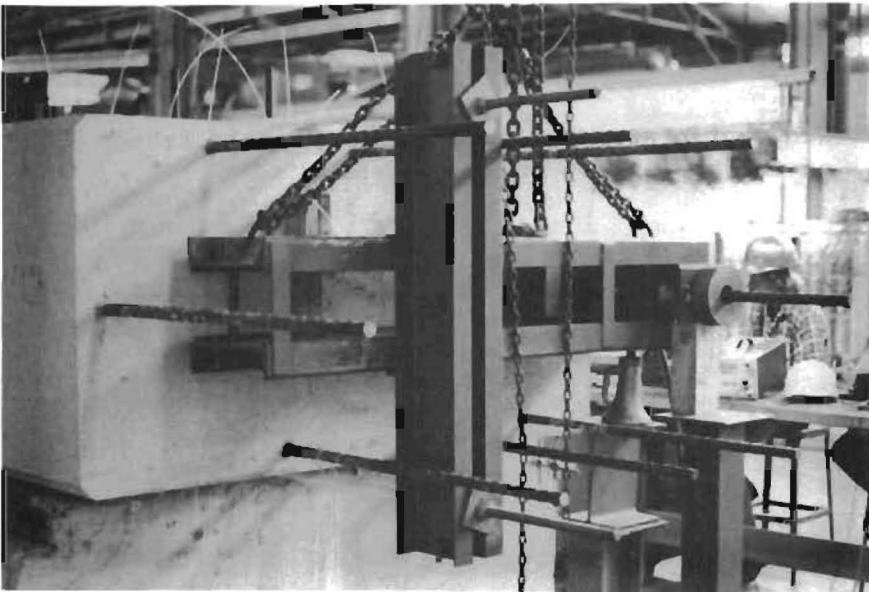


Fig. 4.19 Test frame B used to test the middle top and bottom bars

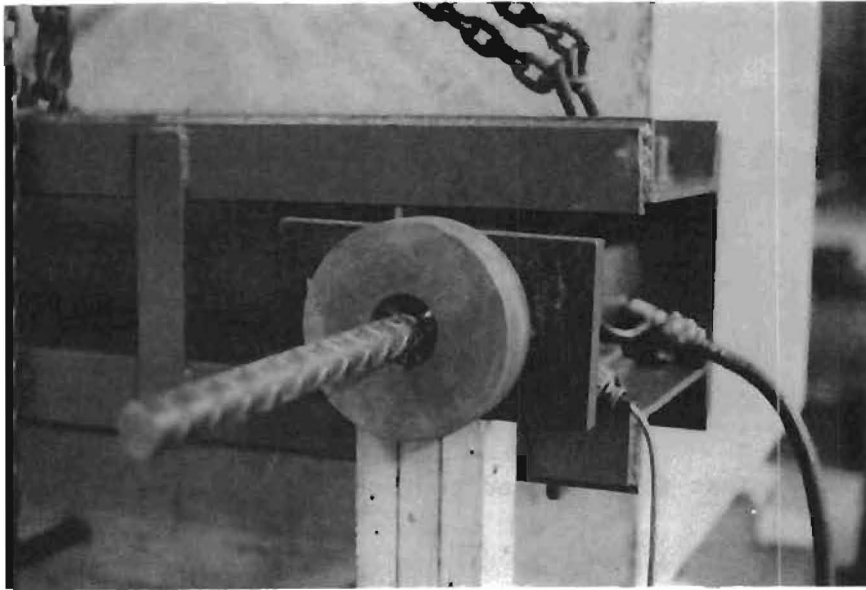


Fig. 4.20 Wedge grip assembly mounted in the test frame of the middle top and bottom bars

inserting it into a hole of equal diameter drilled in the anchored bar. The wire was oriented parallel to the bar axis in the expected direction of slip. As shown in Fig. 4.21 slip was measured at two points along the bar representing the loaded end and free end positions. After the wire was placed in the bar, a plastic tube was placed over the entire length of the wire to prevent bonding and to allow free movement of the piano wire. The plastic tube was sealed at the bar to prevent cement from entering the tube. The amount of sealer was small and the loss of bond surface area was kept to a minimum.

It was necessary to ensure that slip was measured relative to a stable reference point. The slip wires extended from the anchored bars to the specimen faces. Figure 4.22 shows a middle top bar in place in the form prior to casting with the slip wires extending to the specimen face.

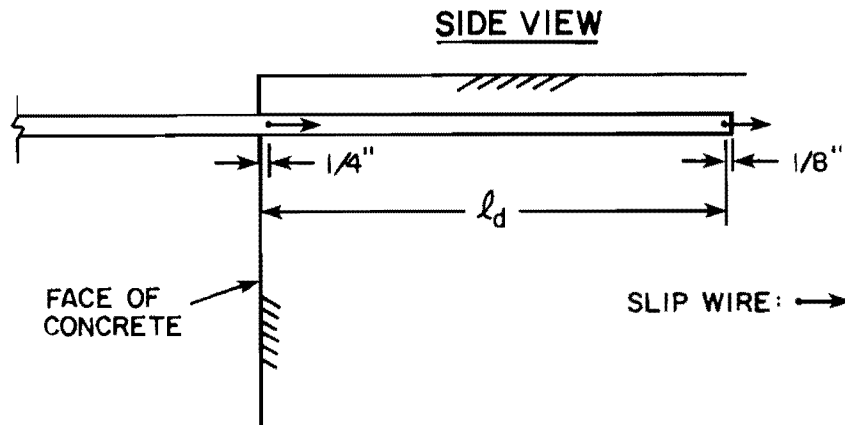


Fig. 4.21 Location of slip wires

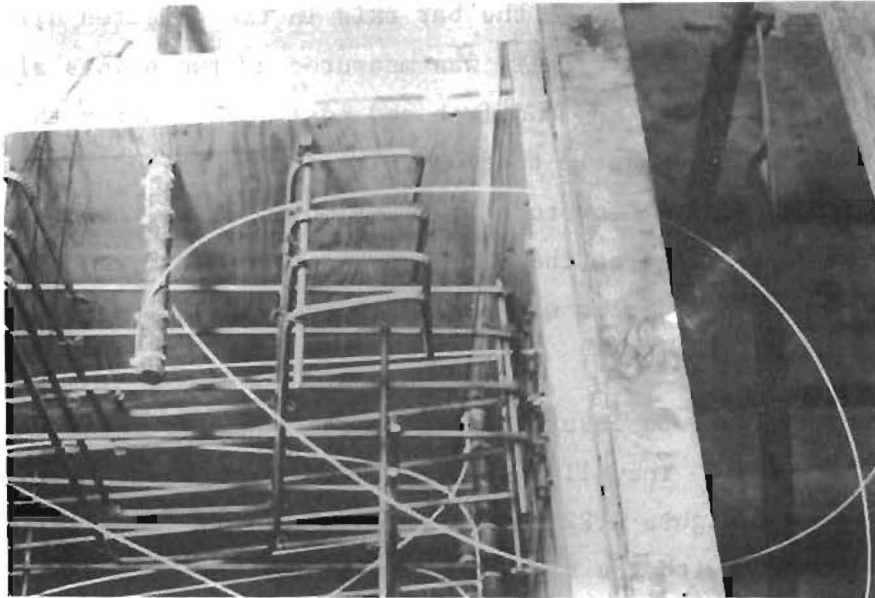


Fig. 4.22 Slip wires extending from a middle top bar to the specimen face

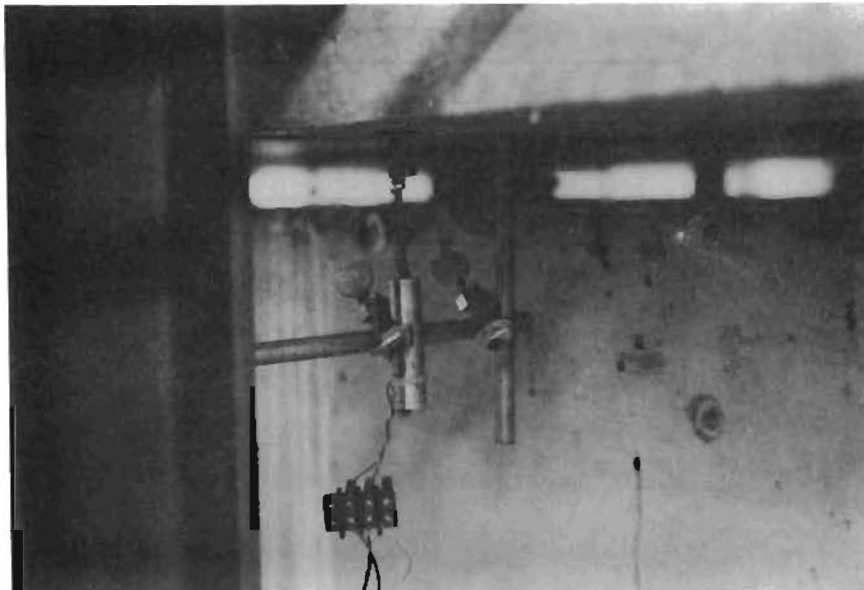


Fig. 4.23 Slip potentiometer mounting

To reduce the wobble of the slip wire in the plastic tube, the wire was placed in tension using a spring between the concrete surface and a small brass plug fastened to the wire with a set-screw. A plunger-type precision potentiometer was used to measure movement of the wire and was mounted on the side of the specimen as shown in Fig. 4.23. The plunger of the potentiometer rested against the brass plug at the end of the slip wire. The resulting change in resistance in the potentiometer was measured by a digital voltmeter. A constant voltage was maintained across the potentiometers which allowed the changes in resistance to be converted into deformations. Slip was measured to 0.0001 in.

Considerable variation between test bars was found for the load required to produce initial loaded end slip. The reasons for the variation were slight differences in the distance from the anchorage point of the slip wire to the specimen face and the differences in resistance to slip, due to friction, of the slip wire inside the PVC tubing. The method used to correct for these differences is shown in Fig. 4.24. The initial straight line portion of the load-slip curve was extended until it crossed the slip axis at point A, thus defining the segment AO ( $\Delta$ ). The load-slip curve was then shifted to the right a distance  $\Delta$  so that it originated at point O.

#### 4.9 Test Procedure

Specimens D1-D3 and S1, S2 were cast in a vertical position and were tested in a horizontal position. By means of lifting inserts in the side faces, the specimen was lowered from the vertical position to the horizontal position. The specimen was placed in the test position for testing the top layer of side bars and the middle top and bottom bars on both end faces of the specimen. The specimen was turned over by means of the lifting inserts to test the other layer of side bars. Specimen D4 required additional rotations to permit testing of all bars.

The first step in placing the specimen in the test frame was to set the specimen on two concrete pedestals each with two 1-1/2 in. thick,

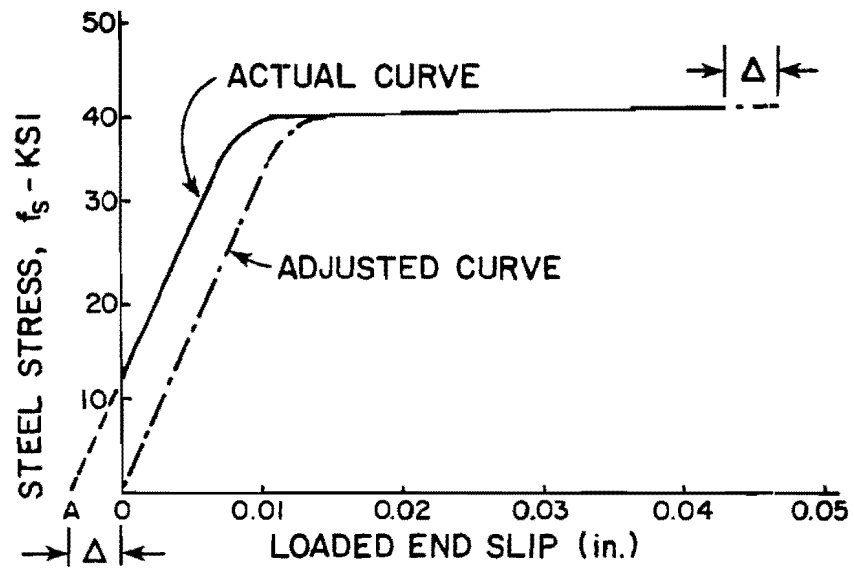


Fig. 4.24 Slip correction method

4 in. x 6 in. steel plates placed on top to allow enough spacing below the specimen for the bottom tie bolt in test frame B (see Figs. 4.16 and 4.17). The specimen was bolted down to the test floor by means of two long anchor rods into the laboratory test floor. The reaction beam was placed over the bar being tested and in both test frames A and B, the hydraulic ram was placed on the reaction beam and centered on the test bar. For the splice tests, two reaction beams were necessary for each test, one for the bar on each face. By connecting both rams (which had the same ram area) to the same pump by means of a T-connection in the hydraulic fluid lines, the same load was applied to each bar.

The test procedure, with the exception of the load increment, was the same for all specimens. Larger load increments were applied with large bars and in the initial load stages (up to about half of ultimate capacity) in all tests. The load was applied by a 60 ton hydraulic ram. The level of the load was measured by an electronic 10000 psi pressure transducer. The load level was also checked at the ram by a 100-kip capacity calibrated load cell. In addition, hydraulic hose pressure was measured at the pump by a calibrated 10000 psi pressure gage. A test was terminated when the anchored bar would not carry additional load or would only maintain a reduced level of load with continued extension of the rams. Normally, loading was halted to avoid causing unnecessary damage to the specimen which might interfere with subsequent tests on the same specimen.

In the T and D series, the load was increased every 90 seconds. After the first 30 seconds, during which a load increment was added, slip potentiometers were read. Immediately prior to applying the next load increment, 60 seconds later, the load cell and pressure transducer were read again to allow an evaluation of the degree of relaxation of the test specimen and the loading system during the load stage. The slip values were read again to detect any change in slip of the bar under the same stress. Because four slip measurements were necessary for each load stage for the splice tests, 2-minute intervals were used between load increments with the final readings being taken with 30 seconds remaining in the interval.

This page replaces an intentionally blank page in the original.

-- CTR Library Digitization Team

## C H A P T E R 5

### BEHAVIOR--DEVELOPMENT TESTS

#### 5.1 Introduction

In this chapter, results from Specimens D1-D4 in which all bars failed in a similar mode are analyzed. The primary variable was the casting position. In Specimens D1-D3, eight bars were embedded on either side. All eight bars had the same anchorage length, bar diameter, and clear cover. The only variation was in casting position. Specimen D1 had #11 bars on both sides with a 20-in. embedment length and 2-in. clear cover (refer to Fig. 4.9). Specimen D2 had #7 bars on one side with a 12-in. embedment length and a 1-in. clear cover and #9 bars on the other side with a 12-in. embedment length and 2-in. clear cover. Specimen D3 was identical to D2 except that the concrete slump was increased from 3 to 8-1/2 in. Specimen D4 had both vertical and horizontal bars. The cover was 2 in. and all bars were #9 (see Fig. 4.2).

#### 5.2 Variation of Concrete Strength

Type III cement was used in the mix design of Specimens D1 and D2 and Type I for all others. During the week of testing required to complete all the bars in a specimen, the concrete compression strength increased slightly. The difference between the concrete strengths on the first day and the last day of testing was less than 400 psi. For comparative purposes, the curves showing steel stress versus loaded end slip were adjusted to the equivalent of 3000 psi concrete. To make the adjustment, it was assumed that the bond strength varied as the square root of  $f'_c$ . For a measured slip the corresponding steel stress was multiplied by  $\sqrt{(3000/f'_c)}$ . A similar adjustment has been made in many previous bond projects [17,19]. The assumption was based on the close relationship between tension and bond stresses and the fact that tension stresses are generally proportional to the square root of the concrete compression strength. The concrete strengths are given in Appendix B.

### 5.3 General Characteristics of Behavior

In almost all tests, the loaded end slip started at an early stage of loading. In some tests it started immediately upon initial loading and progressed with increasing increments of loading, while in others there was a problem of slip wires sticking on initial loading and delaying detection of loaded end slip. The curves were corrected as shown in Fig. 4.24. Bond splitting started over the bar at the loaded end and progressed toward the unloaded free end. Normally the cracks gradually progressed over the entire length before failure, with the ultimate strength being developed about the time the splitting crack reached the free end.

In terms of free end slip, the higher cast bars behaved differently from the lower cast bars. Free end slip of most of the lower cast bars did not usually occur until splitting became prominent near the loaded end and the bar was close to ultimate. With the higher cast bars, free end slip was generally measured before cracking at the loaded end had progressed far. It is likely that the voids under the higher cast bars permitted the bar to slip over the full length without much, if any, splitting of the concrete. The higher cast bars consistently carried much higher loads after the initial free end slip was observed and before failure took place.

The variation of steel stress with loaded end slip was plotted for all bars. Figure 5.1 shows steel stress-slip relationships for #7 bars at two casting positions. The curves are typical examples of the relationship between loaded end and free end slip of bars at different casting positions. The curves illustrate the difficulty in correlating the free end to loaded end slip. The free end slip is relatively small. Consequently, plots of the free end slip are not presented. Many previous investigators have also concluded that the slip at the free or unloaded end of the bar is meaningless. In many cases the first occurrence of slip at the free end coincides with severe bond deterioration and the bar is no longer effective in stress transfer. The test data from this study show that in some cases, especially for the bars at lower heights in the specimen, free end slip did not occur until the bar was close to failure.

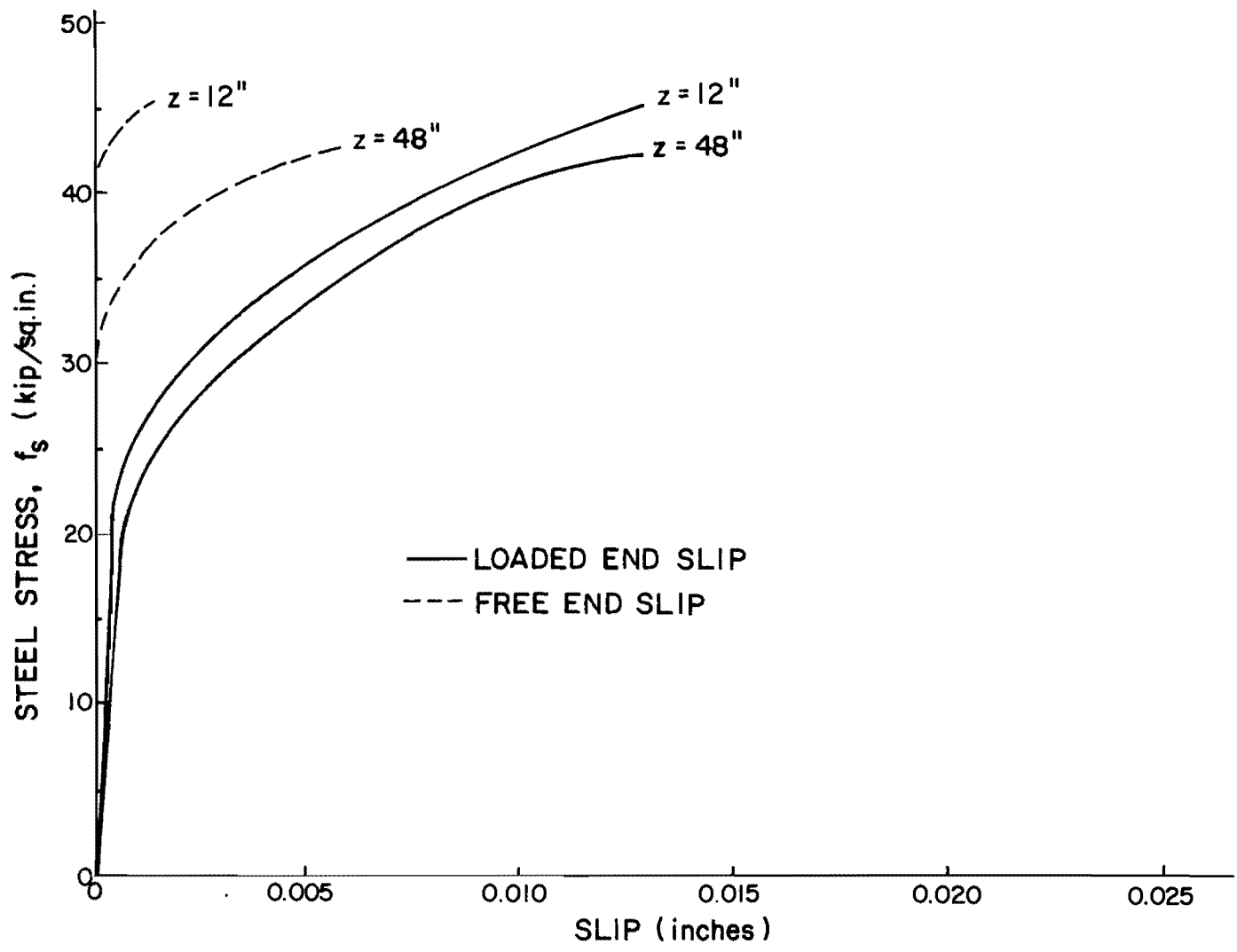


Fig. 5.1 Comparison of stress-slip curves at the loaded end and the free end of #7 bars in Specimen D2

5.3.1 Specimens D1 and D2. When testing the bars, the loading was normally halted when splitting spread over the entire concrete cover along the anchorage length of the reinforcing test bar. The type of failure which describes the crack pattern of these bars is the V-notch failure which was shown schematically in Fig. A.1. Figure 5.2 illustrates the V-notch failure for the side bars in Specimens D1 and D2. The transverse #3 reinforcement prevented cracking from spreading into the zone of adjacent bars. Figure 5.3 shows that the crack interaction between adjacent test bars was limited on the side of the concrete specimen and along the development length of the bars on the face of the specimen. One #7 bar at  $z = 12$  in. failed without splitting the adjacent corner as illustrated in Fig. 5.4. The supplementary transverse #3 reinforcement did not prevent other bars at  $z = 12$  in. from splitting the adjacent corner as shown in Fig. 5.5. splitting of the corner occurred although the number of transverse #3 bars along the embedment length of the anchored bars was increased in Specimens D1 and D2 from that used in Specimens T1, T2, and T3, to attempt to control the cracking pattern of the bar at  $z = 12$  in.

The increase of the specimen width from 21 in., as in the trial specimens, to 36 in. succeeded in forcing a V-notch type of failure for the middle top and bottom bars (see Fig. 5.6) and permitted comparisons between bars on the basis of a common type of crack pattern and mode of failure.

5.3.2 Specimen D3 (High Slump Concrete). The specimen cast using concrete with an extremely high slump contained eight #9 bars with 2 in. cover and eight #7 bars with 1 in. clear cover. The specimen was identical to D2 except that D2 was constructed with concrete having a 3 in. slump, while in Specimen D3 the concrete had an 8-1/2 in. slump.

The effect of a high slump concrete in a very deep beam became apparent even before actual testing began. Excessive concrete shrinkage or settlement due to the high slump was restrained by the test bars and tension cracks formed in the vicinity of the middle top bars in patterns identical to crack patterns resulting from loading. Figures 5.7 and 5.8

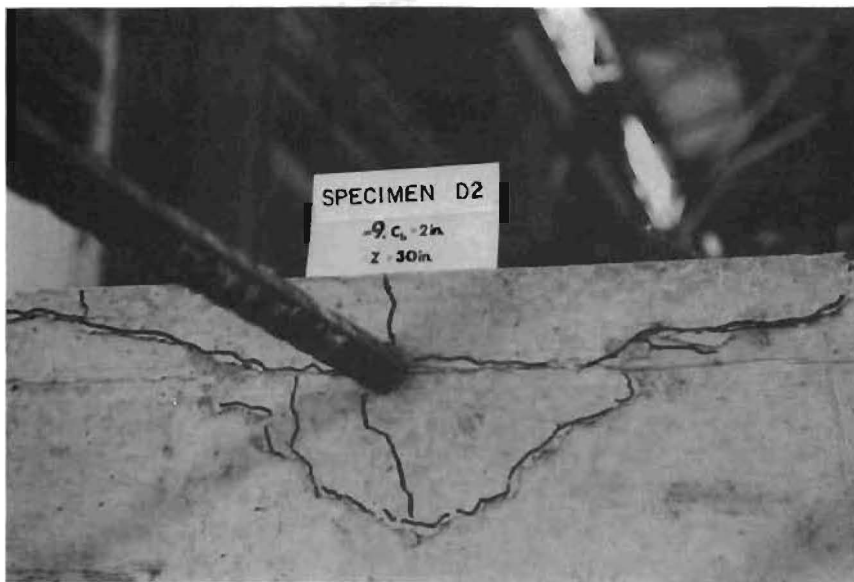
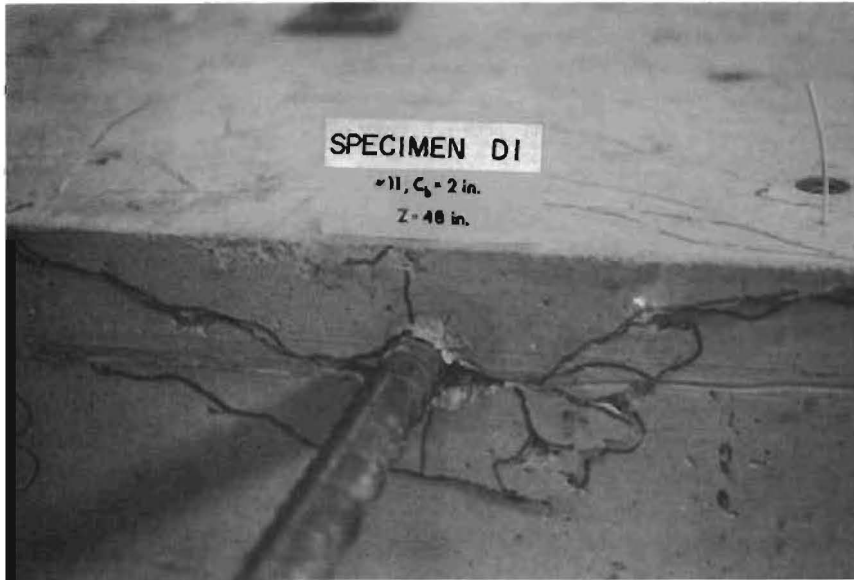
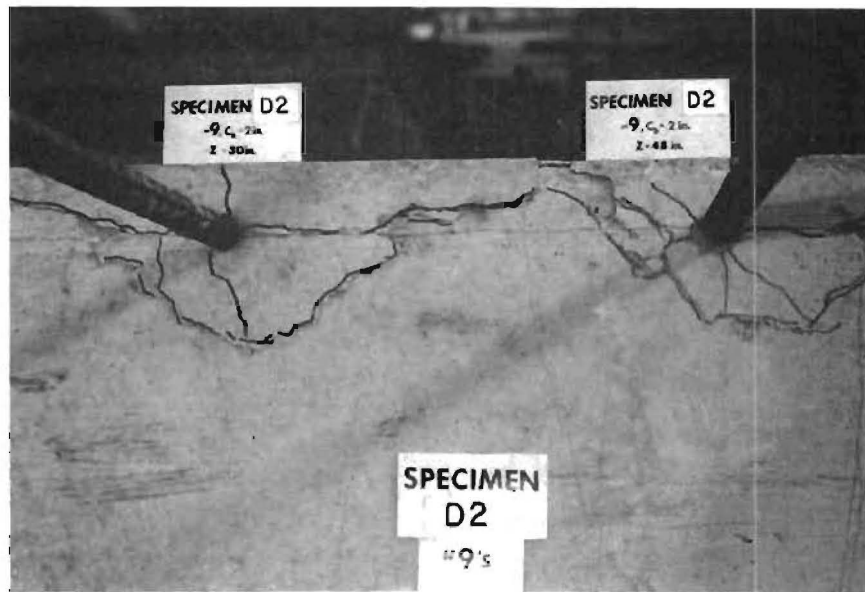
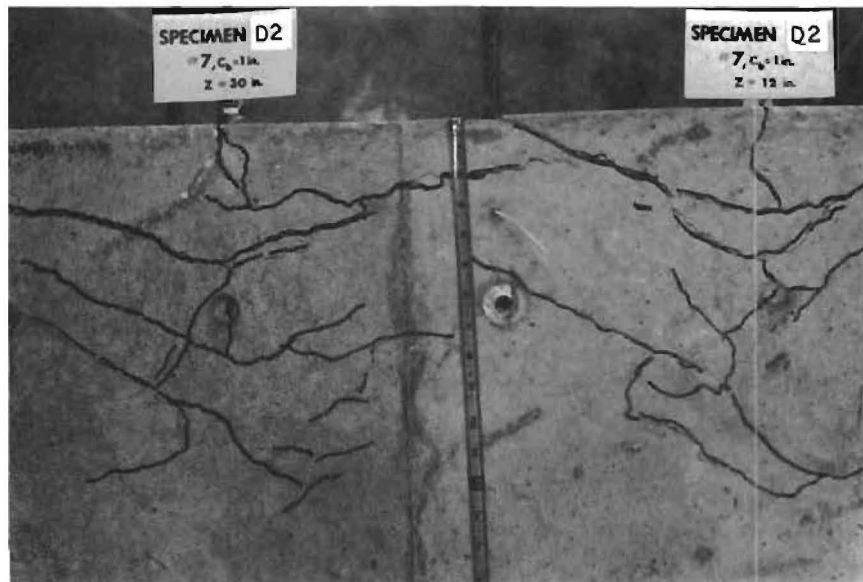


Fig. 5.2 V-notch splitting mode of failure of side bars of test Specimens D1 and D2



(a) Side view



(b) Top view

Fig. 5.3 Interaction of the crack patterns of adjacent side bars in test Specimen D2

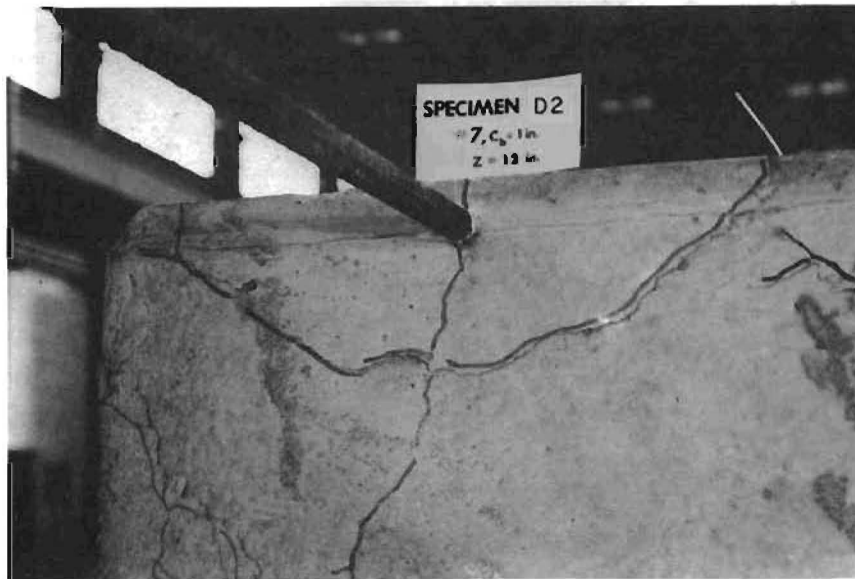


Fig. 5.4 V-notch splitting mode of failure of the #7 bar at  $z = 12$  in. in test Specimen D2

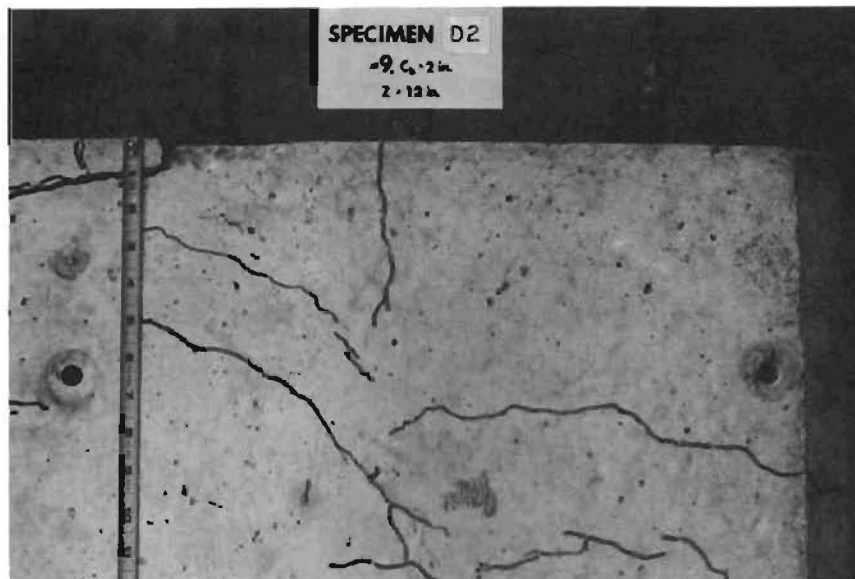
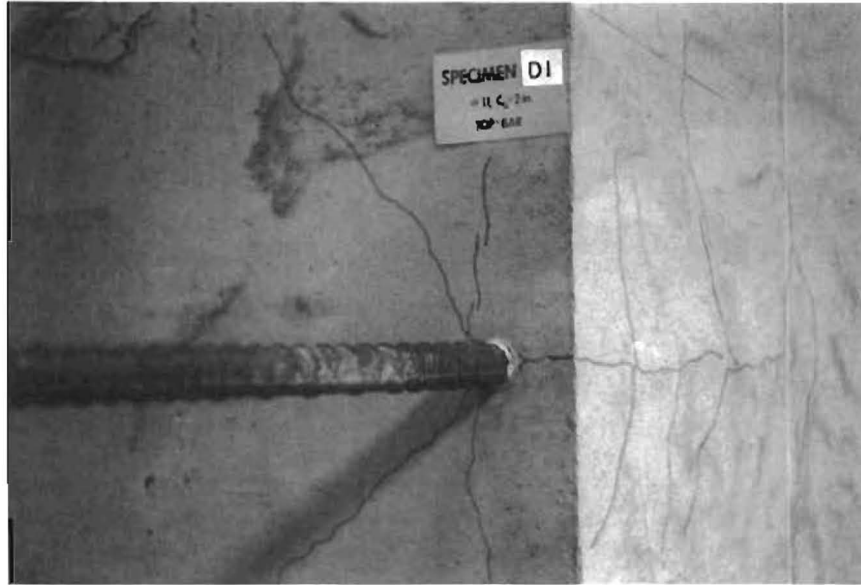
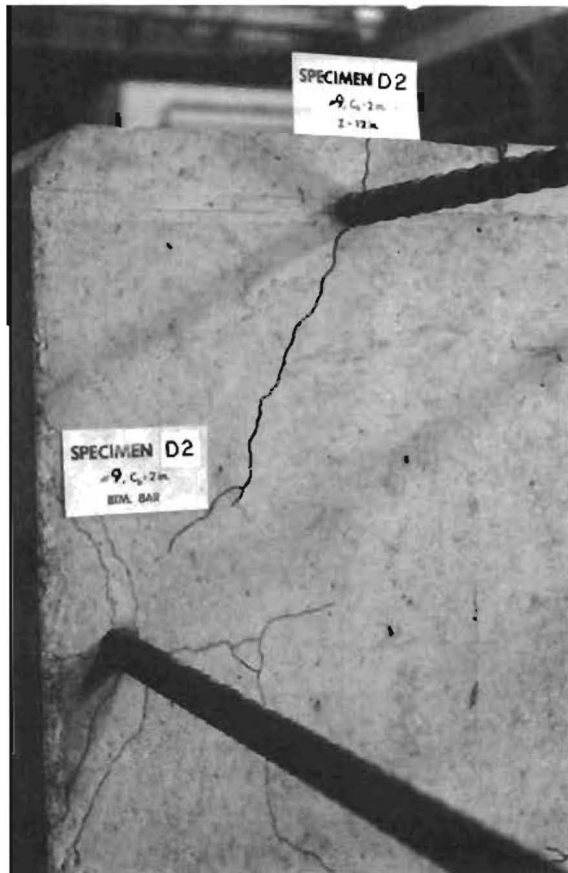


Fig. 5.5 Corner-splitting mode of failure of the #9 bar at  $z = 12$  in. in test Specimen D2



(a) Specimen D1



(b) Specimen D2

Fig. 5.6 Typical crack pattern of the middle top and bottom bars

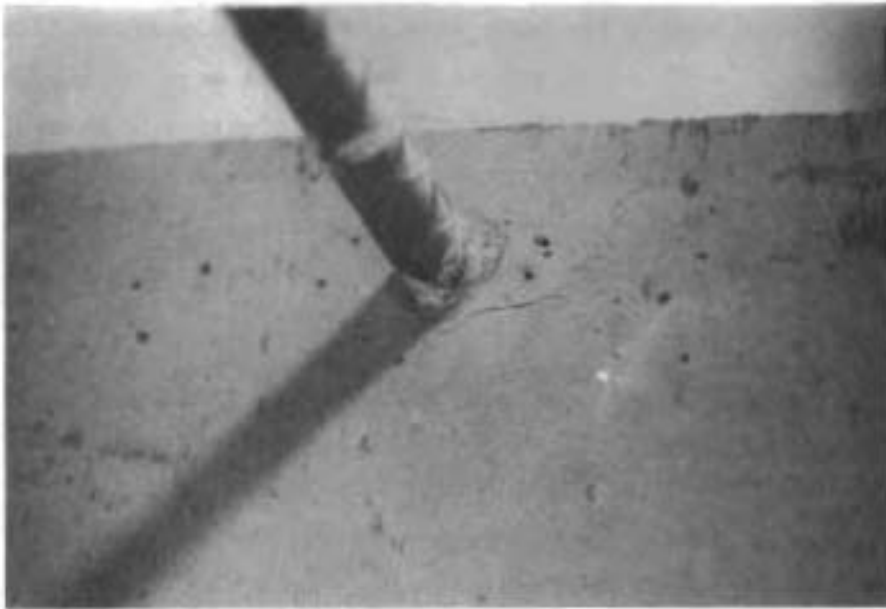


Fig. 5.7 Shrinkage cracks formed around top middle #9 bars on face of high slump specimen

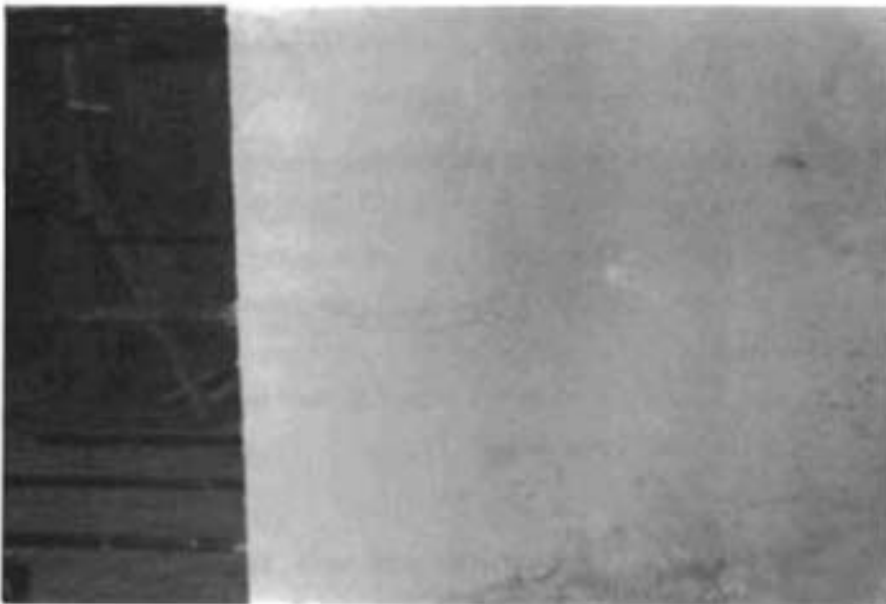


Fig. 5.8 Longitudinal shrinkage cracks formed along cover of top middle #7 bar in high slump specimen

show these cracks before the bars were tested. Only top middle bars exhibited shrinkage or settlement cracks. When loads were applied, the shrinkage cracks opened wider and the bars failed at very low loads. Although some new face cracks and transverse cracks appeared in the cover, no new axial cracks developed under the applied loading. Figure 5.9 shows the longitudinal cover cracking around the middle top bars following completion of the test.

5.3.3 Specimen D4 (Horizontal/Vertical Bars). This series of tests was designed to compare the behavior and capacity between vertical and horizontal bars. The specimen details were shown in Fig. 4.2. At two different heights in the specimen,  $z = 18$  in. and  $z = 48$  in., two test bars were positioned for each of the following cases:

- (1) horizontal
- (2) vertical, pulled in the direction of concrete settlement, and
- (3) vertical, pulled in the direction opposite to that of concrete settlement.

Figure 5.10 shows the top of the specimen formwork with the bars in position before the reinforcing cages were placed around the bars.

The cracking patterns are shown in Figs. 5.11 and 5.12. The straight line represents the effective embedment length of the test bars while the arrow at the end of the line indicates the direction of loading. The number next to the bar is the ultimate load capacity of that bar. The values of load with arrows at the edges of the specimen represent the ultimate load capacity and the direction of loading of the bars in the middle of the 36 in. wide side of the specimen. Figure 5.13 shows the cracking pattern of one of these bars.

The cracking patterns at failure were fairly similar for all bars. The only cracks visible were the longitudinal cracks along the axis of the bars. Some of the bars developed longitudinal cracks at some distance from the axis of the bar and also some transverse cracks. Though the failures were sometimes sudden, they were never explosive and the cover never completely separated from the bar.

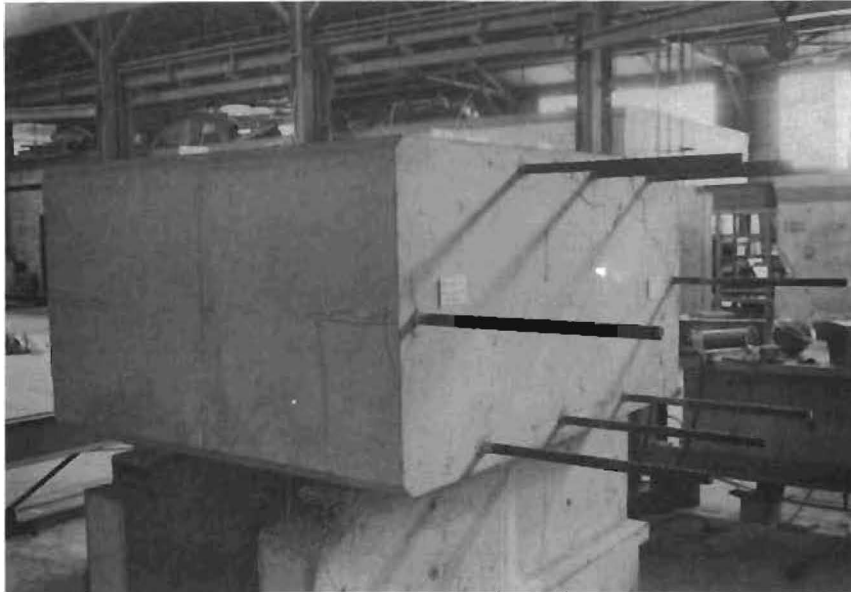


Fig. 5.9 Crack patterns after testing of top middle #9 (on right) and #7 bars of high slump specimen

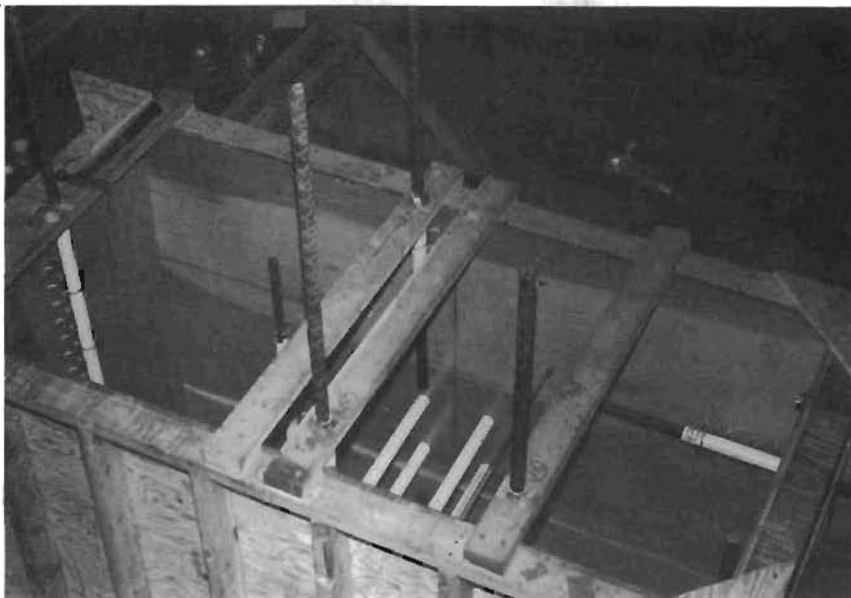


Fig. 5.10 Position of test bars in formwork of horizontal/vertical specimen

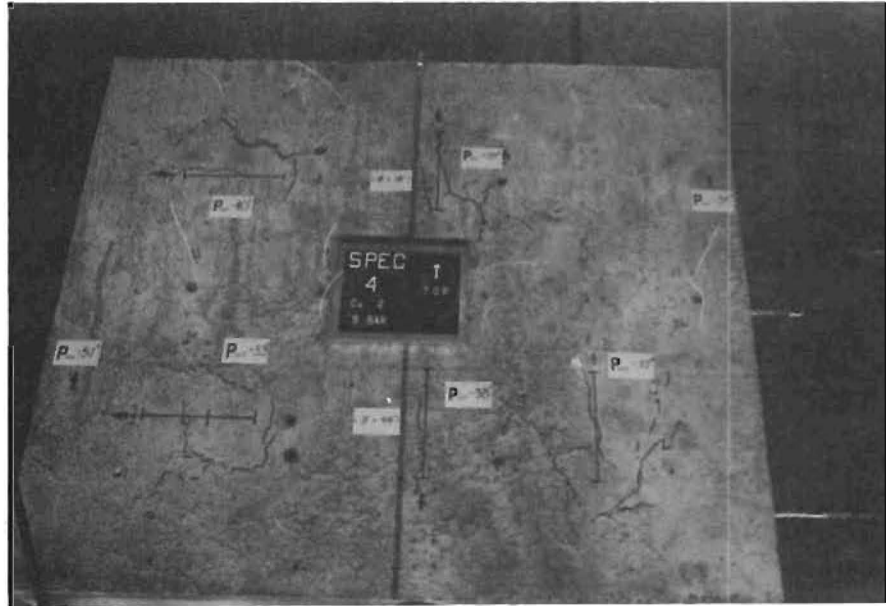


Fig. 5.11 Crack patterns of test bars of horizontal/vertical specimen



Fig. 5.12 Crack patterns of test bars of horizontal/vertical specimen

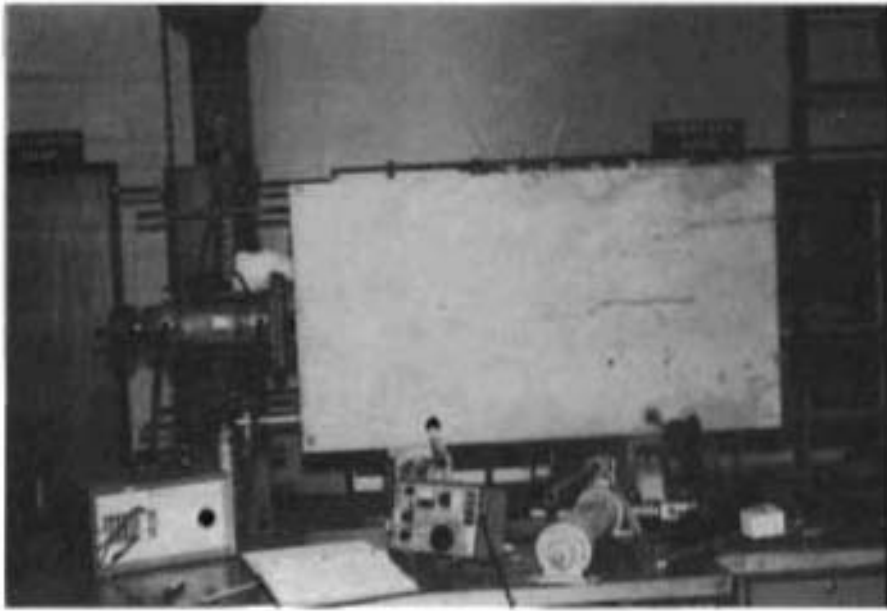


Fig. 5.13 Crack pattern of test bar along the end of horizontal/vertical specimen

#### 5.4 Effect of Casting Position

The stress-slip curves for bars of Specimens D1 and D2 are shown in Figs. 5.14-5.17. The bar stress in the stress-slip curves has been adjusted to 3000 psi concrete strength (Section 5.2). The initial slopes of the stress-slip curves of bars at various casting positions on a given side of a test specimen are quite similar, especially for #7 and #9 bars. Tables 5.1 and 5.2 list the ultimate steel stresses for specimens D1 and D2. Bond efficiency ratios, relative to the adjusted ultimate stress of the middle bottom bar, are listed for the different casting positions on a given side of a test specimen. Similar bond efficiency ratios were calculated for stresses at 0.01-in. loaded end slip for specimens D1 and D2. Table 5.3 summarizes bond efficiency ratios at ultimate and at 0.01-in. loaded end slip. The data in Table 5.3 are plotted in Fig. 5.18. Table 5.3 and Fig. 5.18 show a drop in bond strength with increase in the height of the bar above the bottom of the form. Figure 5.18 shows that up to a height of 48 in., the reduction in bond strength at ultimate is less than 10 percent for #7 and #11 bars and less than 15 percent for #9 bars. The ACI Code and AASHTO specify a 30 percent reduction in bond strength (or a 40 percent increase in development length) for a "top bar". The ACI Code defines a top bar as having more than 12 in. of concrete cast below the bar. AASHTO omits the definition of top bar. The specifications appear to overemphasize the "top bar" effect for normal slump concretes.

Figure 5.18 shows that the reduction in bond strength with height is generally greater at 0.01 -in. loaded end slip than at ultimate. The larger reduction provides some justification for the current specification values for "top bar" when based on a 0.01-in. loaded end slip. However, even using stresses at 0.01-in. loaded end slip, the 30 percent reduction in bond strength for a "top bar" is still greater than the reduction observed in Specimens D1 and D2.

#### 5.5 Effect of Slump

Stress-slip curves for Specimen D3 are shown in Figs. 5.19 and 5.20. The initial slopes did not seem to be related to the height of the bar in the specimen. The lower the bar in the specimen, the higher the load at which the rate of slip began to increase rapidly. The lower bars

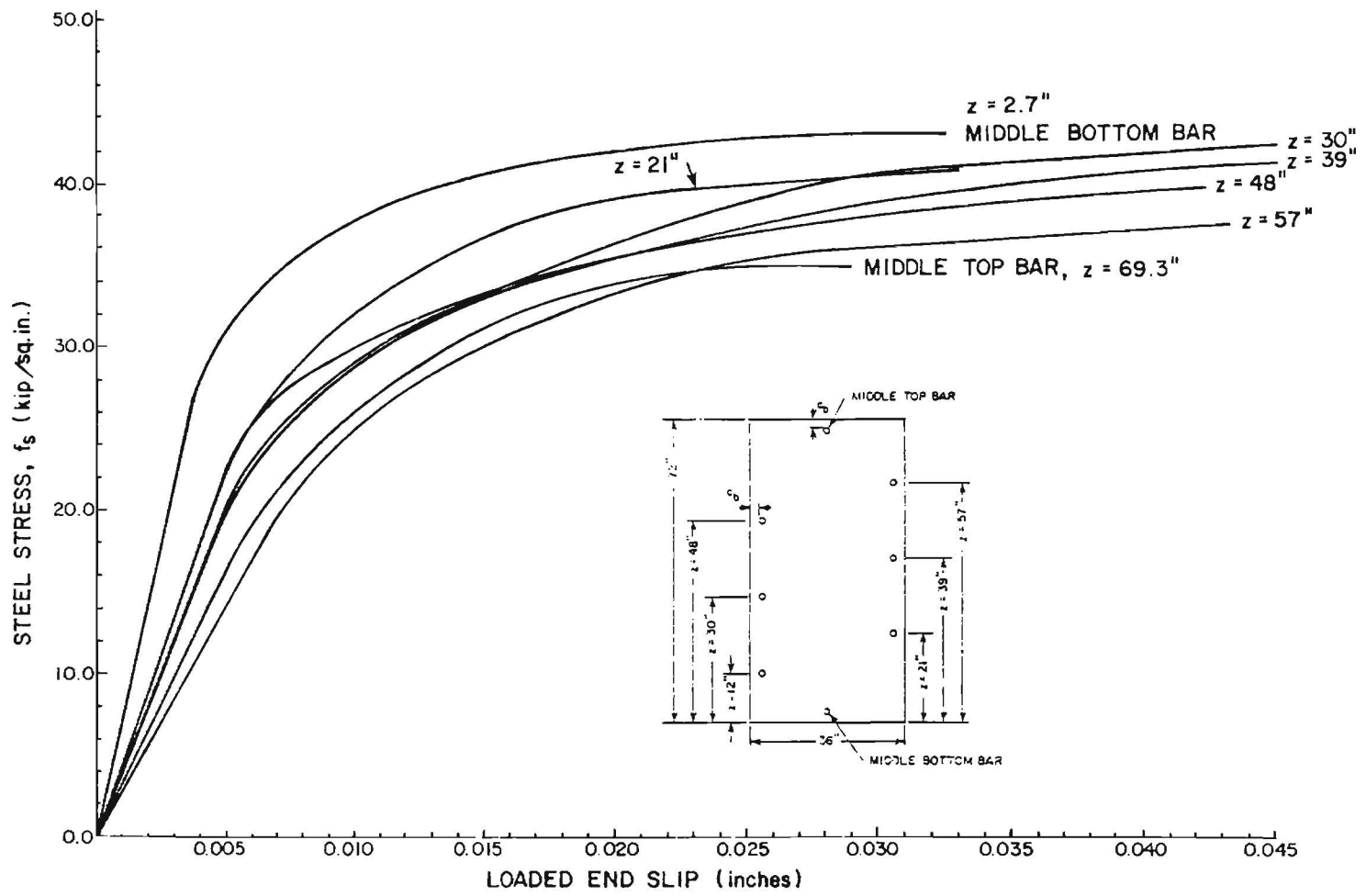


Fig. 5.14 Stress-slip relationship for #11 bars (Specimen D1, Side A)

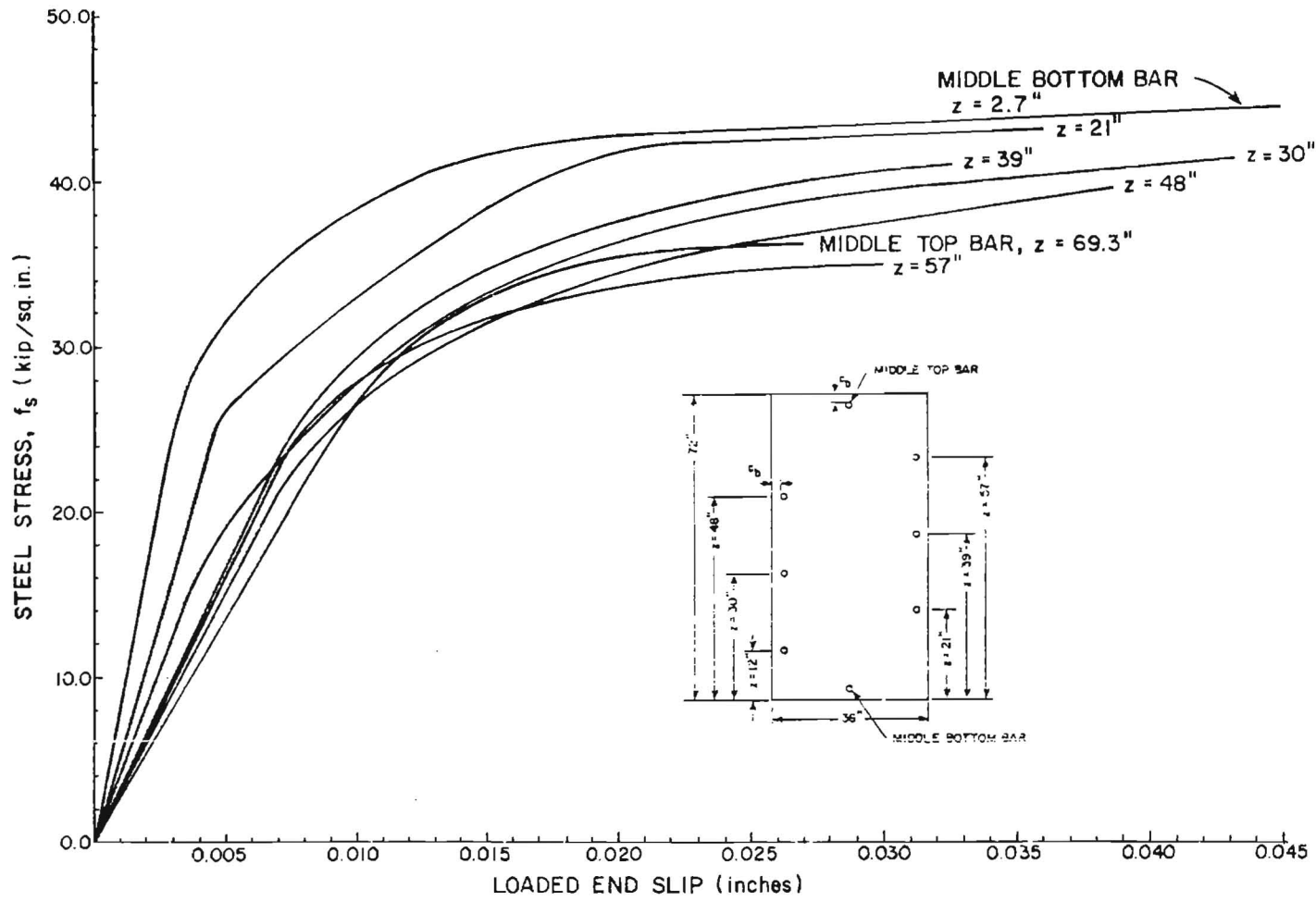


Fig. 5.15 Stress-slip relationship for #11 bars (Specimen D1, Side B)

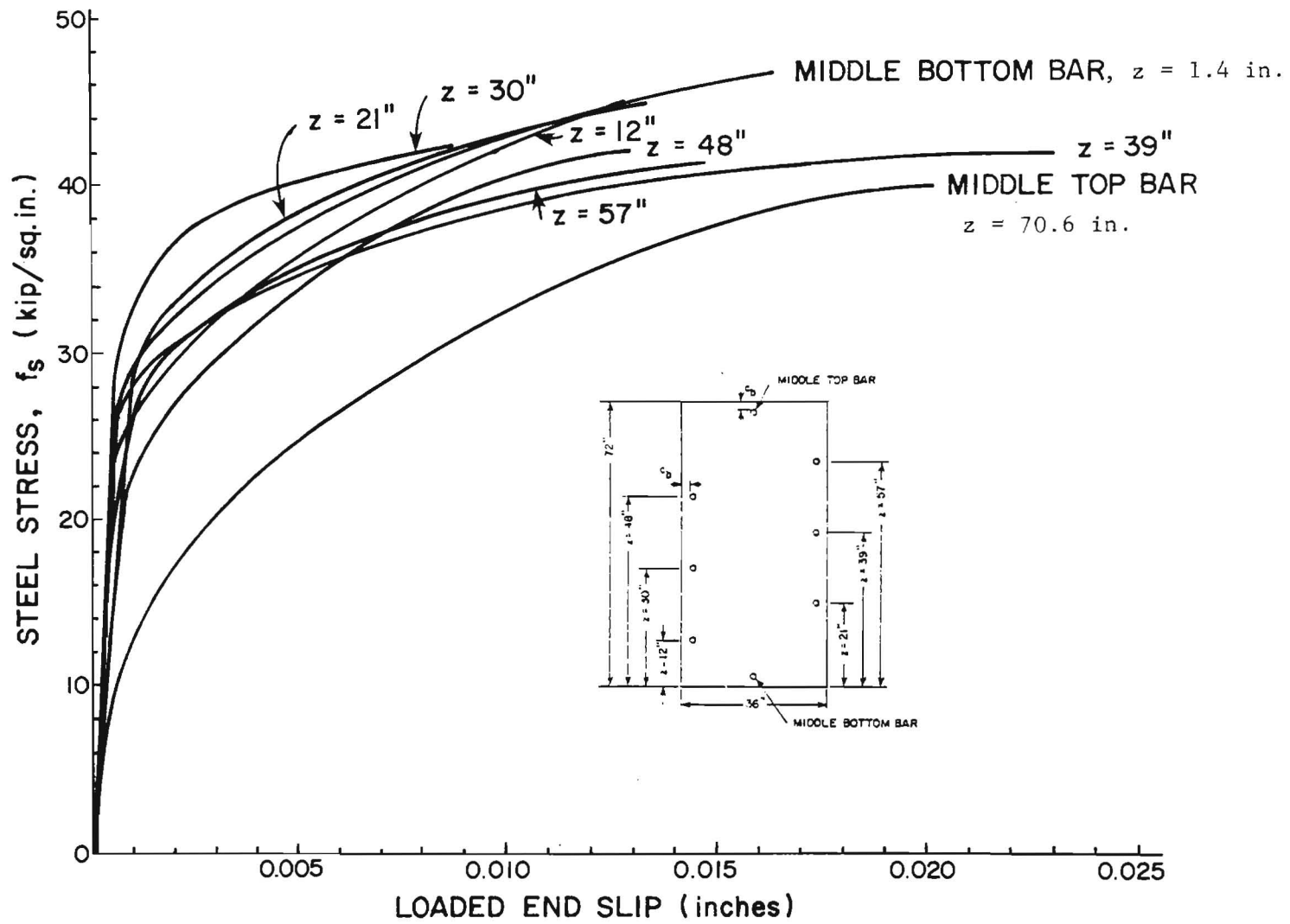


Fig. 5.16 Stress-slip relationship for #7 bars (specimen D2)

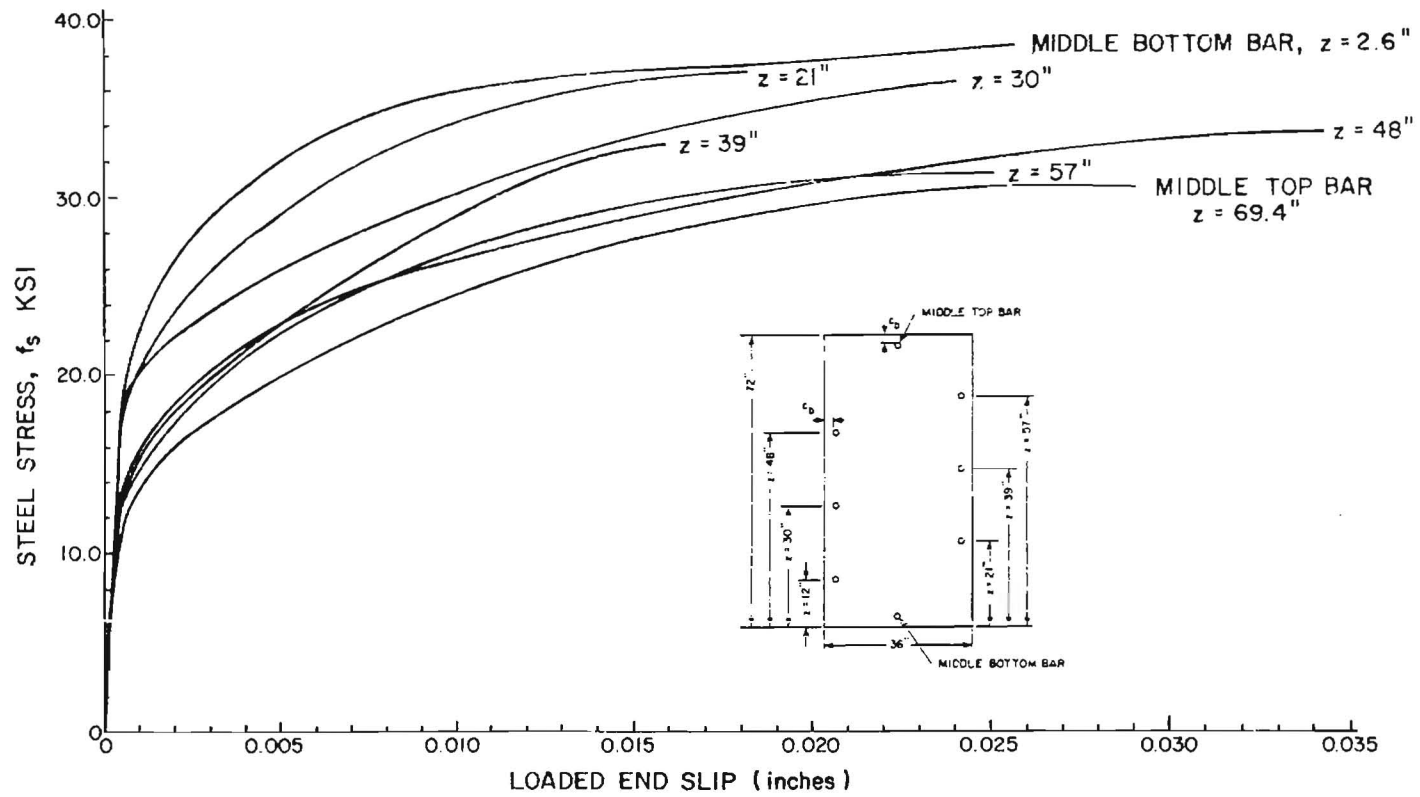


Fig. 5.17 Stress-slip relationship for #9 bars (Specimen D2)

TABLE 5.1 ULTIMATE BAR STRESS, SPECIMEN D1, #11 BARS

Casting position z in.	Side A				Side B				$\left(\frac{f'_{su}}{f'_{su \text{ bot.}}}\right)$ average
	$f'_c$ psi	$f_{su}$ ksi	$f'_{su}^*$ ksi	$\left(\frac{f'_{su}}{f'_{su \text{ bot.}}}\right)$	$f'_c$ psi	$f_{su}$ ksi	$f'_{su}^*$ ksi	$\left(\frac{f'_{su}}{f'_{su \text{ bot.}}}\right)$	
Middle Top Bar	2715	33	35	0.81	2715	35	36	0.82	0.82
57	3150	39	48	0.87	3150	36	35	0.79	0.83
48	3150	40	39	0.90	3000	40	40	0.89	0.90
39	3150	42	41	0.96	3150	42	41	0.93	0.94
30	3150	44	43	0.99	3150	42	41	0.93	0.96
21	3150	42	41	0.96	3150	44	43	0.97	0.96
12	3150	--	--	--	2715	--	--	--	--
Middle Bot. Bar	2715	41	43	1.00	2715	42	44	1.00	1.00

$$*f'_{su} = f_{su} \times \left(\frac{3000}{f'_c}\right)^{\frac{1}{2}}$$

TABLE 5.2 ULTIMATE BAR STRESS, SPECIMEN D2

Casting position z in.	#7 Side				#9 Side			
	f' <sub>c</sub> psi	f <sub>su</sub> ksi	f' <sub>su</sub> * ksi	$\left(\frac{f'_{su}}{f'_{su \text{ bot.}}}\right)$	f' <sub>c</sub> psi	f <sub>su</sub> ksi	f' <sub>su</sub> * ksi	$\left(\frac{f'_{su}}{f'_{su \text{ bot.}}}\right)$
Middle Top Bar	3125	41	40	0.85	3200	32	31	0.80
57	3400	44	41	0.89	3335	33	31	0.82
48	3400	45	42	0.90	3450	36	34	0.88
39	3400	45	42	0.90	3400	35	33	0.86
30	3400	45	42	0.90	3450	39	36	0.95
21	3450	48	45	0.96	3335	39	37	0.97
12	3400	48	45	0.97	3400	--	--	--
Middle Bot. Bar	3200	48	47	1.00	3125	39	38	1.00

$$*f'_{su} = f_{su} \times \left(\frac{3000}{f'_c}\right)^{\frac{1}{2}}$$

TABLE 5.3 COMPARISON OF BOND EFFICIENCY RATIOS,  
SPECIMENS D1 AND D2

Bar number	Casting position z in.	Bond Efficiency Ratio*	
		at ultimate	at 0.01-in. loaded end slip
#7	Middle Top Bar	0.85	0.75
	57	0.89	0.90
	48	0.90	0.93
	39	0.90	0.90
	30	0.90	0.97
	21	0.96	1.00
	12	0.97	0.97
	Middle Bot. Bar	1.00	1.00
#9	Middle Top Bar	0.80	0.68
	57	0.82	0.74
	48	0.88	0.76
	39	0.86	0.81
	30	0.95	0.83
	21	0.97	0.95
	12	--	--
	Middle Bot. Bar	1.00	1.00
#11	Middle Top Bar	0.82	0.78
	57	0.83	0.80
	48	0.90	0.80
	39	0.94	0.85
	30	0.96	0.82
	21	0.96	0.90
	12	--	--
	Middle Bot. Bar	1.00	1.00

\*Ratio is relative to the stress developed in the middle bottom bar ( $f'_{su}/f'_{su \text{ bot}}$ ).

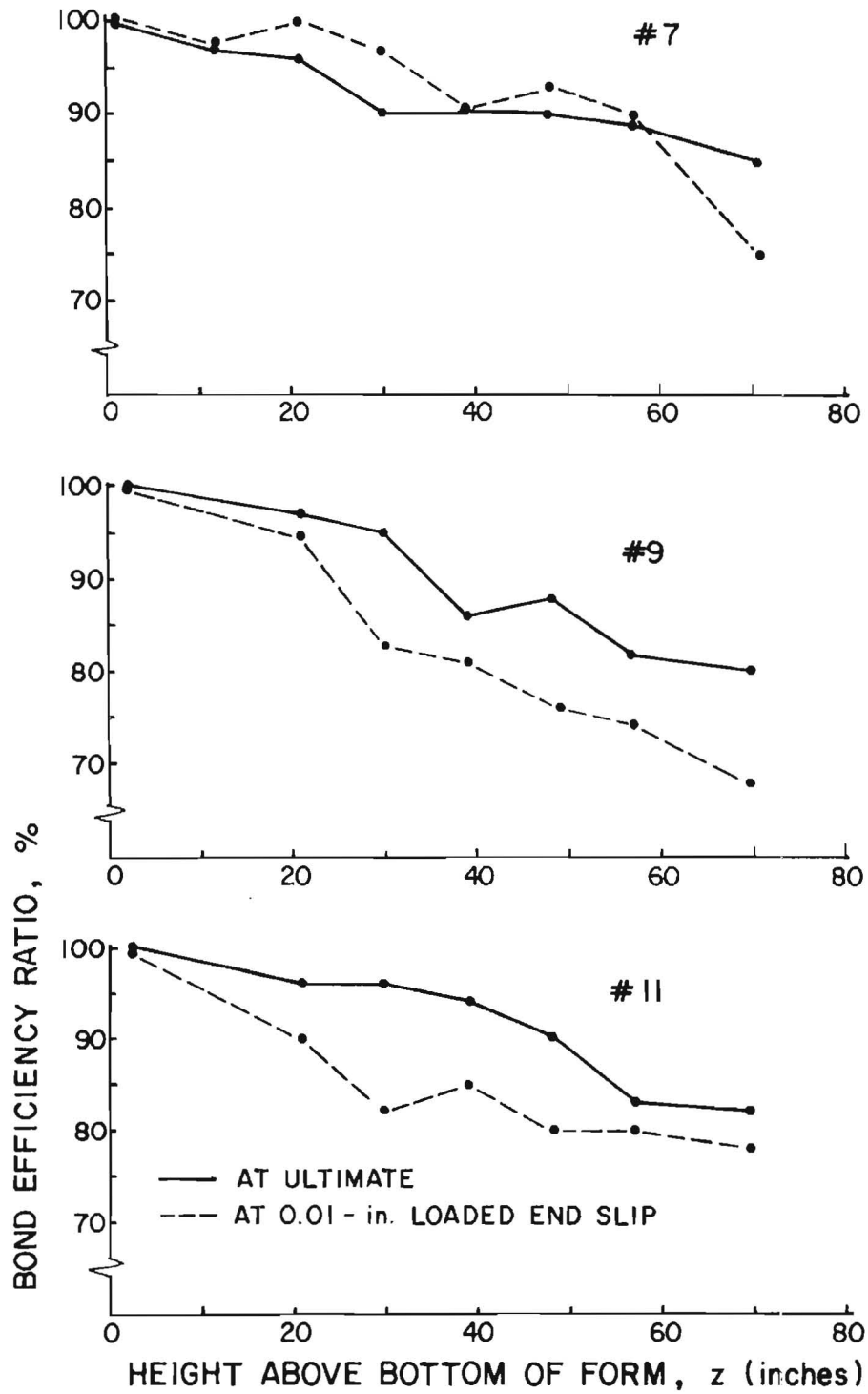


Fig. 5.18 Bond strength reduction--casting position relationship, normal slump specimens

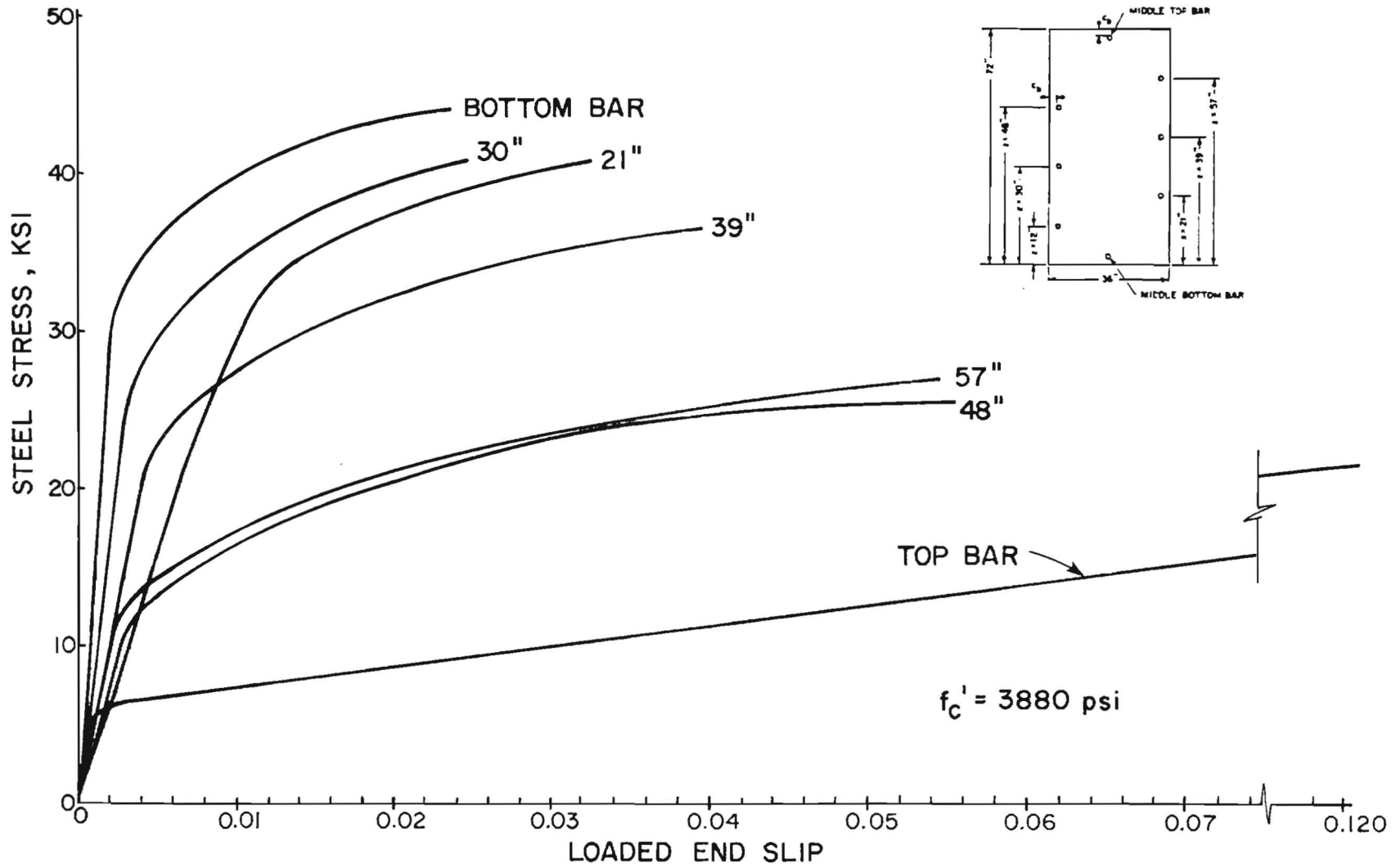


Fig. 5.19 Stress-slip relationship for #9 bars, Specimen D3, high slump

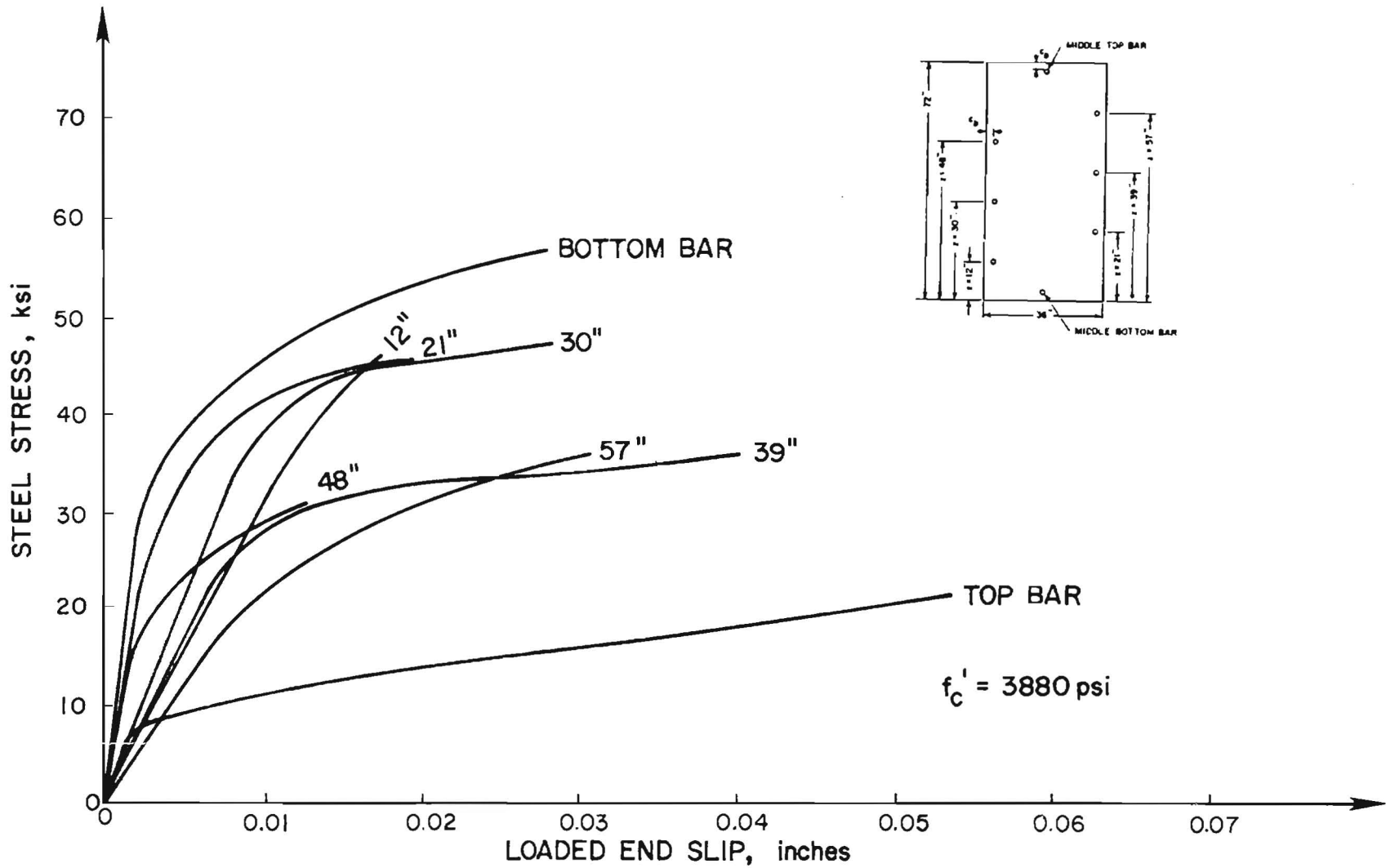


Fig. 5.20 Stress-slip curves for #7 bars, Specimen D3, high slump

in the specimen, and especially the bottom bars, showed a gradual increase in the rate of slip with increased load. However, the upper bars in the specimen showed very sharp increases in the rate of slip at relatively low loads. The #9 bar at  $z = 12$  in. failed in a different mode and is not shown.

Figure 5.21 shows the ultimate bar stress for all bar positions for both the high and the low slump test specimens. It is interesting to note that up to a height of 30 to 39 in. there is little difference in the bar stresses for the high and the low slump concrete specimens. However, for greater heights, the bars in high slump concrete show a dramatic decrease in developed stress.

The effect of an increase in slump becomes even more apparent when the bond efficiency ratio ( $f'_{su} / f'_{su \text{ bottom bar}}$ ) is plotted against bar height in Fig. 5.22. The ratios for the #9 bars remain almost parallel up to a bar height of 39 in. but drop sharply thereafter, reaching a low of 48 percent for the top middle bar position. The capacity of the low slump bar at this same position is only 80 percent of the low slump bottom bar. The ratios for the #7 bars are reduced to 80 percent of that of the bottom bar at a height of only 12 in. The relative capacity of the bar in low slump concrete at this same height was 96 percent. In the worst case, at the top bar position, the relative capacity of the #7 bar was 80 percent for the low slump concrete and only 37 percent for the high slump concrete.

These curves indicate that the #7 bar was affected to a much greater degree by the increase in slump than the #9 bar. Most likely, this stemmed from the fact that the #7 bar had a 1 in. cover while the #9 bar had a 2 in. cover. One of the most serious side effects of an increase in slump (or water content) is an increase in shrinkage, and with shrinkage cracks are more likely to occur with small cover than with large cover. This difference shows up to an even greater extent if the performance at a slip of 0.01 in. is compared in Fig. 5.23. Note that for the uppermost bars, stresses at 0.01 in. slip reached values of only 20 to 30 percent of the stresses reached by the bottom bar.

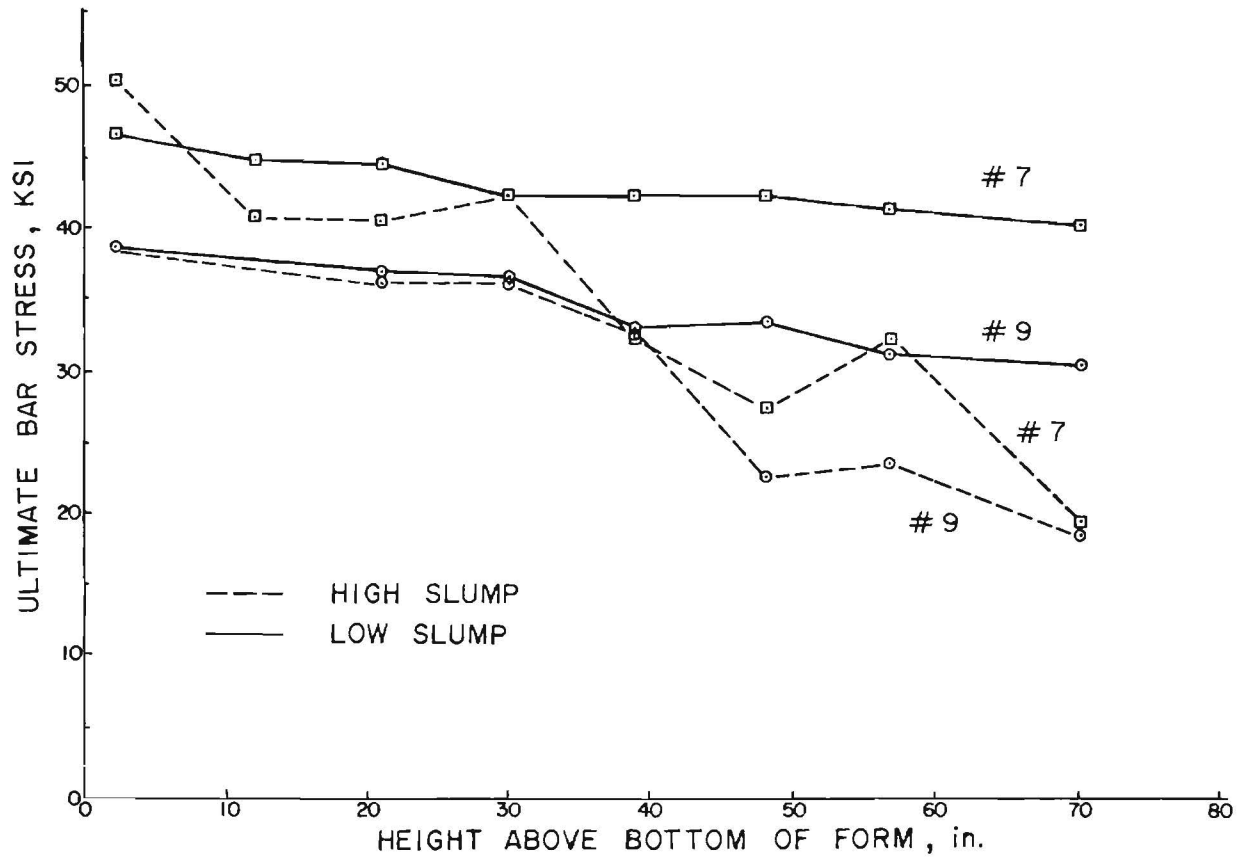


Fig. 5.21 Bar stress at ultimate vs. bar height for high slump (9-1/2 in.) and low slump (3 in.) specimens

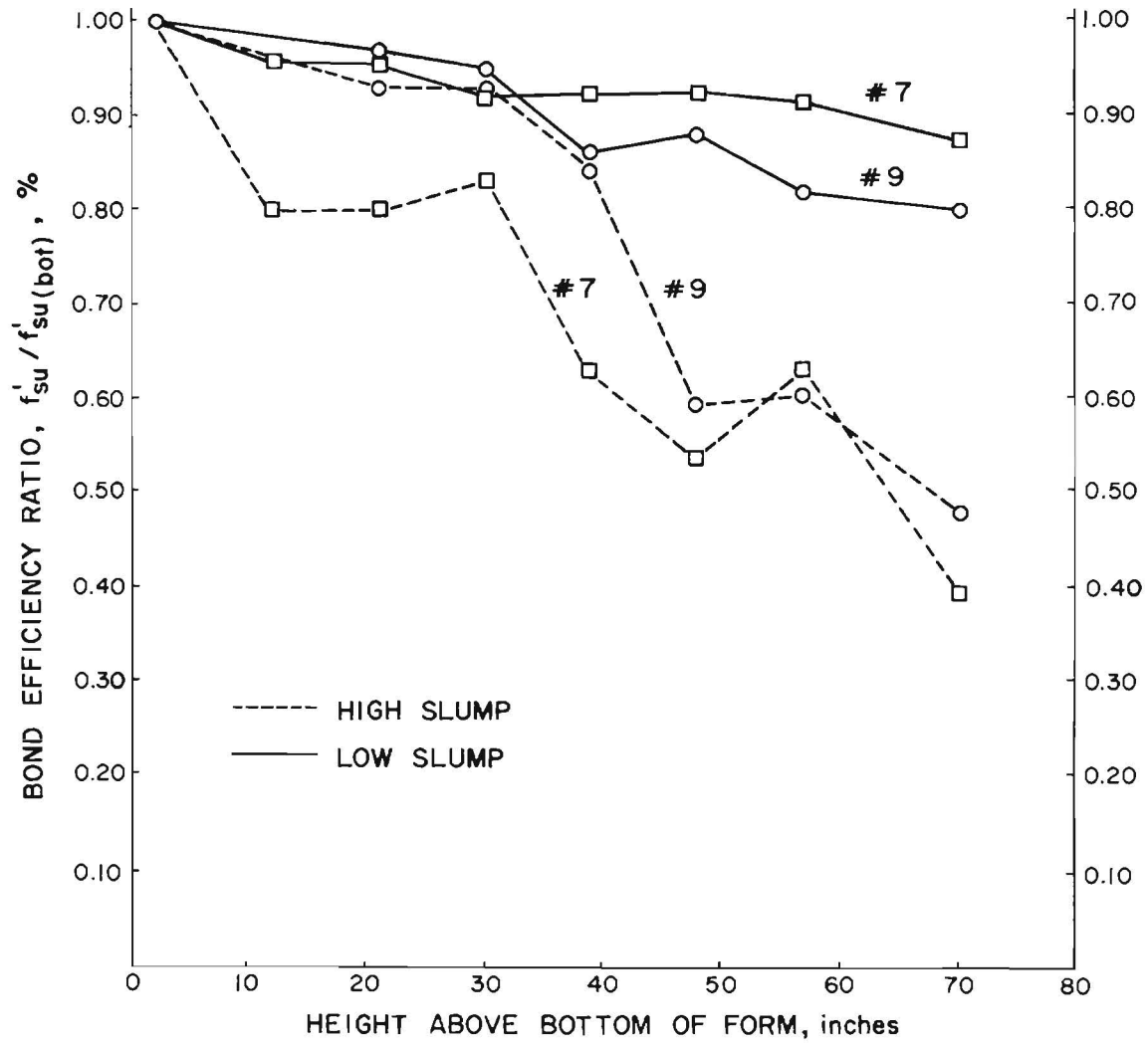


Fig. 5.22 Ultimate bond efficiency ratio vs. bar height, influence of slump

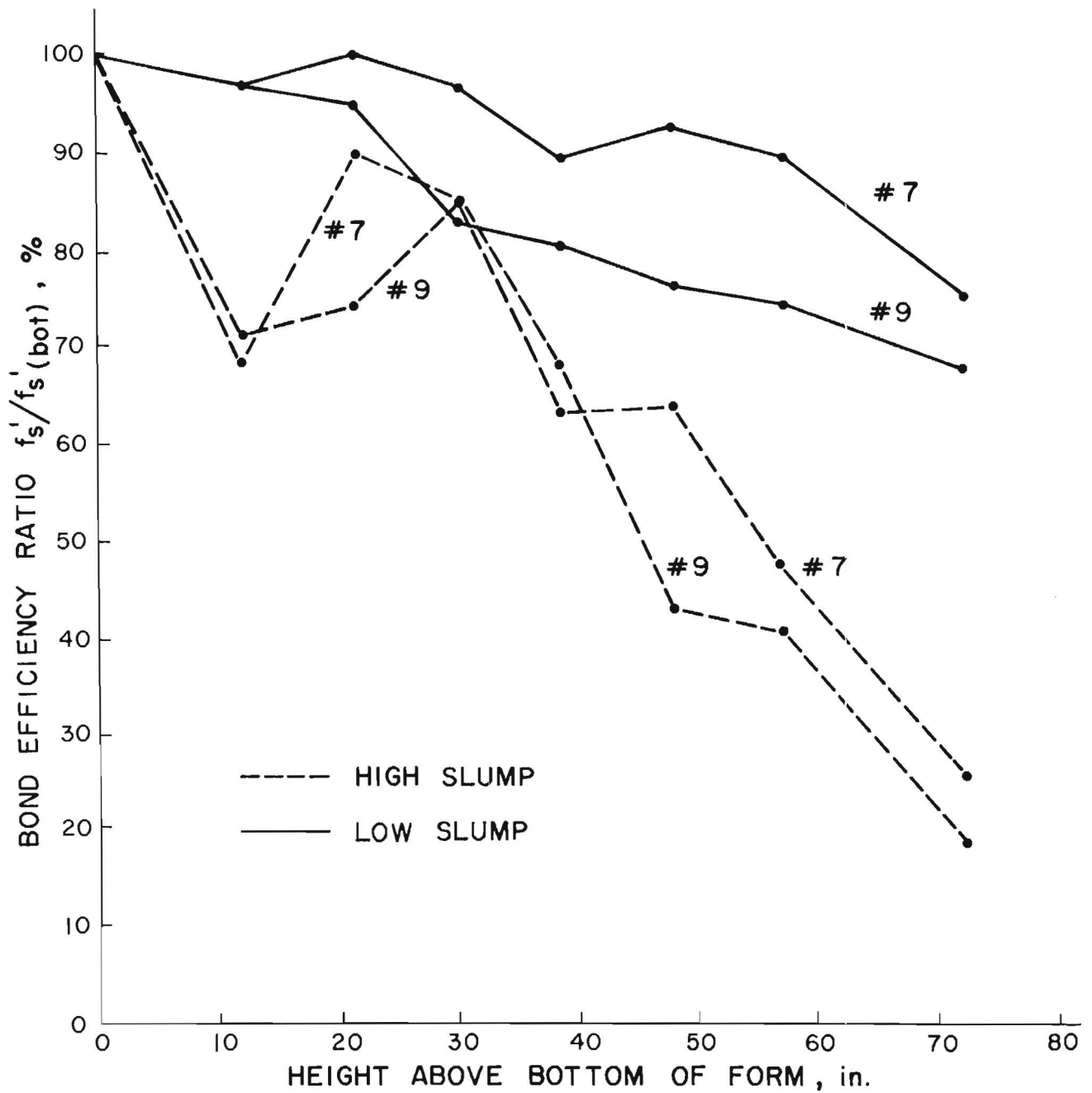


Fig. 5.23 Bond efficiency ratio at 0.01 in. slip, influence of slump

## 5.6 Horizontal vs. Vertical Bars

Specimen D4 provided the data for comparing influence of the orientation of bars and the direction of loading (see Fig. 1.2) on the bond characteristics of the bars. The bars were all #9 and  $f'_c$  was about 3100 psi during the period of testing. Two bars were tested in each position and at each height (see Fig. 4.2).

Figure 5.24 shows the load-slip curves for the bars at  $z = 18$  in. There was a tendency for the horizontal bars to be the strongest and the vertical bar pulled in the direction of concrete settlement to be the weakest. The values of ultimate stress for the vertical bar pulled against the direction of concrete settlement showed considerable variation with one bar reaching an ultimate stress in the range of the horizontal bars and the other in the range of the vertical bars pulled in the direction of concrete settlement. Figure 5.25 shows the load-slip curves for the bars at  $z = 48$  in. In this case both the horizontal bars and the vertical bars pulled against the direction of concrete settlement show similar capacities and load-slip response. The vertical bars pulled in the same direction as concrete settlement failed at much lower stresses and exhibited more slip. However, the scatter between test values makes evaluation difficult since one of the bars with only 18 in. of concrete cast below exhibited considerably more slip and also slightly less load-carrying capacity than a bar of the same type with 48 in. of concrete cast below.

The effect of the height of the bar during casting appears to be much clearer for the horizontal bars than for either type of vertical bar. The ultimate load capacity for both horizontal bars at  $z = 18$  in. is substantially greater than that of both bars at  $z = 48$  in. Obviously, it is much easier for the water and weak concrete to build up under the horizontal bar than under the lugs of the vertical bars because of the greater area involved. The amount of inferior concrete under the lugs of the vertical bars is likely to be highly variable and a function of method of compaction, bar congestion, and workability of concrete.

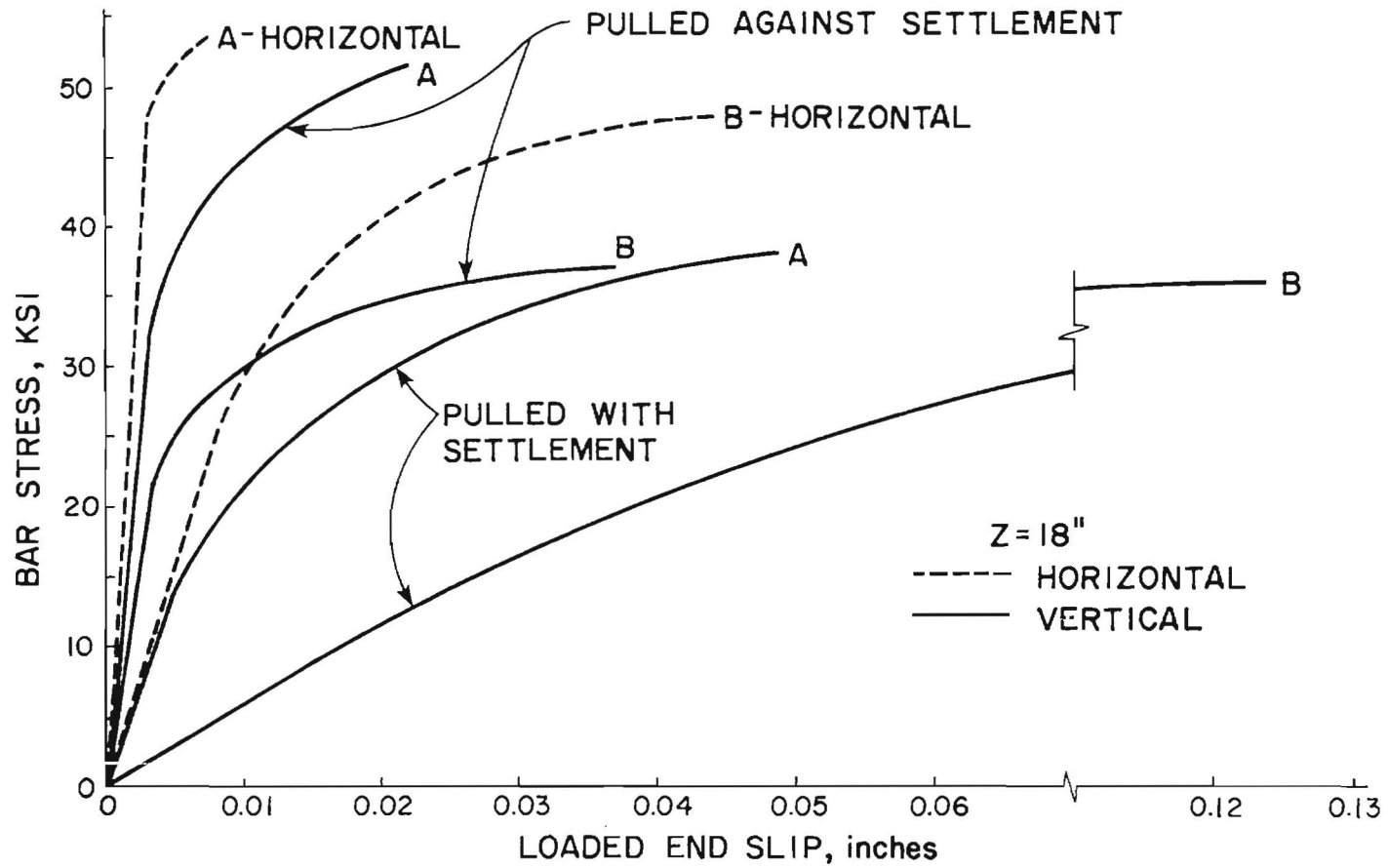


Fig. 5.24 Stress-slip curves for bars at  $z = 18$  in., Specimen D4

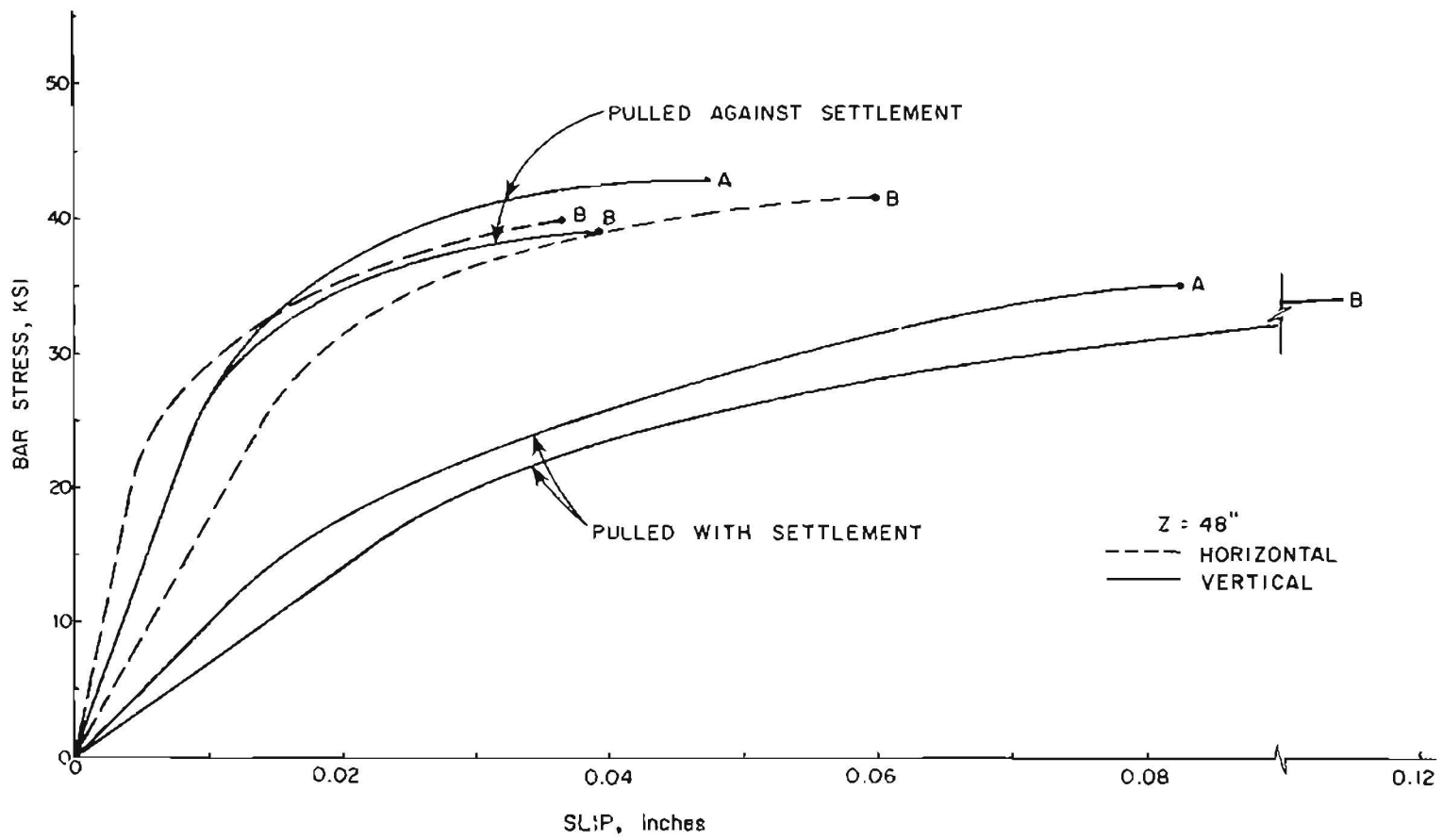


Fig. 5.25 Stress-slip curves for bars at  $z = 48$  in., Specimen D4

### 5.7 The Influence of Slip Level

The degree to which deformed bars are influenced by the depth of concrete cast below them is highly dependent on the value of slip used as a basis for comparison. The current ACI Code specifications on the "top bar effect" are based on values of stress measured at a loaded end slip of 0.01 in. As shown by the results discussed herein, the effects of casting position are exaggerated and it has been suggested that comparisons be made on the basis of ultimate steel stress values. The anchored bars in specimens with high slump concrete generally showed a great deal of slip before reaching ultimate capacity and provide an extreme example of the differences between stresses at 0.01 in. slip and at ultimate. A comparison of the changes in the bond efficiency ratio for slip at 0.01 in. and at ultimate indicates that the use of bar stress at a slip of 0.01 in. is very conservative for ultimate strength design purposes.

Thus it would appear that the use of 0.01 in. slip as a failure criterion, as was true for the early investigations of Abrams [1] and Clark [9], led to an overestimation of the influences of casting position. The rationale behind the use of 0.01 in. slip as a criterion was that slip values greater than 0.01 in. would lead to excessive crack widths in the concrete. However, in the tests in this study development lengths were intentionally kept short to prevent yielding of the bar prior to bond failure. Such results may be inappropriate for typical structural applications. As noted earlier, the beginning of the free end slip usually coincided with a sharp increase in the rate of loaded end slip and implies that, had the embedment lengths been longer, excessive slip would not have occurred. It should also be noted that current codes for ultimate strength design contain serviceability provisions to prevent excessive cracking.

## C H A P T E R 6

### BEHAVIOR--SPLICE TESTS

#### 6.1 Introduction

The behavior of splice bars is discussed in terms of load-slip curves and cracking patterns. In all splices very little free end slip was measured before failure, indicating, as previous investigators have suggested (Zipprodt [41]), that free end slip is a very poor basis for the comparison of the behavior of anchored bars. Figures 6.1 and 6.2 show free and loaded end slip for several splices (Figs. 4.3 and 4.4 show splice details). In this chapter loaded end slip is used exclusively for making comparisons between tests.

#### 6.2 Influence of Splice Orientation

The splice test results clearly indicate that the most significant variable influencing the failure of a splice, regardless of the depth of concrete cast below the splice,  $z$ , is the orientation of the splice (Fig. 6.3) relative to the surface of the concrete; that is, whether the splice is face-parallel or face-perpendicular. In all cases where the depth of concrete below the splice was greater than 21 in., the face-parallel splices failed at lower ultimate loads than the face-perpendicular splices.

At the time the specimens were designed, it was anticipated that the face-parallel splice would be the weaker of the two orientations, since both bars had a 2-in. cover, while the face-perpendicular splice had one bar with a 2-in. cover and the other bar with a 3-in. cover. However, when these splices were placed along the side of the specimen, the face-perpendicular splice had two bars under which air and sand particles could accumulate while in the face-parallel splice only the lower bar of the splice had any accumulation. It therefore seemed likely that as the depth of concrete cast below the splice was increased for splices along the side of the specimen, the relative superiority of the face-perpendicular

### STACKED SPLICE TOP AND BOTTOM SPLICES

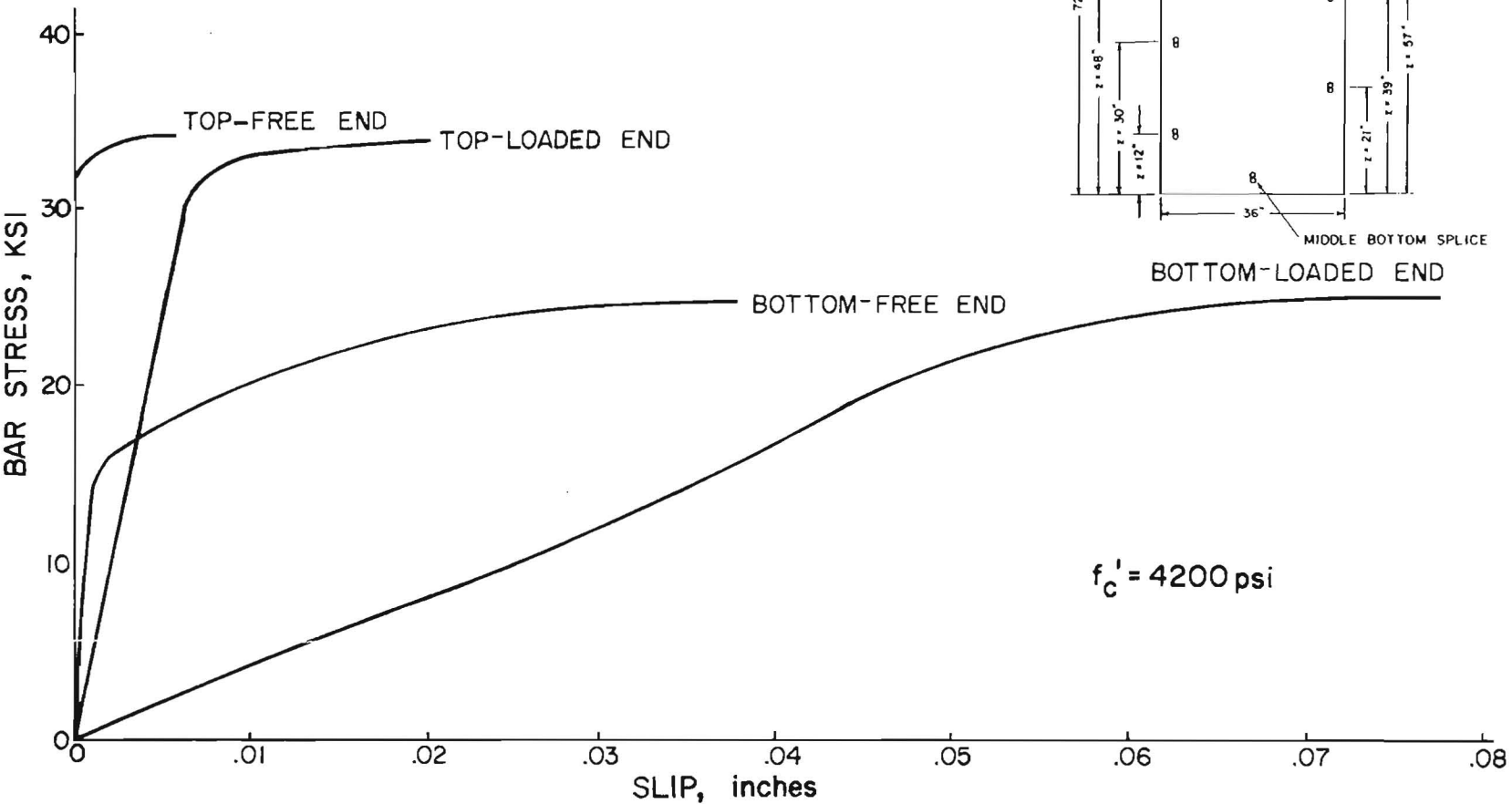


Fig. 6.1 Load-slip curves for stacked splices (S1)

## SIDE-BY-SIDE SPLICE TOP AND BOTTOM SPLICES

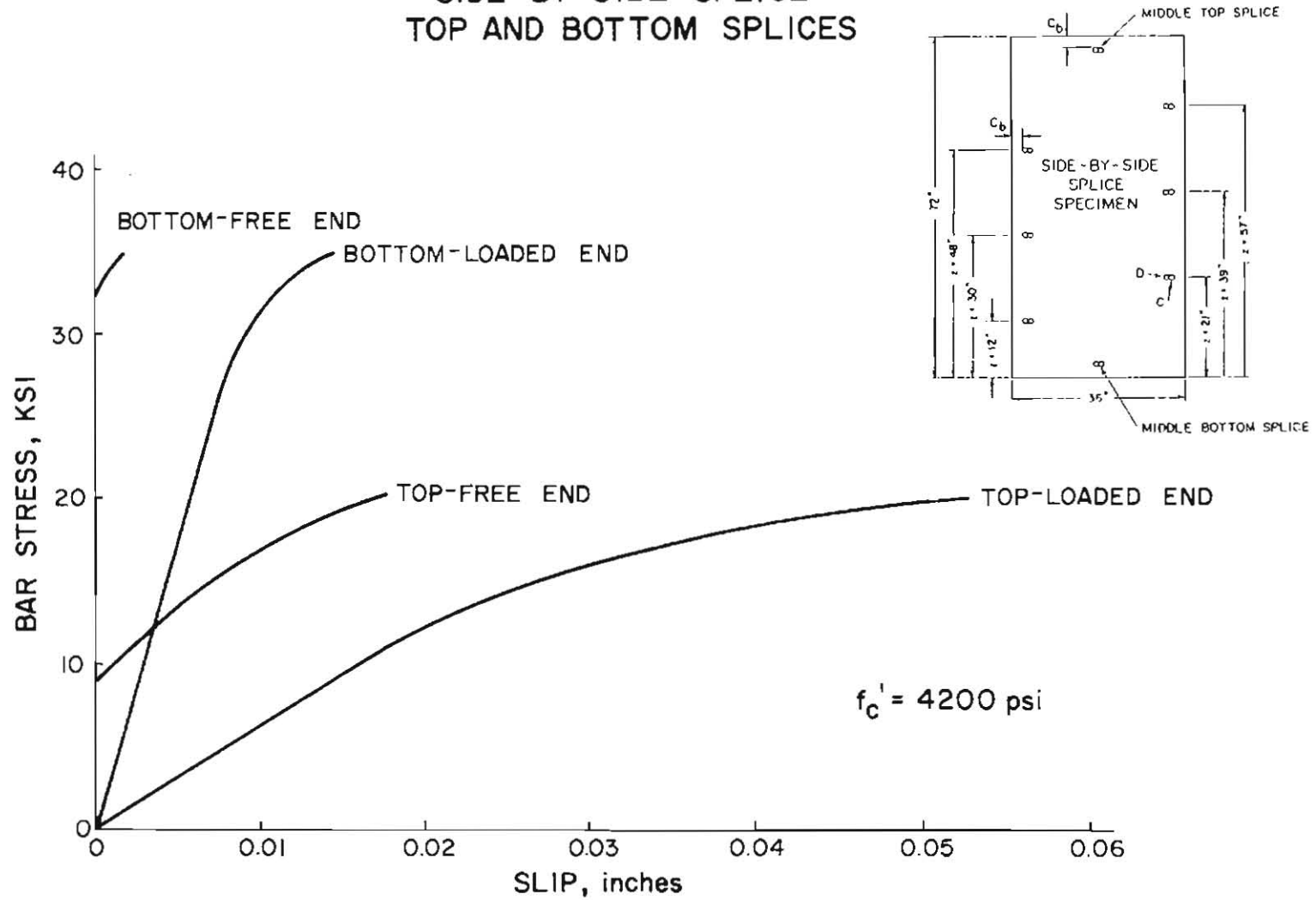


Fig. 6.2 Load-slip curves for side-by-side test (S2)

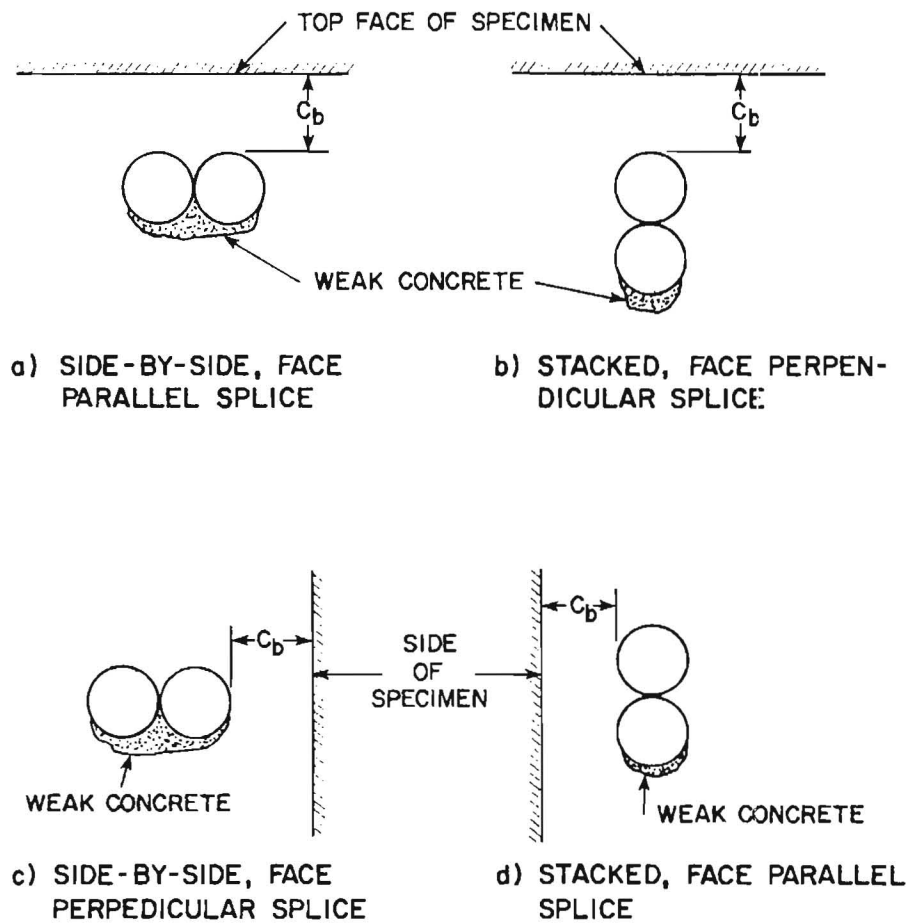


Fig. 6.3 The effect of splice orientation on accumulation of inferior concrete

splice would diminish; however, this trend was not observed in the test program.

### 6.3 Crack Patterns

The cracking patterns for the face-parallel and face-perpendicular splices at  $z = 30$  in. are shown in Figs. 6.4 and 6.5, respectively. Note that in the case of the face-parallel splice, cracks propagate from the splice along a line nearly parallel to the plane of the splice. Failure resulted when the cover over both bars was forced away from the splice. Longitudinal cracks perpendicular to the cover surface of the specimen and extending from the bar to the surface, characteristic of a single bar tested in this manner, did not develop.

An indication of the magnitude of the radial forces normal to the plane of the splice is seen from the crack pattern of the face-perpendicular splice at  $z = 30$  in. (Fig. 6.5). The radial forces were sufficient to split the specimen nearly in half. The crack shown developed over the entire length of the splice (from face-to-face of the specimen) and extended from the spliced bars almost to the opposite edge of the specimen. Longitudinal cracks from the splice through the cover occurred in this case as they did in all other face-perpendicular splice tests.

The crack through the specimen due to the testing of the face-perpendicular splice at  $z = 30$  in. affected the results of the tests on the opposite side of the specimen. The cracks from the splices at  $z = 21$  in. and  $z = 39$  in. propagated to the crack formed by the test of the splice at  $z = 30$  in. It is very likely that this resulted in the low stresses recorded for the splice at  $z = 21$  in.

### 6.4 Stress-Slip Curves

Table 6.1 lists the values of stress at failure for the various splices studied in this investigation. Figure 6.6 shows bar stress vs. splice height,  $z$ , for the two specimens cast in the splice series. Specimen S1, represented by the V line, was cast with stacked splices while the other,

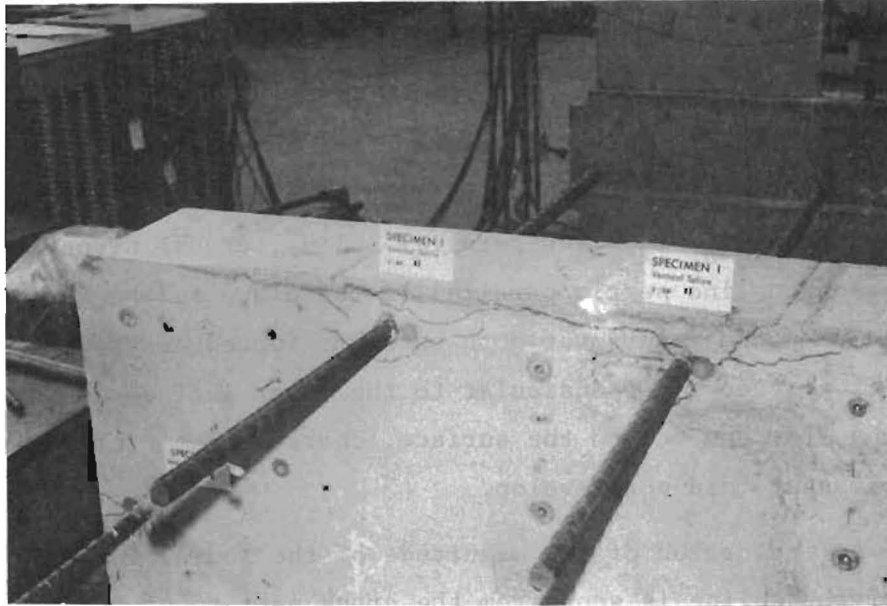


Fig. 6.4 Crack patterns for stacked splices along specimen side

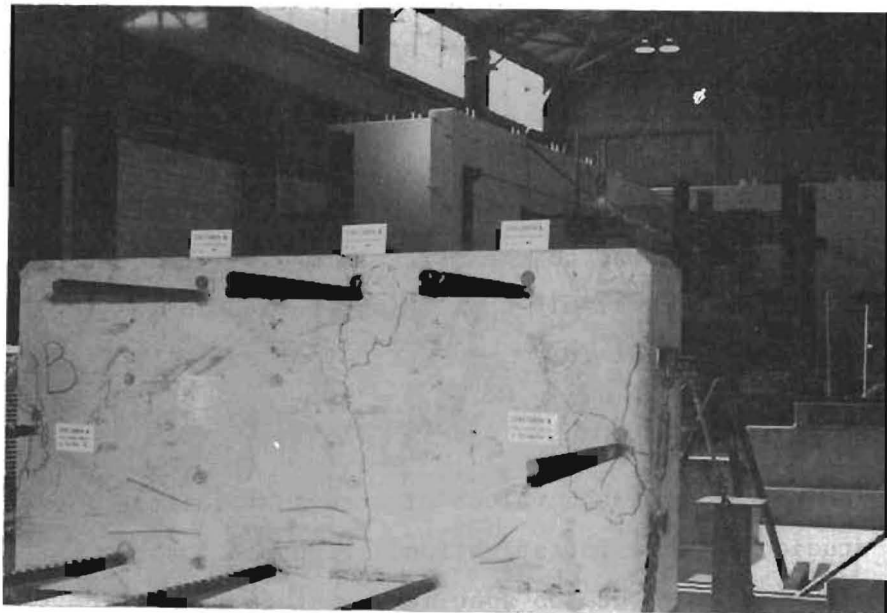


Fig. 6.5 Crack patterns for side-by-side splices

TABLE 6.1 SUMMARY OF STRESSES AT FAILURE - SPLICE TESTS - S1 AND S2

Casting Position	Stacked Splice - ●			Side-by-Side Splice - ●●		
	$f_{su}$ ksi	$f'_{su}$ * ksi	$\frac{f'_{su}}{f'_{su\ bot}}$	$f_{su}$ ksi	$f'_{su}$ ksi	$\frac{f'_{su}}{f'_{su\ bot}}$
z = in.						
Top Bar	25	21	0.74	21	18	0.60
57	31	26	0.91	33	28	0.94
48	27	23	0.79	34	29	0.97
39	35	30	1.03	37	31	1.06
30	34	29	1.00	39	33	1.11
21	38	32	1.12	35	30	1.00
12	29	25	0.85	29	25	0.83
Bottom Bar	34	29	1.00	35	30	1.00

$$* f'_{su} = f_{su} \times \left[ \frac{3000}{f'_c} \right]^{1/2}$$

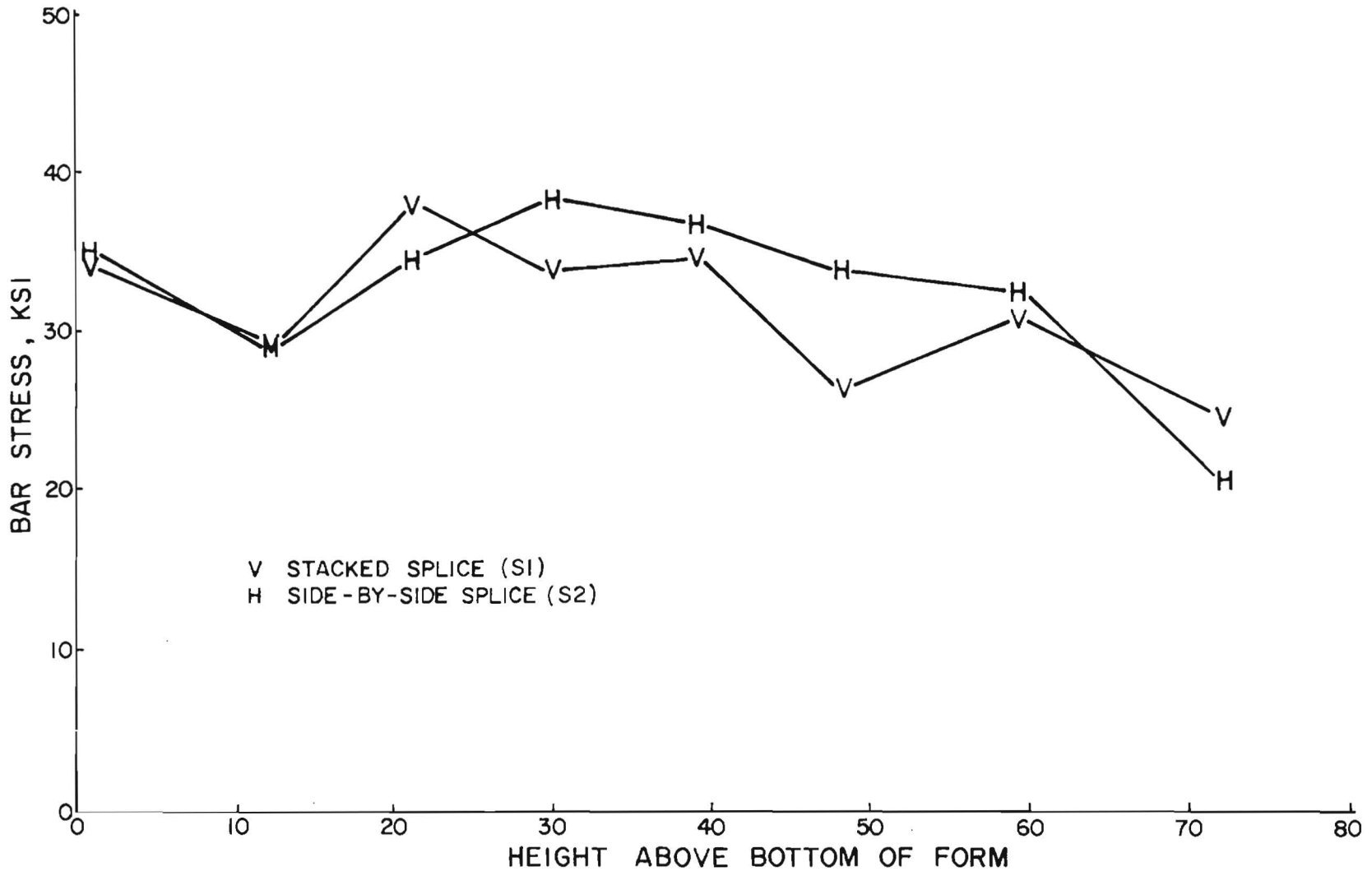


Fig. 6.6 Bar stress vs. height for stacked and side-by-side splices

S2, represented by the H line, contained all side-by-side splices. There is little discernible difference between the two curves in Fig. 6.6. However, when the face-parallel and face-perpendicular splices are separated, as in Table 6.2, there is a more obvious difference between the two curves, with the face-perpendicular splice showing a slight superiority (11 percent average) in capacity. This is especially true as the depth of concrete cast below the splice is increased.

Figure 6.7 shows the load-slip curves for both types of splice at  $z = 30$  in. Both bars in the face-perpendicular orientation displayed a greater amount of initial and ultimate slip than either of the two bars in the face-parallel orientation. This behavior was typical of other splices and indicates that the side-by-side splice arrangement leads to an increase in the accumulation of weak concrete under the bars which in turn leads to an increase in slip but little change in strength.

The initial portion of the load-slip curves is the same for both bars in the face-parallel splice with the lower bar showing slightly more slip at higher loads. This was characteristic of most splices of this type because the weak concrete build-up was concentrated under the lower bar in the splice.

In beams, the longitudinal reinforcement is generally placed along the top and bottom surfaces rather than along the side surfaces as the majority of the test splices were in this program. Therefore, a comparison of the splices at the tops and bottoms of the two test specimens should give a good indication of the differences in behavior between top and bottom splices in beams, and, as the depth of the specimen was greater than that of most beams, the differences should be magnified.

Figure 6.8 shows stress-slip curves for the top and bottom splices of Specimens S1 and S2. It can be seen that there is very little difference in the ultimate load capacity of the bottom splices. The initial straight line portions of the curves are also quite similar. Bar A of the top splice shows a great deal more slip near ultimate than either of the two bars of

TABLE 6.2 SUMMARY OF STRESS AT FAILURE - INFLUENCE OF SPLICE ORIENTATION

Casting Position	Face Parallel Splice - ●			Face Perpendicular Splice - ●●			
	$f_{su}$ ksi	$f'_{su}$ * ksi	$\frac{f'_{su}}{f'_{su \text{ bot}}}$ (1)	$f_{su}$ ksi	$f'_{su}$ ksi	$\frac{f'_{su}}{f'_{su \text{ bot}}}$ (2)	$\frac{(2)}{(1)}$
$z = \text{in.}$							
Top Bar	21	18	0.60	25	21	0.74	1.23
57	31	26	0.89	33	28	0.97	1.09
48	27	23	0.77	34	29	1.00	1.30
39	35	30	1.00	37	31	1.09	1.09
30	34	39	0.97	39	33	1.15	1.18
21	38	32	1.09	35	30	1.03	0.94
12	29	25	0.83	29	25	0.85	1.02
Bottom Bar	35	30	1.00	34	29	1.00	1.00
						Average	1.11

$$* f'_{su} = f_{su} \times \left[ \frac{3000}{f'_c} \right]^{1/2}$$

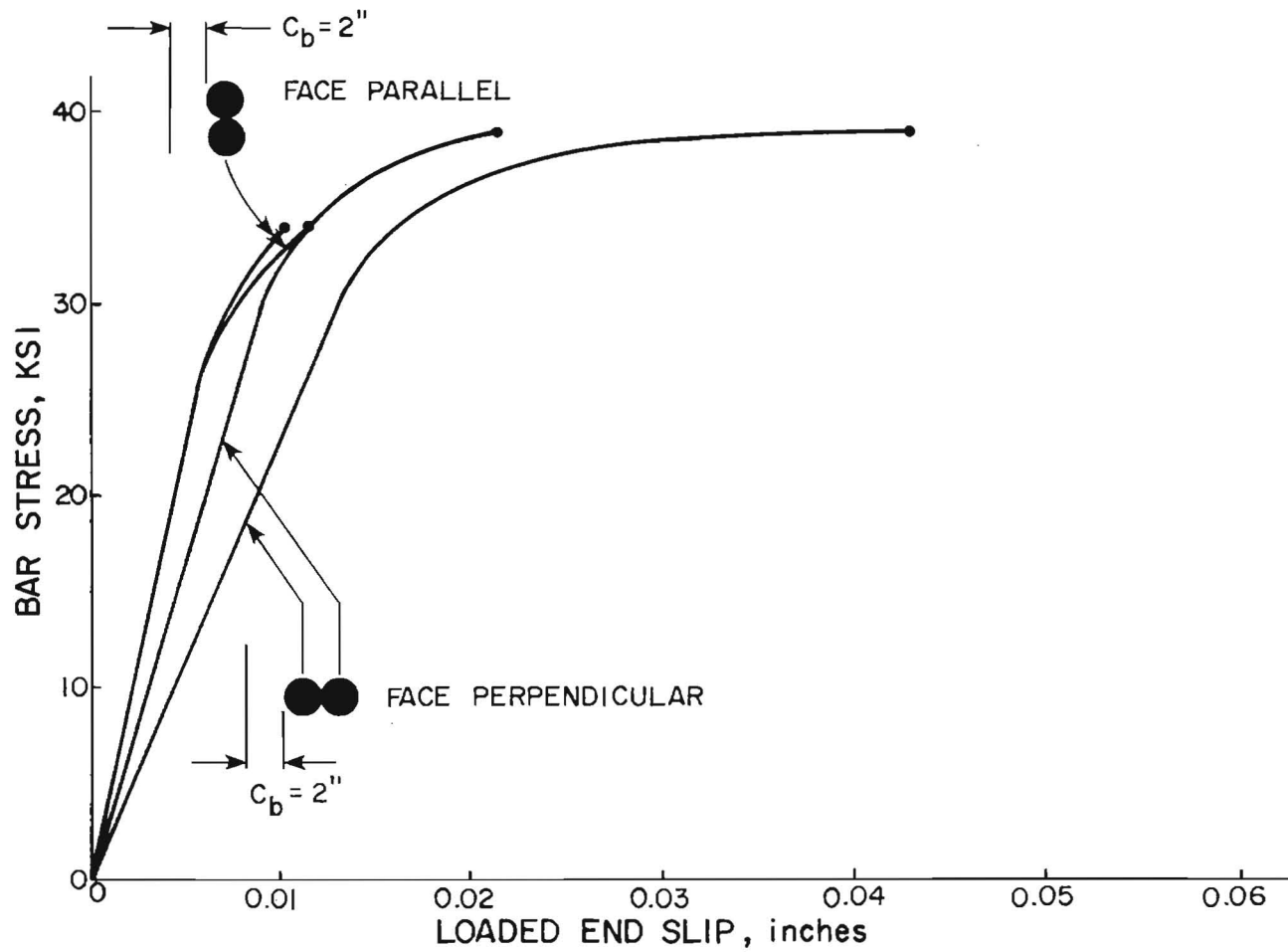


Fig. 6.7 Comparison of stress-slip curves for face-parallel and face-perpendicular splices at  $z = 30$  in.

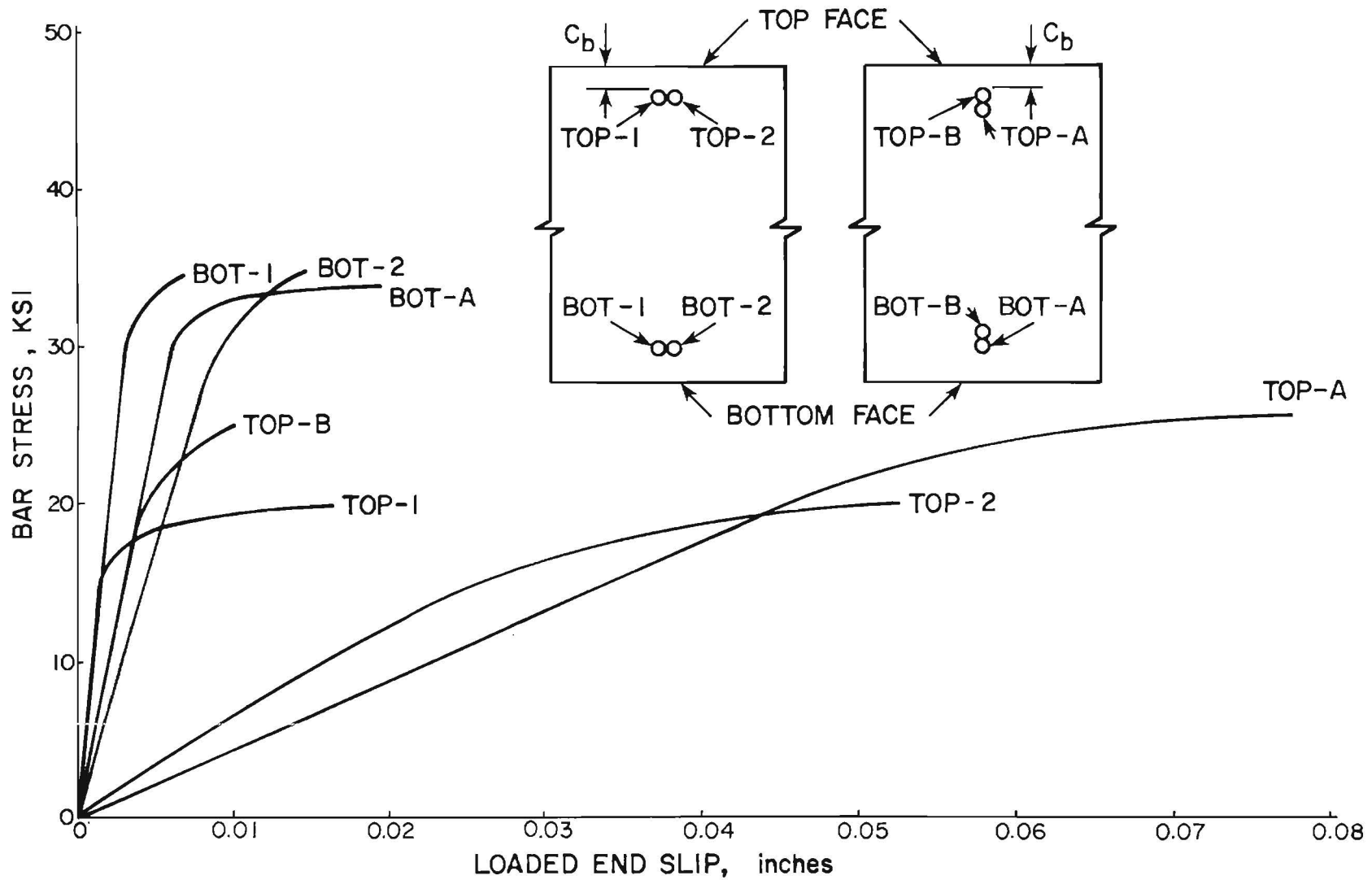


Fig. 6.8 Stress-slip curves for top and bottom splices in S1 and S2

the face-parallel splice. It appears that the lower bar (bar A) failed as a single bar rather than as a spliced bar. The top face-perpendicular splice reached a stress about 25 percent greater than the top face-parallel splice.

### 6.5 Splice Tests vs. Development Length Tests

The results of tests to determine the effects of casting position on development length (Chapter 5) provide an excellent opportunity to compare both the absolute and relative values of splice capacity to that of anchored bars placed at varying heights in a mass of concrete. Figure 6.9 shows the values of the adjusted bar stress at ultimate, for both splice types and for the #9 development tests (from Specimen D2).

The splice tests give lower absolute values of ultimate bond stress at all bar and splice levels. This is to be expected because of the difference in specimen geometry. The splice test specimen was only as long as the splice--that is, 12 in. The anchored bar specimen, on the other hand, was 72 in. long in order that bars could be tested at each end of the specimen. Therefore, there was a great deal of concrete beyond the free end of the bar.

More important than the absolute values of ultimate bar stress are the values of bar stress at ultimate relative to that of the bottom bar or splice.

As can be seen in Fig. 6.10, the splice tests show considerably more variation than the anchored bars. The splices at intermediate heights show greater relative strengths than the anchored bars at the same levels. Both top splices had lower relative strength than the top anchored bar. The ultimate capacity of the face-perpendicular splice at  $z = 30$  in. is 15 percent greater than that of the bottom splice and, neglecting the splice at  $z = 12$  in., the first splice of this type to show a drop in relative capacity is at  $z = 57$  in. In the case of the face-parallel splice, there is no drop in capacity up to  $z = 48$  in.

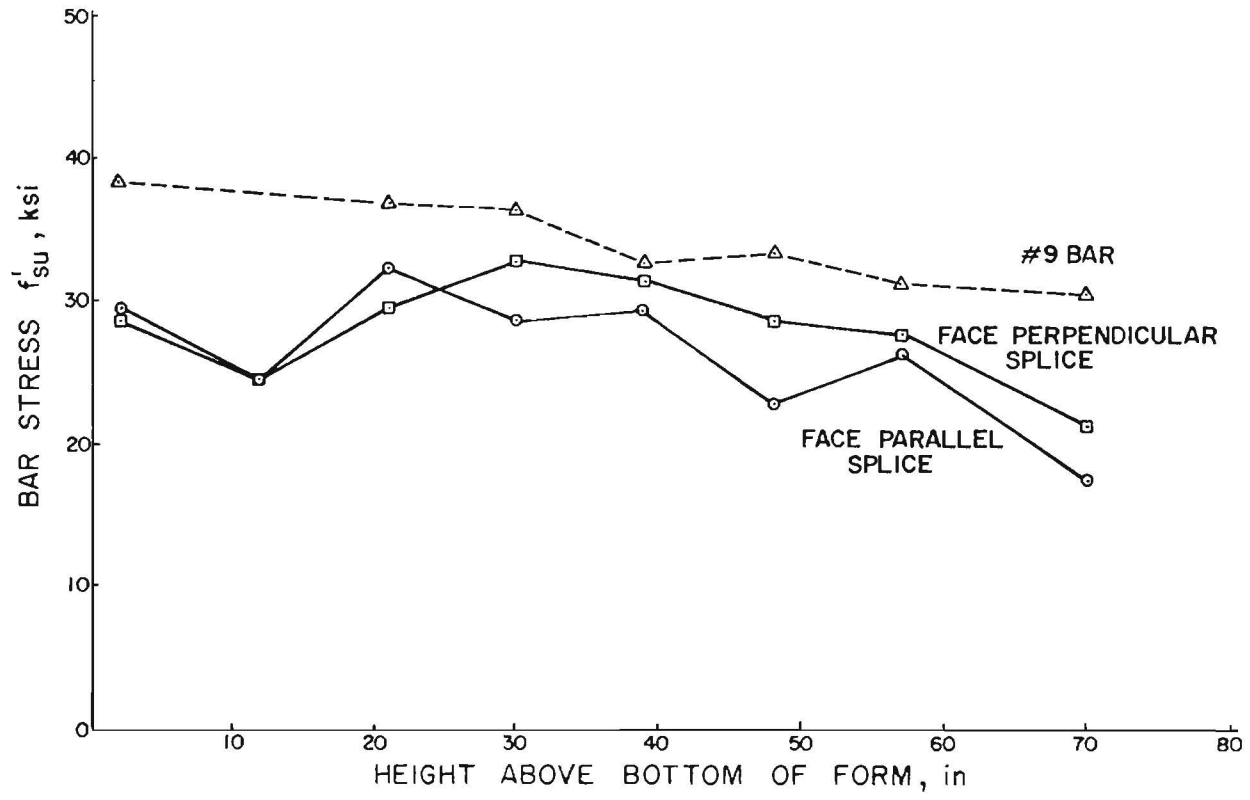


Fig. 6.9 Bar stress vs. height for splice and development tests

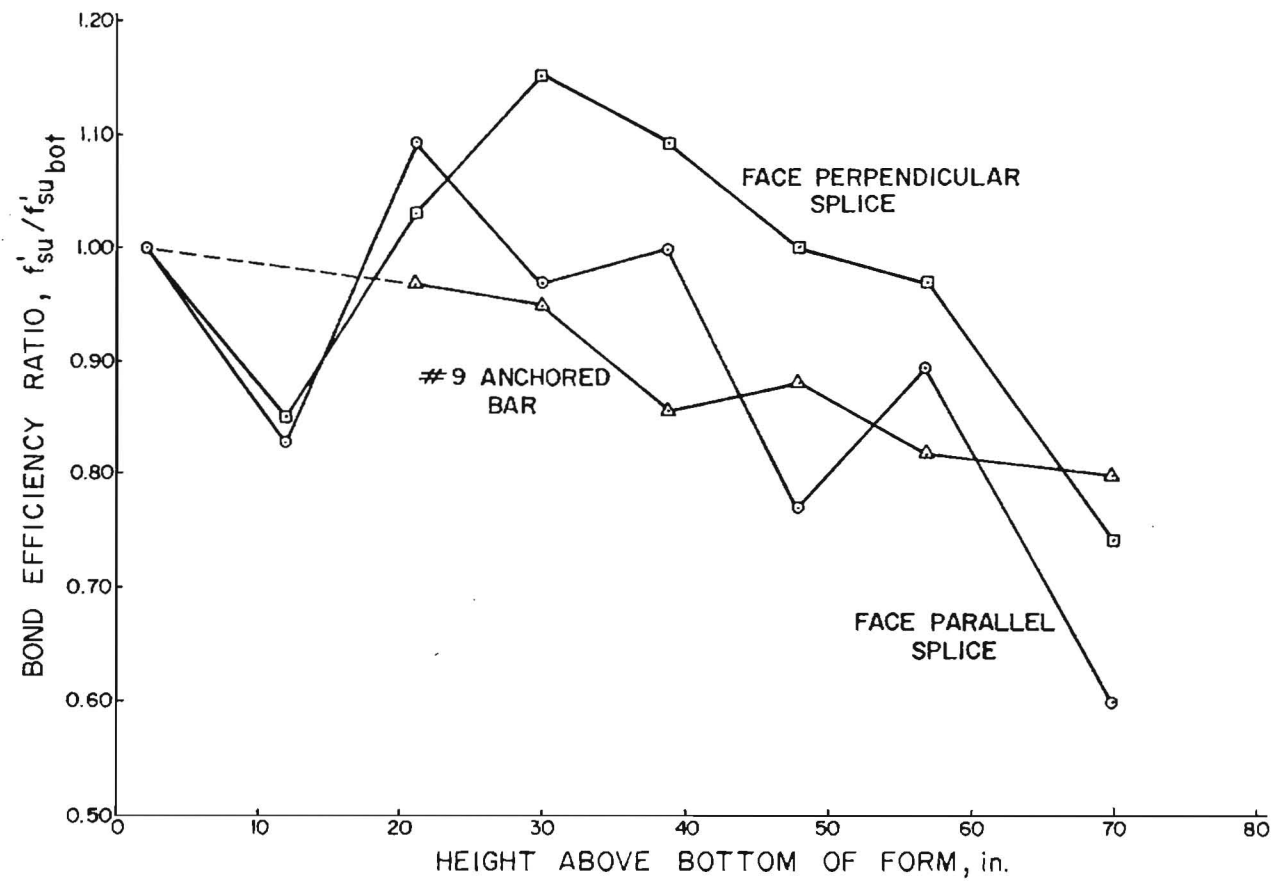


Fig. 6.10 Bond efficiency ratio vs. height for splice and development tests

It was expected that there would be some complications because of the orientations of the splices (for example, the face-perpendicular splices on the sides of the specimen were oriented parallel to the bottom of the specimen while the top and bottom face-perpendicular splices were oriented perpendicular to it). However, the values of ultimate load capacity for both types of splices in the bottom position are very nearly equal. In the limiting case--that is, the top bar and splice values relative to the values of respective bottom tests--the splices appear to show a larger drop in capacity than the anchored bars. It cannot be directly concluded, though, that splices are influenced more by casting position than anchored bars. It is likely that the relative inferiority of the splices results from the fact that the splice test specimens were cast with a slump of 5.5 in. while the anchored bar specimen was cast with a slump of 3 in.

## C H A P T E R 7

### SUMMARY AND CONCLUSIONS

#### 7.1 Summary

The primary objective of this study was to evaluate the effect of casting position, concrete consistency, and bar orientation on the bond strength of horizontally embedded deformed bars. The magnitude of bond strength reduction with top casting, as a function of the amount of concrete cast below the bar, was investigated in a series of four test specimens.

Three specimens consisting of 72-in. high and 56-in. long wall panels were cast vertically. Bars were placed horizontally and held rigidly during casting. A test specimen included bars on either side with the same anchorage length, bar diameter, and clear cover. The only variation in a given specimen was in casting position. Three bar sizes were investigated, #7, #9 and #11. Both low slump (3 in.) and high slump (8-1/2 in.) concrete were utilized. One specimen contained bars in a vertical and horizontal position with the vertical bars loaded either in the direction of concrete settlement or against settlement. Bars were tested in sequence in an arrangement simulating flexure. The bond strengths of bars at different casting positions were compared to the bond strength of a bottom cast bar or splice at ultimate. A series of trial specimens was conducted to develop test details which would ensure the same mode of failure for all bars in a test specimen to make bond strength comparisons valid. A total of 60 bars in development and 16 lap splices were tested.

#### 7.2 Conclusions

Based on the test results and observations of the specimens tested, the following conclusions were drawn:

(1) The bond strength decreased with an increase in the depth of concrete cast below the bar. The bar size had very little effect on the pattern of strength reduction with height.

(2) Changes in slump were found to influence significantly the effect of the depth of concrete cast below bars and splices. The higher the slump, the greater the reduction in bond capacity as the depth of concrete was increased.

(3) The effects of bar orientation were two-fold. First, that the vertical bar pulled with and pulled against the direction of concrete settlement showed less reduction of ultimate bond capacity than horizontal bars when the depth of concrete cast below was increased from 18 to 48 in. Second, in all cases, the vertical bars displayed less actual bond capacity than horizontal bars at the same level.

(4) The use of arbitrary values of slip as a failure criterion, rather than ultimate values, gave significantly different values for the effect of the depth of concrete cast below the bar. In general, the lower the level of slip used as a criterion, the greater the calculated effect of casting position.

(5) The current design specification for top cast bars appears to be conservative when compared with the test results for 3 in. slump concrete. Even for a bar located about 70 in. above the bottom of the form, the 40 percent increase in development length specified in the ACI Code (318-77) [4] for a "top bar" is very large.

(6) Bar size did not appear to change the observed effects of casting position. The sharp reduction in bond capacity of the #7 bar in the upper levels of the specimen appeared to result more from the effects of concrete shrinkage on the small bar cover than from the effect of bar size.

(7) The response of lapped splices did not appear to be significantly different from the response of anchored bars. Stacked splices showed no superiority to the side-by-side splices when both were placed in the bottom of the specimen. However, the stacked splices showed significantly greater capacity when placed in the top of the specimen because of the greater amount of weak concrete buildup under the side-by-side splice.

## REFERENCES

1. Abrams, D. A., "Tests of Bond Between Concrete and Steel," Bulletin 71, Engineering Experiment Station, University of Illinois, 1913.
2. ACI Committee 318, "Building Code Requirements for Reinforced Concrete (ACI 318-47)," Journal of the American Concrete Institute, Proc. V. 19, Sept. 1947.
3. ACI Committee 318, "Building Code Requirements for Reinforced Concrete (ACI 318-51)," Journal of the American Concrete Institute, Proc. V. 47, April 1951.
4. ACI Committee 318, Building Code Requirements for Reinforced Concrete (ACI 318-77), American Concrete Institute, Detroit, 1977. (Same reference title for ACI 318-57, ACI 318-63, and ACI 318-71.)
5. ACI Committee 408, "Bond Stress--The State of the Art," Journal of the American Concrete Institute, Proc. V. 63, Nov. 1966.
6. ACI-ASME Technical Committee Report on Concrete Pressure Components for Nuclear Service. Internal Memo.
7. American Society for Testing and Materials, "Deformed and Plain Billet-Steel Bars for Concrete Reinforcement, ASTM A615-76a.
8. Chinn, J., Ferguson, P. M., and Thompson, J. W., "Lapped Splices in Reinforced Concrete Beams," Journal of the American Concrete Institute, Proc. V. 52, No. 2, October 1955.
9. Clark, A. P., "Comparative Bond Efficiency of Deformed Concrete Reinforcement Bars," Journal of the American Concrete Institute, Proc. V. 43, No. 4, December 1946.
10. Clark, A. P., "Bond of Concrete Reinforcing Bars," Journal of the American Concrete Institute, Proc. V. 46, No. 3, November 1949.
11. Collier, S. T., "Bond Characteristics of Commercial and Prepared Reinforcing Bars," Journal of the American Concrete Institute, Proc. V. 43, June 1947.
12. Edwards, L. N., and Greenleaf, H. L., "Experimental Tests of Concrete-Steel Bond," American Society for Testing and Materials (ASTM), Proc. V. 28, II, 1928.
13. Ferguson, P. M., Breen, J. E., and Thompson, J. N., "Pull-out Tests on High Strength Reinforcing Bars," Journal of the American Concrete Institute, Proc. V. 62, No. 8, August 1965.

14. Ferguson, P. M., Breen, J. E., and Thompson, J. N., "Comparative Bond Efficiency of Large High-Strength Deformed Bars," Unpublished Report of Bureau of Engineering Research, The University of Texas at Austin, February 1962.
15. Ferguson, P. M., and Breen, J. E., "Lapped Splices for High Strength Reinforcing Bars," Journal of the American Concrete Institute, Proc. V. 62, No. 9, September 1965.
16. Ferguson, P. M., and Briceno, E. A., "Tensile Lap Splices--Part 1: Retaining Wall Type, Varying Moment Zone," Research Report 113-2, Center for Highway Research, The University of Texas at Austin, July 1969.
17. Ferguson, P. M., and Thompson, J. N., "Development Length of High Strength Reinforcing Bars in Bond," Journal of the American Concrete Institute, Proc. V. 59, No. 7, July 1962.
18. Ferguson, P. M., and Krishnaswamy, C. N., "Tensile Lap Splices--Part 2: Design Recommendations for Retaining Wall Splices and Large Bar Splices," Research Report 113-3, Center for Highway Research, The University of Texas at Austin, April 1971.
19. Ferguson, P. M., and Thompson, J. N., "Development Length of Large High Strength Reinforcing Bars," Journal of the American Concrete Institute, Proc. V. 62, No. 1, January 1965.
20. Ferguson, P. M., Reinforced Concrete Fundamentals, 3rd ed., John Wiley and Sons, Inc., New York, 1972.
21. Gilkey, H. J., Chamberlin, S. J., and Beal, R. W., "The Bond Between Concrete and Steel," Journal of the American Concrete Institute, Proc. V. 35, No. 1, September 1938.
22. Goto, Y., "Cracks Formed in Concrete Around Deformed Tension Bars," Journal of the American Concrete Institute, Proc. V. 68, No. 4, April 1971.
23. Hajnal-Kónyi, K., "Bond Between Concrete and Steel," Paper presented to Reinforced Concrete Association, London, November 1962.
24. Commissie voor Uitvoering van Research Ingesteld door de Betonvereniging, "Onderzoek naar de Samenwerking van geprofileerd staal met beton," Report No. 23, 1963, The Netherlands (Translation No. 112, 1964, Cement and Concrete Association, London, "An Investigation of the Bond of Deformed Steel Bars with Concrete").

25. Hognestad, E., and Siess, C. P., "Effect of Entrained Air on Bond Between Concrete and Reinforcing Steel," Journal of the American Concrete Institute, Proc. V. 46, No. 8, April 1950.
26. Kluge, R. W., and Tuma, E. C., "Lapped Bar Splices in Concrete Beams," Journal of the American Concrete Institute, Proc. V. 42, No. 1, September 1945.
27. Losberg, A., "Bond Failure of Deformed Reinforcement Bars Based on the Longitudinal Splitting Effect of the Bars," Unpublished Research Report Presented at the American Concrete Institute Fall Convention, October, 1976.
28. Lutz, L. A., and Gergely, P., "Mechanics of Bond and Slip of Deformed Bars in Concrete," Journal of the American Concrete Institute, Proc. V. 64, March 1964.
29. Mathey, R. G., and Watstein, D., "Investigation of Bond in Beam and Pull-out Specimens with High Yield-Strength Deformed Bars," Journal of the American Concrete Institute, Proc. V. 57, No. 9, March 1961.
30. Menzel, C. A., "Some Factors Influencing Results of Pull-out Bond Tests," Journal of the American Concrete Institute, Proc. V. 35, June 1939.
31. Minor, J., and Jirsa, J. O., "Behavior of Bent Bar Anchorages," Journal of the American Concrete Institute, Proc. V. 72, No. 4, April 1975.
32. Mylrea, T. D., "Bond and Anchorage," Journal of the American Concrete Institute, Proc. V. 44, No. 7, March 1948.
33. Orangun, C. O., Jirsa, J. O., and Breen, J. E., "The Strength of Anchored Bars: A Reevaluation of Test Data on Development Length and Splices," Research Report 154-3F, Center for Highway Research, The University of Texas at Austin, January 1975.
34. Park, R., and Paulay, T., Reinforced Concrete Structures, John Wiley and Sons, Inc., New York, 1975.
35. Reese, R. C., "New Style Deformed Reinforcing Bars," Journal of the American Concrete Institute, Proc. V. 46, No. 9, May 1950.
36. Rehm, G., "Über die Grundlagen des Verbundes Zwischen Stahl und Beton," Report No. 138, Deutscher Ausschuss für Stahlbeton, 1961, The Netherlands (Translation No. 134, 1968, Cement and Concrete Association, London, "The Basic Principles of the Bond Between Steel and Concrete").

37. Richart, F. E., "Hi-Bond Reinforcing Bars," Published by Inland Steel Co., 1928.
38. Tepfers, R., "A Theory of Bond Applied to Overlapped Tensile Reinforcement Splices for Deformed Bars," Publication 73:2, Division of Concrete Structures, Chalmers University of Technology, 1973.
39. Tepfers, R., "Cracking of Concrete Cover Along Anchored Deformed Reinforcing Bars," Magazine of Concrete Research, V. 31, No. 106, March 1979.
40. Welch, G. B., and Patten, B. J. F., "Reduction in Concrete-Steel Bond with Horizontally Embedded Reinforcement," UNCIV Report No. R-8, The University of New South Wales, February 1967.
41. Zipprodt, R. R., Posey, C. J., Abeles, P. W., Gilkey, H. J., and Clark, A. P., Discussion of "Comparative Bond Efficiency of Deformed Concrete Reinforcing Bars," by Clark, A. P., Journal of the American Concrete Institute, Proc. V. 43, June 1947.

## A P P E N D I X A

### DIMENSIONING THE TEST SPECIMENS

#### A.1 General

Specimen geometry has always been a very important factor in bond studies. It affects both the type of failure or crack pattern and the bond strength of anchored bars. Ferguson and Thompson [17,19] found that a single #7 bar in an 18-in. wide beam and a single #11 bar in a 24-in. beam failed in bond splitting. Based mainly on the work by Ferguson and Thompson, ACI Committee 408 [5] considered the problem of specimen geometry. The committee report indicated that a single bar under tension would split a wide beam as is shown in Fig. A.1(a). The report mentioned that a #3 bar in a 6-in. width, a #7 bar in a 16-in. or 18-in. width, or a #11 bar in a 24-in. width seemed to follow this failure pattern. Figure A.1(b) shows the failure pattern of a single tension bar in a "very wide" beam. The report could not bound the term "very wide" due to the lack of test data.

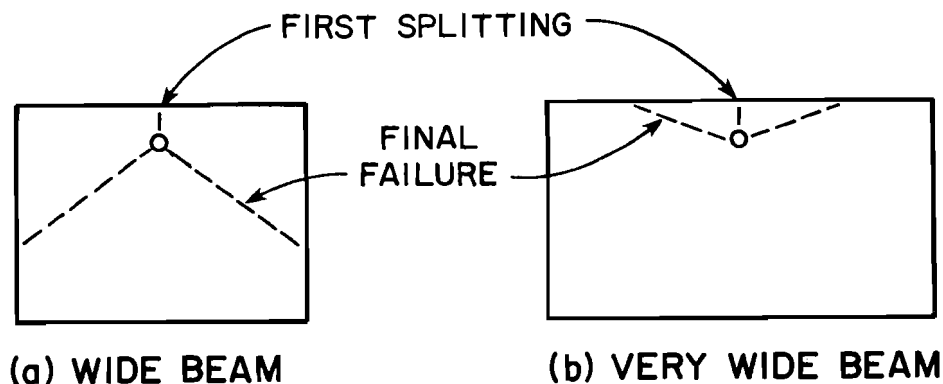


Fig. A.1 Splitting cracks for a single tension bar,  
ACI Committee 408 [5]

At the time this study started, the specimen dimensions were based on the background information discussed above. Two important conditions had to be satisfied to meet the objectives of the study:

(1) The mode of failure of the middle top and bottom bars should be the same as that of the side bars so that realistic comparisons of the stresses could be made.

(2) The spacing between adjacent side bars should be large enough to minimize the interaction of splitting cracks which would invalidate the test data.

## A.2 Trial Specimens

The first Specimen T0 built was a 72-in. high, 56-in. long, and 15-in. wide wall panel with a bar arrangement shown in Fig. A.2. Figure A.3 shows the formwork with the bars in place before placing the other side form. Twenty-four #7 bars, twelve on each side, were placed with a 1-in. side and bottom cover. The spacing between adjacent side bars was 12 in. No middle top bar was placed in Specimen T0. The bar arrangement on one end was a mirror image of the bar arrangement on the other end; that is, for every casting position the wall specimen included two test bars, one on either end. This was done to check the reliability of the loading system and the uniformity of the concrete mix. The anchorage length used, 17.5 in., was based on assuming an ultimate concrete compression strength of 3000 psi and a steel stress of 40 ksi (see Table 3.1). However, the 28-day strength was almost 4000 psi.

The loading system worked as expected. After testing the side bars, it was clear that the results were not as useful as anticipated based on the following observations:

(1) The 12-in. bar spacing did not prove to be large enough. Splitting cracks radiating out from one test bar intersected yet untested bars, thus invalidating the test results of these bars (see Fig. A.4). Moreover, the concrete face on which the compression plate was supposed to bear was not

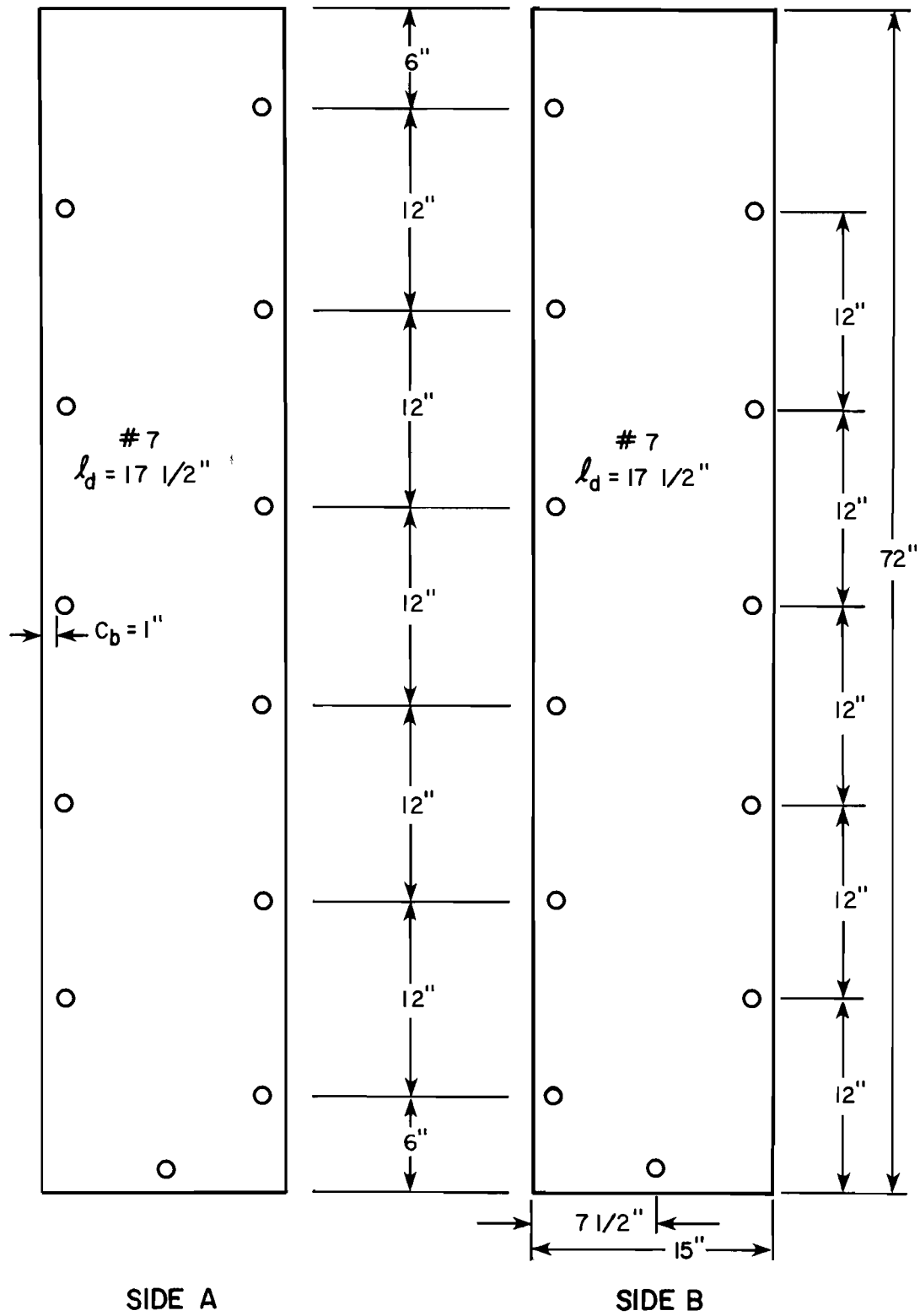


Fig. A.2 Bar arrangement in Specimen T0

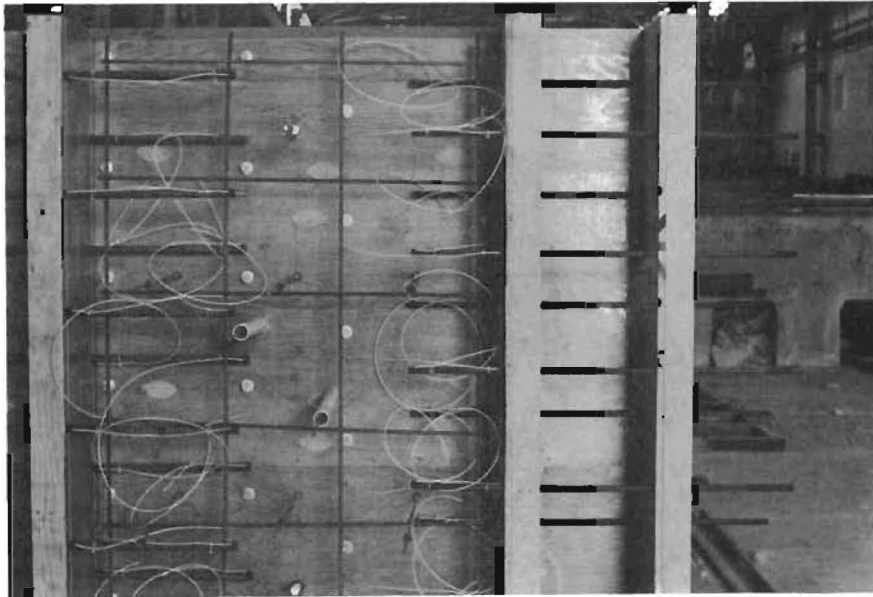


Fig. A.3 Specimen T0 prior to casting

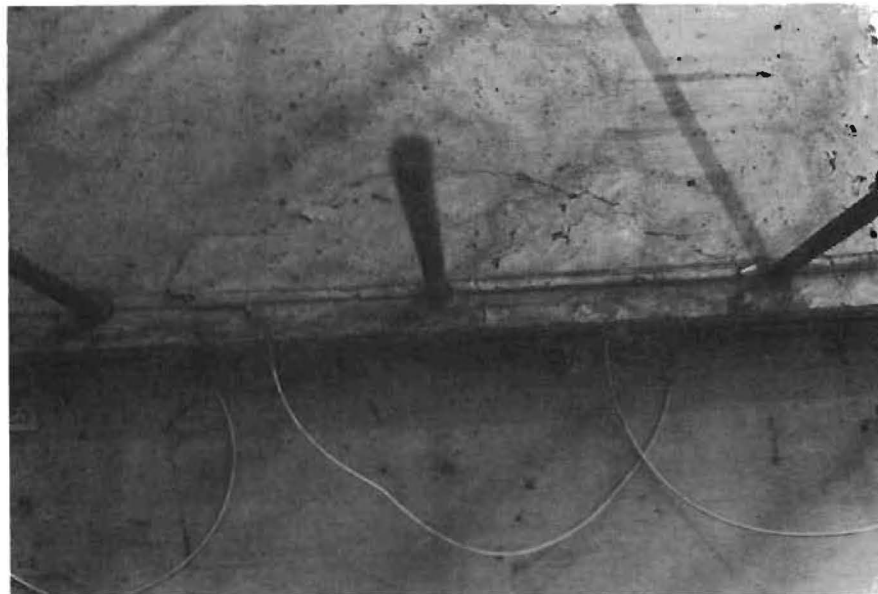


Fig. A.4 Splitting cracks radiating out from one test bar intersecting adjacent untested bar in Specimen T0

sound due to the cracking from the layer of side bars already tested.

(2) A few bars yielded although the anchorage length was chosen to force splitting failure for all test bars. This resulted in even wider and more scattered cracks along the bar and in the test zone. Yielding of a few bars could be related to the higher ultimate concrete compression strength than that used in the anchorage length calculation. This increase counteracted the reduction in the steel stress used in the calculated development lengths.

The crack interaction due to the close spacing of adjacent test bars and yielding of some test bars also seemed to affect the soundness of the area of concrete where the free end slip gage assembly was to be mounted. That zone of concrete could no longer be considered as a stable reference plane, thus invalidating the readings of the slip potentiometer.

(3) The middle bottom bar was not tested on either side of the wall specimen due to the fact that cracks from the nearby side bars intersected the untested bottom bars.

(4) The specimen width, 15 in., seemed to be unsatisfactory since the cracks radiating from some side bars on one layer tended to intersect untested bars on the other layer about a specimen width away.

(5) Bars 6 in. from the top and bottom, on either side of the wall specimen, split the adjacent corner upon failure. The failure occurred at relatively low loads.

After T0 was tested, the specimen was redesigned. The following modifications were considered:

(1) The bar spacing on a given side was increased from 12 in. to 18 in. and the specimen width was increased from 15 in. to 21 in. This was done primarily to prevent the crack pattern of one test bar from spreading into the test zone of adjacent bars or bars in a layer about a specimen width away.

(2) To help in minimizing the spread of cracks, a series of supplementary transverse bars similar to stirrups in the form of zigzag #3 bars was added

to the specimen design. The transverse bars did not cross the immediate failure zone of a test bar and did not provide confinement for edge splitting cracks.

(3) To make sure that the bars would not yield due to an unexpected high concrete strength; i.e., all would exhibit a brittle splitting failure, the calculated anchorage length based on a concrete compression strength of 3000 psi and a steel stress two-thirds of yield were further reduced as shown in Table 3.1. The reduction of anchorage lengths does not affect the objectives of the study as long as the bars all have the same embedment length.

Three specimens, T1, T2 and T3, were cast utilizing the above modifications. These three specimens were 72-in. high, 56-in. long, and 21-in. wide. Figures A.5 and A.6 show the bar arrangement on one side of each of the three wall specimens. The bar arrangement on the other side was a mirror image of the one shown for each of the specimens.

Specimen T1 was the first specimen to be tested in the revised series. After testing the side bars, it was obvious that the middle top and bottom bars would be invalid tests since the cracks from bars at  $z = 57$  in. and  $z = 12$  in. spread into the test zones of the middle top and bottom bars (see Figs. A.7 and A.8). Subsequently, these bars were tested, and as anticipated gave low strengths. The sequence of testing was changed in later specimens to get more valid information about the mode of failure of the middle top and bottom bars.

Side bars in all three test specimens gave a V-notch type of failure (see Fig. A.9) and exhibited a reduction of bond strength with increase in depth of concrete below the test bar. The ultimate bond strengths of bars at the same casting position on either end of the specimens were less than 10 percent different. Cracks seemed to be better contained; that is, interaction was avoided in most cases (see Fig. A.9). The result from T1-T3 supported the use of the supplementary transverse zigzag #3 bars. Figures A.10 and A.11 show the additional reinforcement in place before casting.

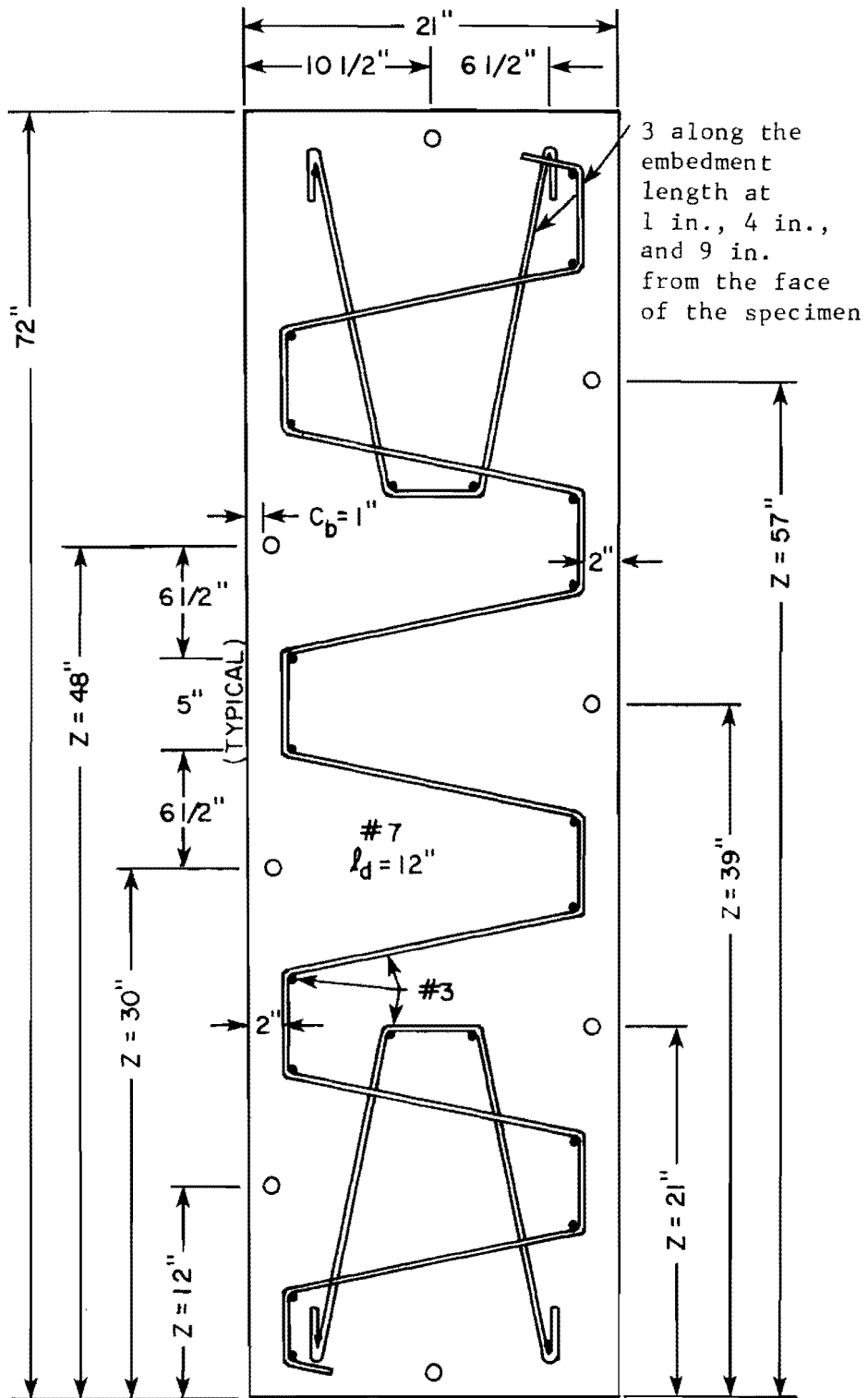


Fig. A.5 Bar arrangement on one side of Specimen T1

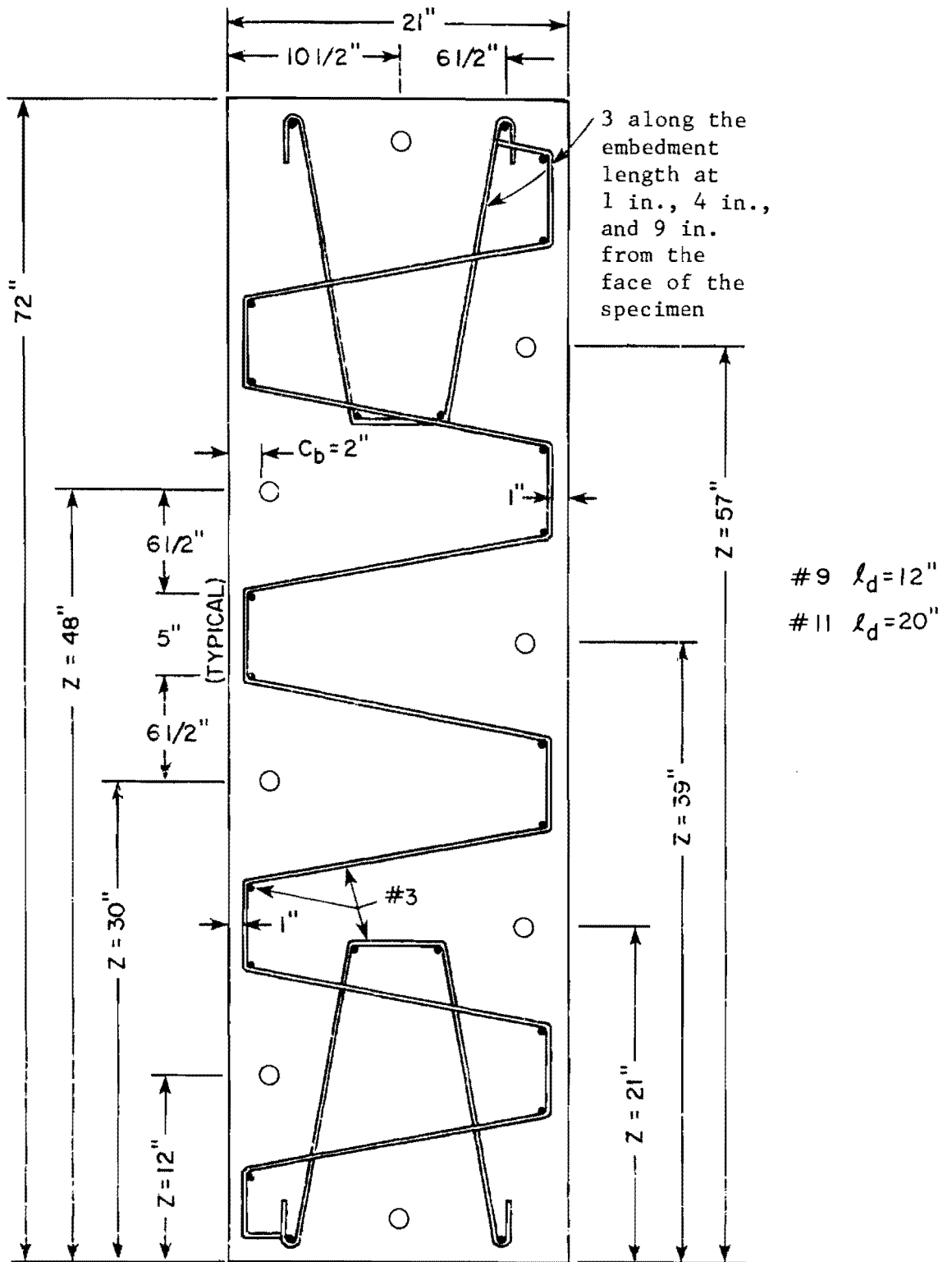


Fig. A.6 Bar arrangement on one side of trial Specimen T3

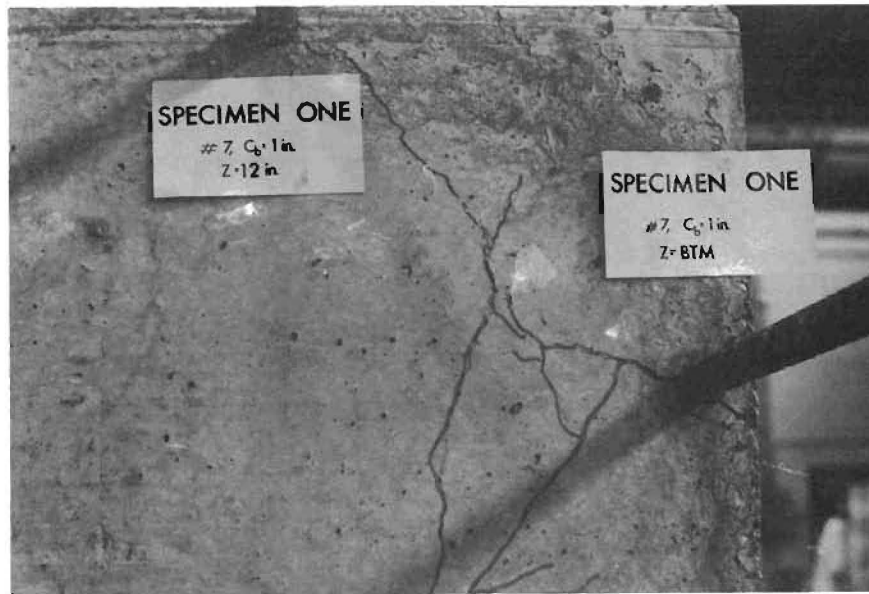
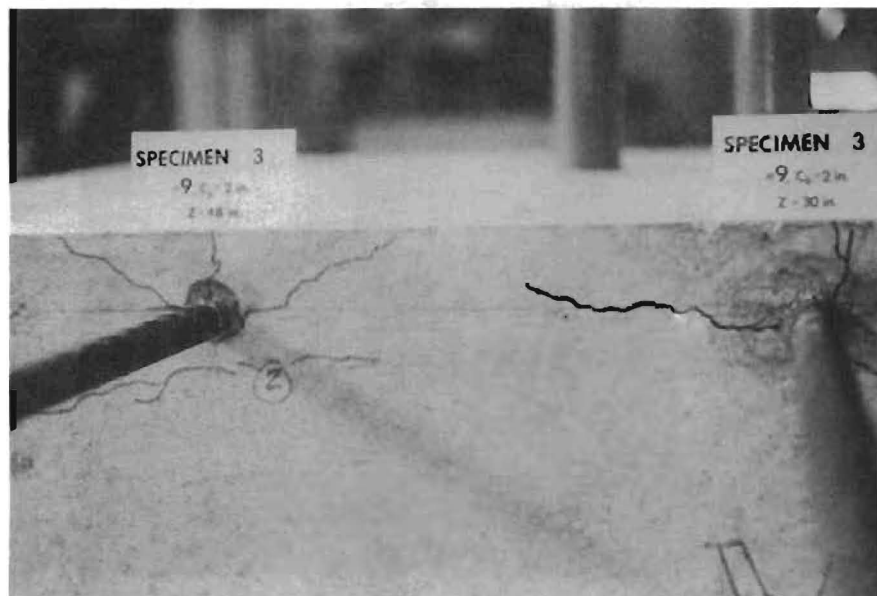


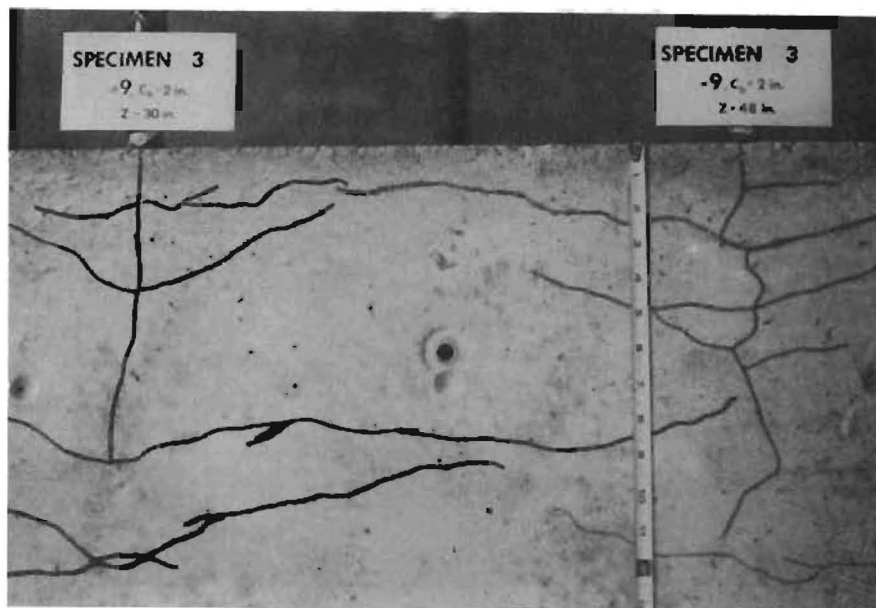
Fig. A.7 Cracks from bar at  $z = 12$  in. spreading into the test zone of the middle bottom bar, Specimen T1



Fig. A.8 Cracks from bar at  $z = 57$  in. spreading into the test zone of the middle top bar, Specimen T1



(a) Side view



(b) Top view

Fig. A.9 V-notch splitting mode of failure for side bars of Specimen T3

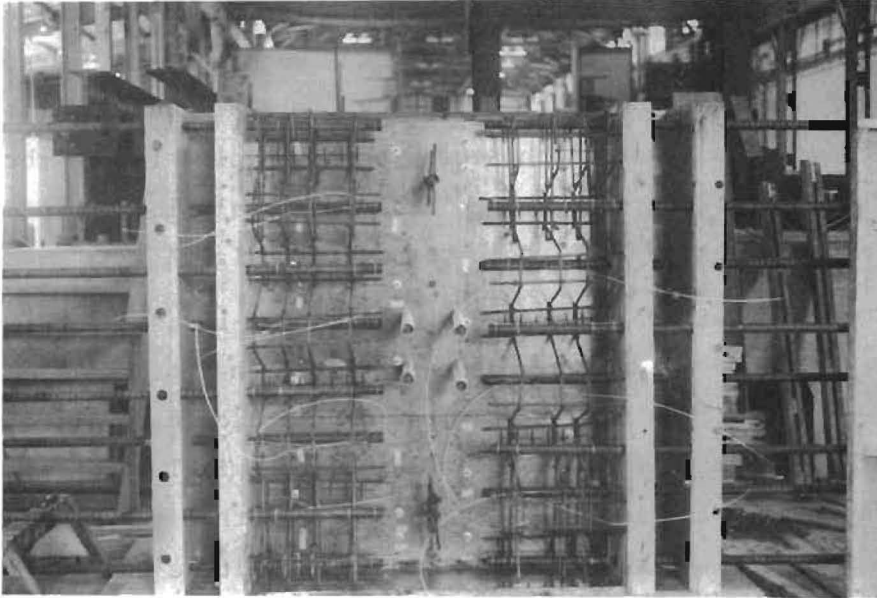


Fig. A.10 Specimen T2 with the additional #3 reinforcement in place



Fig. A.11 Additional #3 reinforcement on one side of Specimen T3

The slip measurement setup worked as anticipated and the concrete zone where the free end slip gage assembly was mounted remained sound. The reduction in the embedment length of the test bars prevented all bars from yielding. The only test bar which seemed to be invalid in the three test specimens was at  $z = 12$  in. It failed at a relatively low stress with the cracks tending to break off the whole corner (see Fig. A.12).

The mode of failure exhibited by the middle top and bottom bars of Specimens T2 and T3 was completely different from that of the side bars; that is, a V-notch failure similar to that of the side bars did not take place. Figure A.13 shows the crack pattern of the middle top and bottom bars. The observed splitting appeared to indicate that the width of the specimen, 21 in., fit the term "wide" that ACI Committee 408 [5] described in its 1966 report.

Even though the middle top and bottom bars could be compared to each other, the significant difference between the modes of failure made the comparison between the test values of all test bars on a given side of a specimen impossible and invalidated the main objective of the study. Test results of Specimen T1 are shown in Table A.1 and Fig. A.14, those of Specimen T2 are shown in Tables A.2 and A.3 and Fig. A.15, and those of Specimen T3 are shown in Tables A.4 and A.5 and Fig. A.16.

### A.3 Final Dimensions of the Test Specimens

Specimens T1-T3 were based on the design modifications concluded after testing Specimen T0 and performed better than the initial Specimen T0. The modifications proved to isolate the side bars fairly well, but the failure of the middle top and bottom bars was different from that of the side bars.

A further redesign of the wall specimen was undertaken with the following modifications:

- (1) The specimen width was increased from 21 in. to 36 in. This was done to get a "very wide" specimen as far as the middle top and bottom bars were

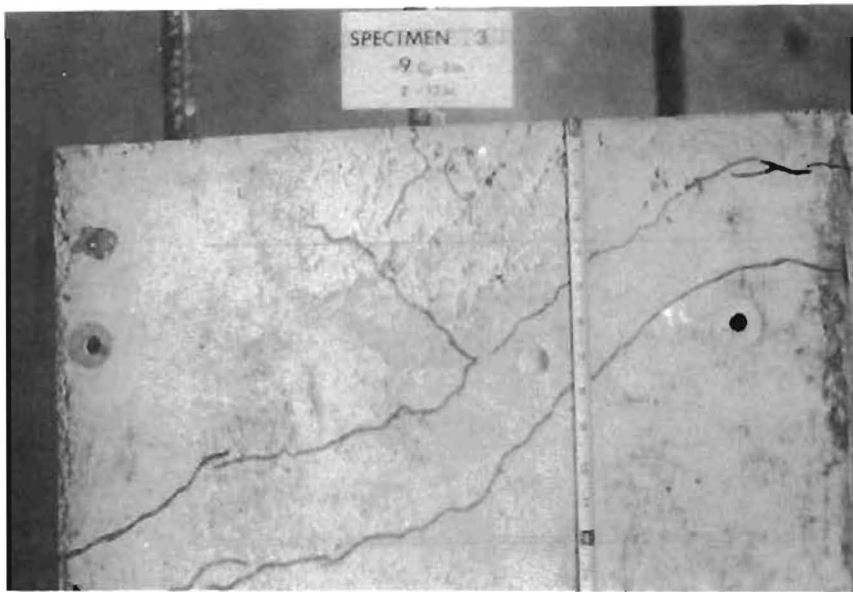


Fig. A.12 Corner-splitting mode of failure of bar at  $z = 12$  in., Specimen T3



Fig. A.13 Typical crack pattern of the middle top and bottom bars of trial Specimen T2

TABLE A.1 TEST RESULTS OF SPECIMEN T1

z in.	$P_u$ kips	$f_{su}$ ksi
21	26	44
30	23	38
39	21	35
48	21	34
57	20	33

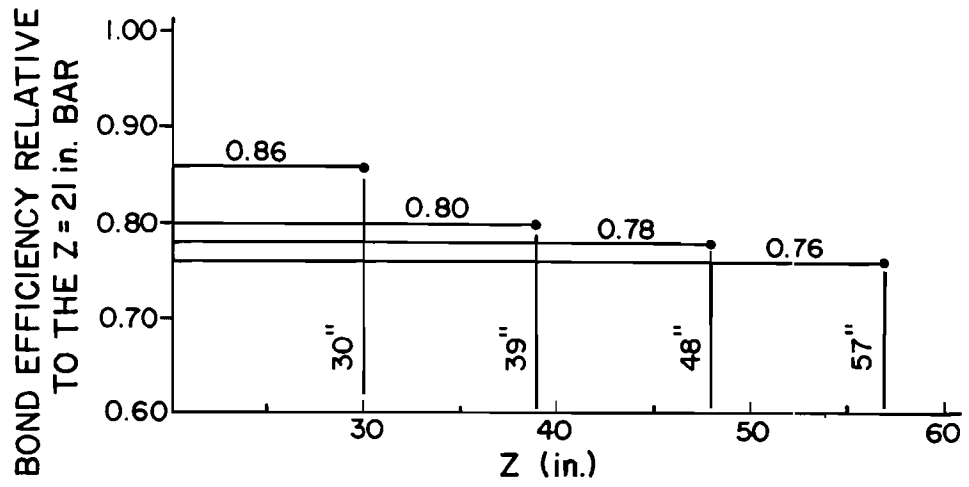


Fig. A.14 Test results of Specimen T1

TABLE A.2 TEST RESULTS OF MIDDLE TOP AND BOTTOM BARS OF SPECIMEN T2

	$P_u$ kips	$f_{su}$ ksi	Bond efficiency relative to bottom bar
Middle bottom bar	51	33	1.00
Middle top bar	40	26	0.78

TABLE A.3 TEST RESULTS OF SIDE BARS OF SPECIMEN T2

z in.	$P_u$ kips	$f_{su}$ ksi
21	58	37
30	55	35
39	53	34
48	52	33
57	47	30

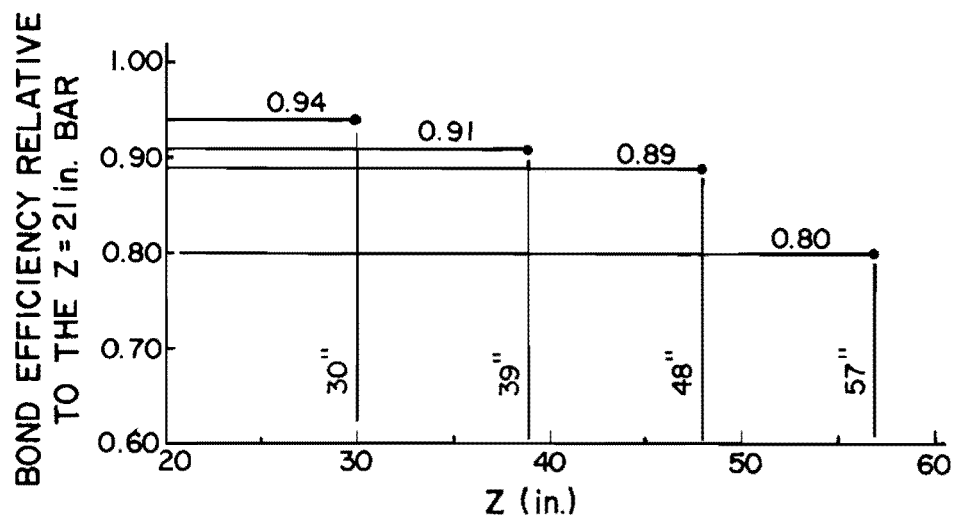


Fig. A.15 Test results of Specimen T2

TABLE A.4 TEST RESULTS OF MIDDLE TOP AND BOTTOM BARS OF SPECIMEN T3

	$P_u$ kips	$f_{su}$ ksi	Bond efficiency relative to bottom bar
Middle bottom bar	29	29	1.00
Middle top bar	25	25	0.85

TABLE A.5 TEST RESULTS OF SIDE BARS OF SPECIMEN T3

$z$ in.	$P_u$ kips	$f_{su}$ ksi
21	34	34
30	32	32
39	31	31
48	30	30
57	27	27

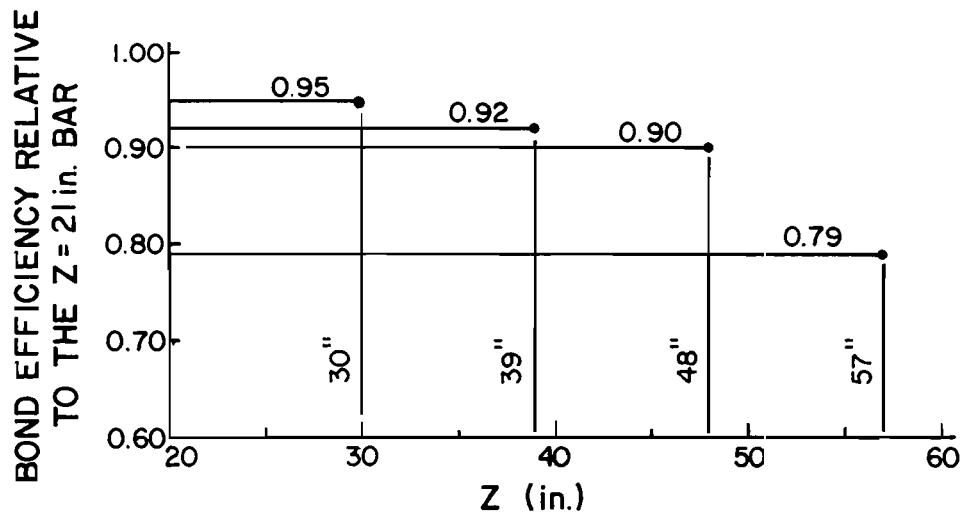


Fig. A.16 Test results of Specimen T3

concerned to force a V-notch mode of failure similar to that of the side bars.

(2) More supplementary reinforcement in the form of zigzag #3 bars was placed along the anchorage length of the test bars in an effort to control the cracking of the middle top and bottom bars and the bar at  $z = 12$  in.

Specimens D1-D3 were constructed using these dimensions. Specimen D1 had #11 bars at a side and bottom cover of 2 in. The bar arrangement on one side was a mirror image of that on the other side to check the uniformity of the concrete mix and the reliability of the loading system. With the exception of the bar at  $z = 12$  in., the specimen performed satisfactorily. The middle top and bottom bars did not split out the shoulders and a failure quite similar to that of the side bars occurred. Specimen D2 had #7 bars with a 1-in. cover on one end and #9 bars with a 2-in. cover on the other end. This specimen also performed satisfactorily. The bar at  $z = 12$  in. still showed a corner effect on the end with the #9 bars. Figure 4.9 shows the dimensions and reinforcement used in the D-series.

This page replaces an intentionally blank page in the original.

-- CTR Library Digitization Team

## A P P E N D I X B

### MATERIALS

#### B.1 Concrete

The concrete mix was designed to meet the Texas Highway Department Standard Specifications for Class A non-air entrained concrete with a specified minimum compression strength ( $f_c'$ ), at twenty-eight days of age, of 3000 psi. These specifications required a slump range of 2.0 to 4.0 in. which would result in a relatively dry mix. A stiff mix would generally lead to a high bond strength. However, an improvement in bond stress at failure with a stiff mix can only be expected when the concrete is placed very carefully around the bar by proper vibration during the casting process.

Before casting any specimen, several concrete mixes were tried in the lab using a half cubic yard commercial mixer. The trials were done to achieve a mix design meeting both requirements of minimum compression strength at 28 days, of 3000 psi, and a slump within the range of 2.0 to 4.0 in. In these trials high-early strength cement was used meeting the current standard specifications of ASTM for Type III cement. The intention was that using Type III cement, the 7-day compression strength, based on standard 6 x 12 cylinders, might approximate the 28-day compression strength had cement meeting the current standard specifications of ASTM for Type I cement been used. Type III cement was used to avoid some time delay in deciding the desired mix design. Sand and gravel were of the same properties as those used later in all mix designs. Colorado River sand, largely siliceous, was used. Colorado River gravel, 1.0 in. maximum size, was used. The gravel was largely a hard limestone gravel with some quartz and siliceous particles.

After several mix trials to get a 7-day compressive strength of 3000 psi and a slump in the range 2.0 to 4.0 in., the following mix design was chosen to be satisfactory:

Cement (Type III)	358 lb./cu. yd.
Coarse Aggregate	1847 lb./cu. yd.
Fine Aggregate	1484 lb./cu. yd.
Water	293 lb./cu. yd.

Average 7-day compression strength = 2900 psi  
 Slump  $\approx$  3.0 in.

The above mix design was used for proportioning the concrete mix for Specimen T0. However, cement used for trial specimens T1, T2 and T3 met the current standard specifications of ASTM for Type I cement. Type III cement was used for test specimens D1 and D2. It should be noted that the amount of water ordered from the readymix plant was about 80 percent of the calculated amount. Upon arrival of the truck carrying the concrete mix, and before casting, additional water was added in small increments until the desired slump of about 3.0 in. was reached. While adding water to the concrete mix for Specimen D1, the sensitivity of the slump to the amount of water was observed. Mix designs and the variation in strength with time for all test specimens are presented in this appendix.

#### Concrete Mix Design

Texas Highway Department Standard Specifications for Class A concrete were used. General characteristics common to all mix designs used are

(1) Non-air entrained concrete

(2) Minimum compressive strength ( $f'_c$ )

Using Type I cement = 3000 lb./sq. in., at 28 days of age

Using Type III cement = 3000 lb./sq. in., at 7 days of age

(3) Desired Slump = 2 in. to 4 in.

(4)  $G_s$  = Specific Gravity

= 2.61 Coarse Aggregate

= 2.61 Fine Aggregate

= 3.10 Cement

(5) Concrete Yield =  $\frac{(\text{cu. ft.})}{(\text{cu. yd.})} \div (\text{cement factor})$   
 =  $27 \div (\text{cement factor})$

- (6) Volume Fine Aggregate = Mortar - Paste  
 Mortar = Concrete Yield - Coarse Aggregate  
 Paste = Water + Cement + Air
- (7) Weight (lb./sac) = Volume (cu. ft./sac)  
 $\times$  Water density (lb./cu. ft.)  
 $\times G_s$
- Water density = 62.4 lb./cu. ft.

## B.2 Steel

The requirements for deformations of a deformed bar meeting the ASTM A615-76a are the following [7]:

- 5.1 Deformations shall be spaced along the bar at substantially uniform distances. The deformations on opposite sides of the bar shall be similar in size and shape.
- 5.2 The deformations shall be placed with respect to the axis of the bar so that the included angle is not less than 45 degrees. Where the line of deformations forms an included angle with the axis of the bar of from 45 to 70 deg. inclusive, the deformations shall alternately reverse in direction on each side, or those on one side shall be reversed in direction from those on the opposite side. Where the line of deformation is over 70 deg. a reversal in direction is not required.
- 5.3 The average spacing or distance between deformations on each side of the bar shall not exceed seven-tenths of the nominal diameter of the bar.
- 5.4 The overall length of deformations shall be such that the gap between the ends of the deformations on opposite sides of the bar shall not exceed 12-1/2 percent of the nominal perimeter of the bar. Where the ends terminate in a longitudinal rib, the width of the longitudinal rib shall be considered the gap. Where more than two longitudinal ribs are involved, the total width of all longitudinal ribs shall not exceed 25 percent of the nominal perimeter of the bar; furthermore, the summation of gaps shall not exceed 25 percent of the nominal perimeter of the bar. The nominal perimeter of the bar shall be 3.14 times the nominal diameter.

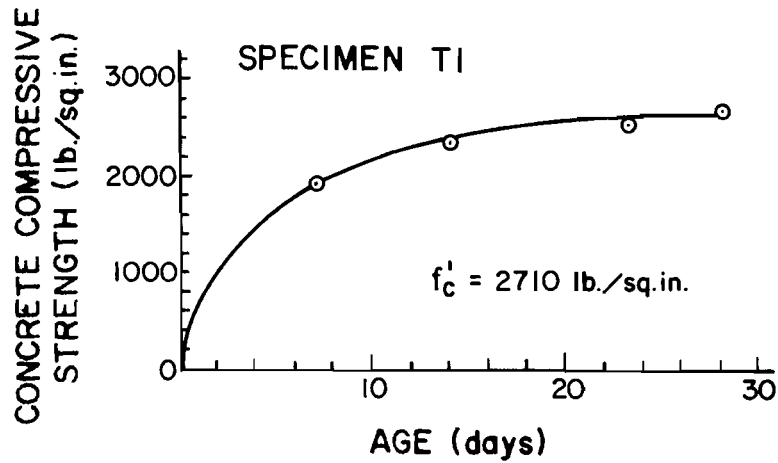


Fig. B.1 Variation of concrete compression strength with age--Specimen T1

TABLE B.1 CONCRETE MIX DESIGN FOR SPECIMEN T1

Material	Batch Design			Full Size Batch lb./cu. yd.
	Volume cu. ft./sac	% Volume	Weight lb./sac	
Coarse Agg.	2.976	42.0	484.7	1847
Water	1.234	17.4	77.01	293
Cement	0.486	6.9	94.0	358
Air	0.0	0.0	0.0	0
Fine Agg.	2.392	33.7	389.6	1484

Cement Factor = 3.81 sac/cu. yd.

Water Factor = 9.26 gal./sac

Water/Cement (by weight) = 0.82

Actual Water Factor used = 7.87 gal./sac

Actual Water/Cement used = 0.70

Slump = 6.0 in.

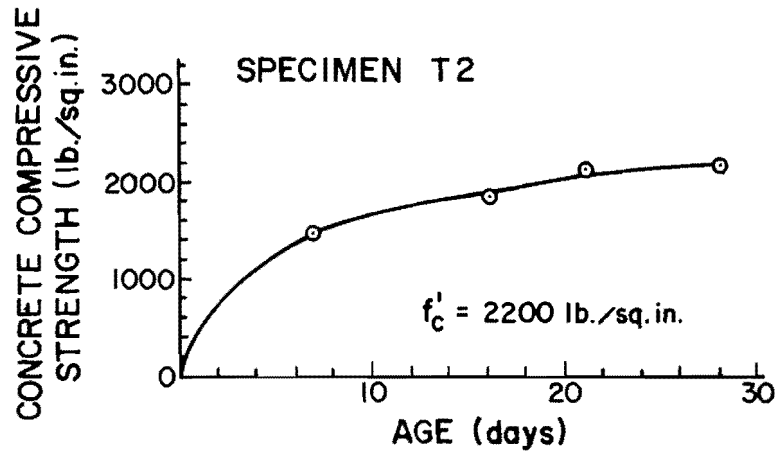


Fig. B.2 Variation of concrete compression strength with age--Specimen T2

TABLE B.2 CONCRETE MIX DESIGN FOR SPECIMEN T2

Material	Batch Design			Full Size Batch lb./cu. yd.
	Volume cu. ft./sac	% Volume	Weight lb./sac	
Coarse Agg.	3.121	43.3	508.3	1906
Water	1.085	15.1	57.7	254
Cement	0.486	6.8	94.0	353
Air	0.0	0.0	0.0	0
Fine Agg.	2.509	34.8	408.6	1532

Cement Factor = 3.75 sac/cu. yd.

Water Factor = 8.14 gal./sac

Water/Cement (by weight) = 0.72

Actual Water Factor used = 7.11 gal./sac

Actual Water/cement = 0.63

Slump = 3.0 in.

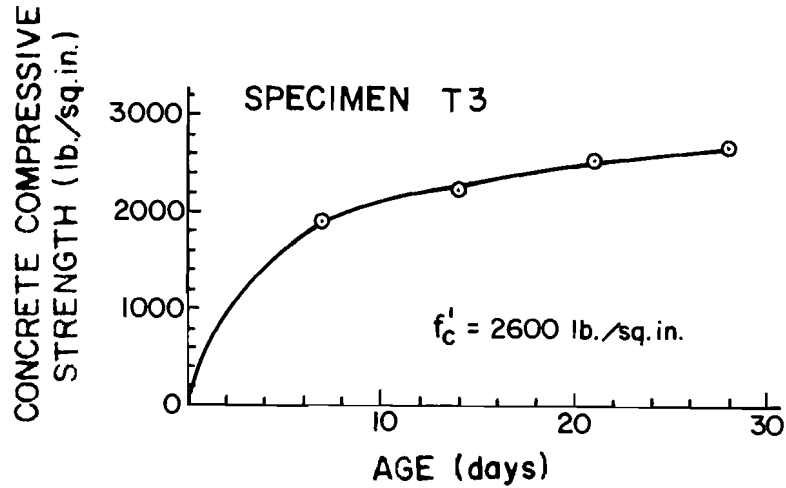


Fig. B.3 Variation of concrete compression strength with age--Specimen T3

TABLE B.3 CONCRETE MIX DESIGN FOR SPECIMEN T3

Material	Batch Design			Full Size Batch lb./cu. yd.
	Volume cu. ft./sac	% Volume	Weight lb./sac	
Coarse Agg.	2.976	43.4	484.7	1907
Water	1.008	14.7	62.9	247
Cement	0.486	7.1	94.0	370
Air	0.0	0.0	0.0	0
Fine Agg.	2.392	34.8	389.6	1533

Cement Factor = 3.94 sac/cu. yd.

Water Factor = 7.56 gal./sac

Water/Cement (by weight) = 0.67

Actual Water Factor used = 7.15 gal./sac

Actual Water/Cement used = 0.63

Slump = 3.5 in.

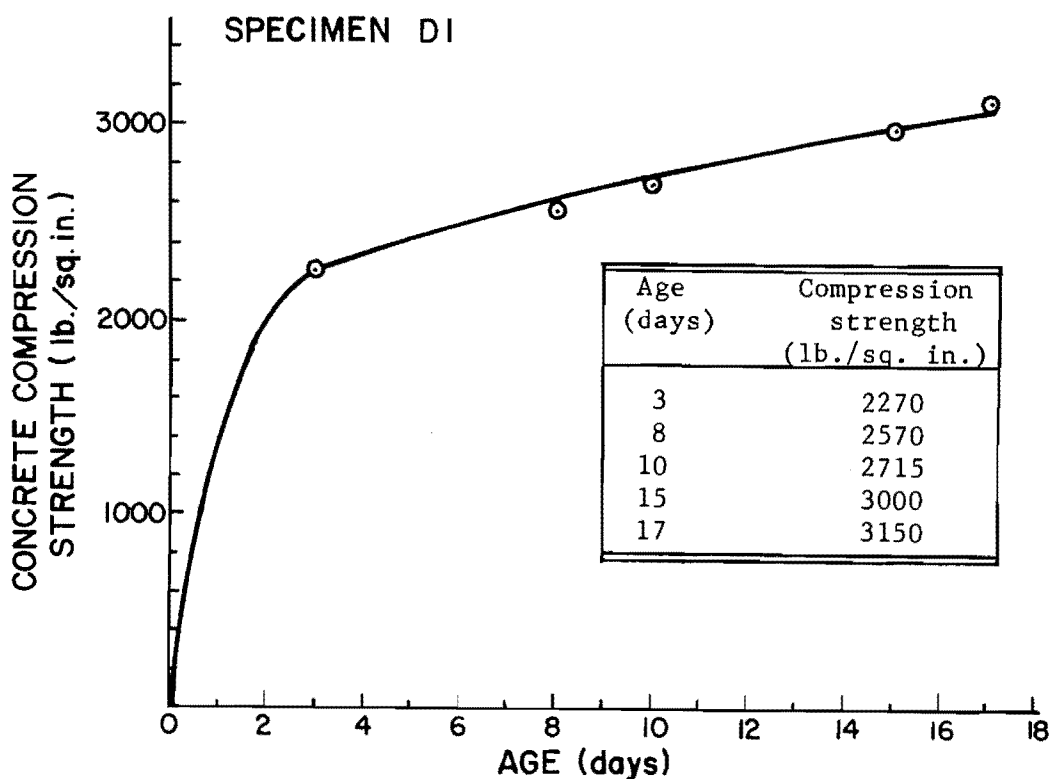


Fig. B.4 Variation of concrete compression strength with age--Specimen D1

TABLE B.4 CONCRETE MIX DESIGN FOR SPECIMEN D1

Material	Batch Design			Full Size Batch lb./cu. yd.
	Volume cu. ft./sac	% Volume	Weight lb./sac	
Coarse Agg.	2.976	43.4	484.7	1907
Water	1.008	14.7	62.9	247
Cement	0.486	7.1	94.0	370
Air	0.0	0.0	0.0	0
Fine Agg.	2.392	34.8	389.6	1533

Cement Factor = 3.94 sac/cu. yd.

Water Factor = 7.56 gal./sac

Water/Cement (by weight) = 0.67

Actual Water Factor used = 7.02 gal./sac

Actual Water/Cement used = 0.62

Slump = 5.5 in.

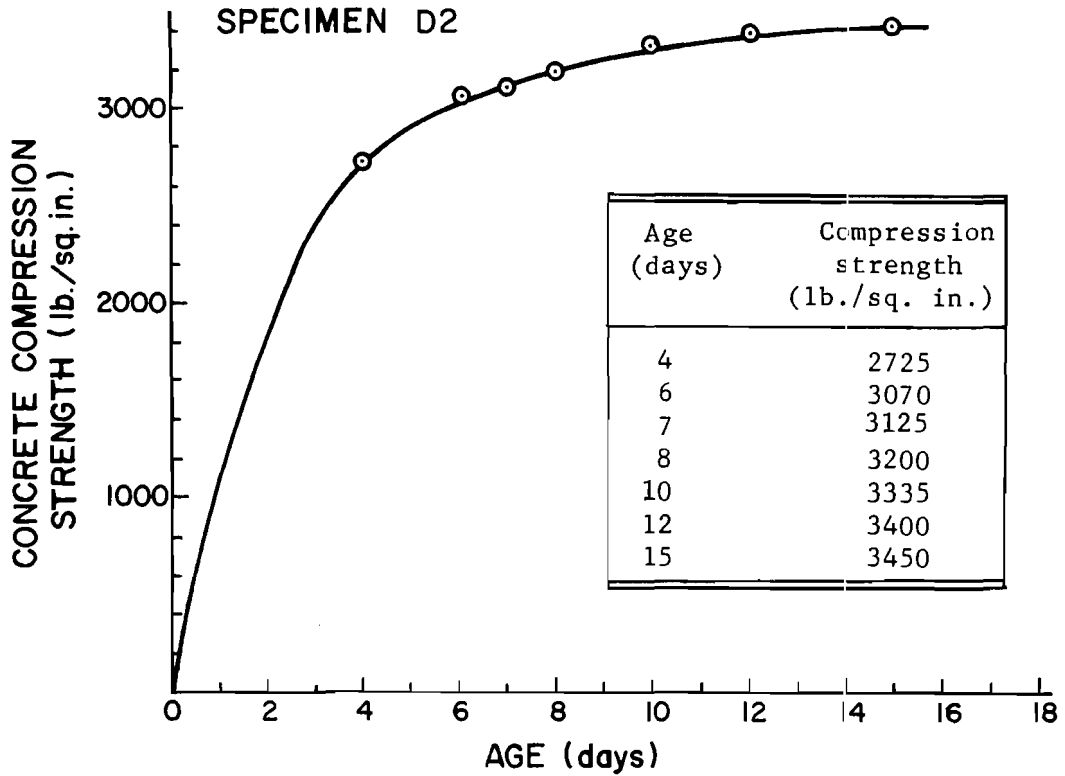


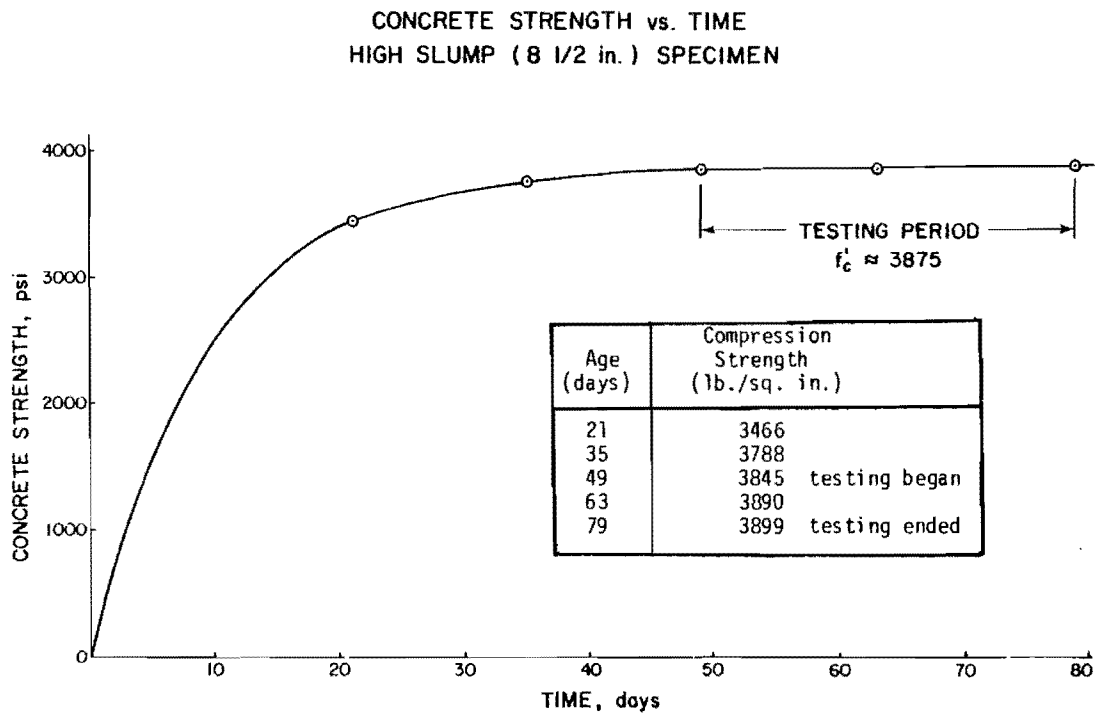
Fig. B.5 Variation of concrete compression strength with age--Specimen D2

TABLE B.5 CONCRETE MIX DESIGN FOR SPECIMEN D2

Material	Batch Design			Full Size Batch lb./cu. yd.
	Volume cu. ft./sac	% Volume	Weight lb./sac	
Coarse Agg.	2.976	43.4	484.7	1907
Water	1.008	14.7	62.9	247
Cement	0.486	7.1	94.0	370
Air	0.0	0.0	0.0	0
Fine Agg.	2.392	34.8	389.6	1533

Cement Factor = 3.94 sac/cu. yd.  
 Water Factor = 7.56 gal./sac  
 Water/Cement (by weight) = 0.67

Actual Water Factor used = 6.89 gal./sac  
 Actual Water/Cement used = 0.61  
 Slump = 3.0 in.



Concrete Mix Design for High Slump Test Specimens

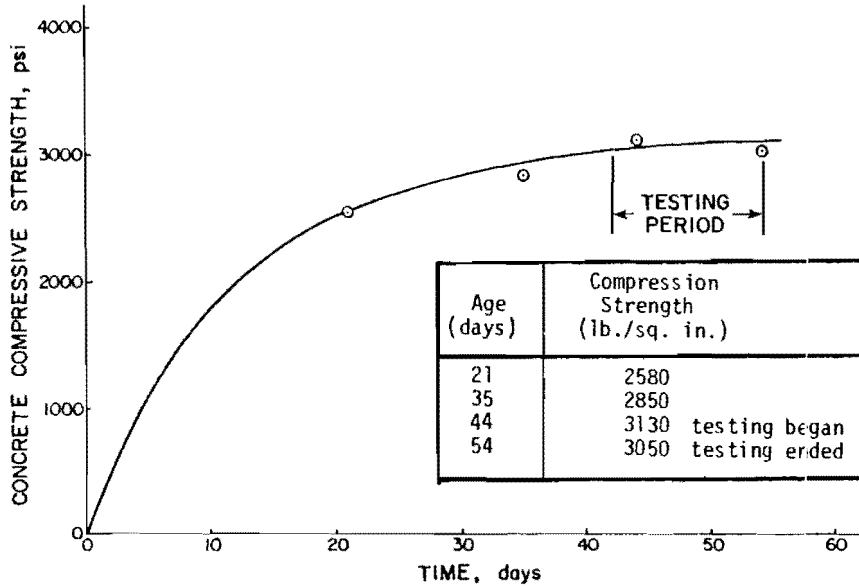
Material	Batch Design		Weight lb./sac	Full Size Batch lb./cu. yd.
	Volume cu. ft./sac	% Volume		
Coarse Agg.	2.983	44.06	485.9	1937.3
Water	.905	13.36	56.5	225.2
Cement	.486	7.18	94.0	1374.8
Air	0.000	0.00	0.0	0.0
Fine Agg.	2.397	35.40	390.4	1556.5

Cement Factor = 3.99 sac/cu. yd.  
Water Factor = 11.32 gal./sac

Water/Cement (by weight) = .60  
Slump = 8-1/2 in.

Fig. B.6 Concrete data--Specimen D3

CONCRETE STRENGTH vs. TIME  
HORIZONTAL / VERTICAL SPECIMEN



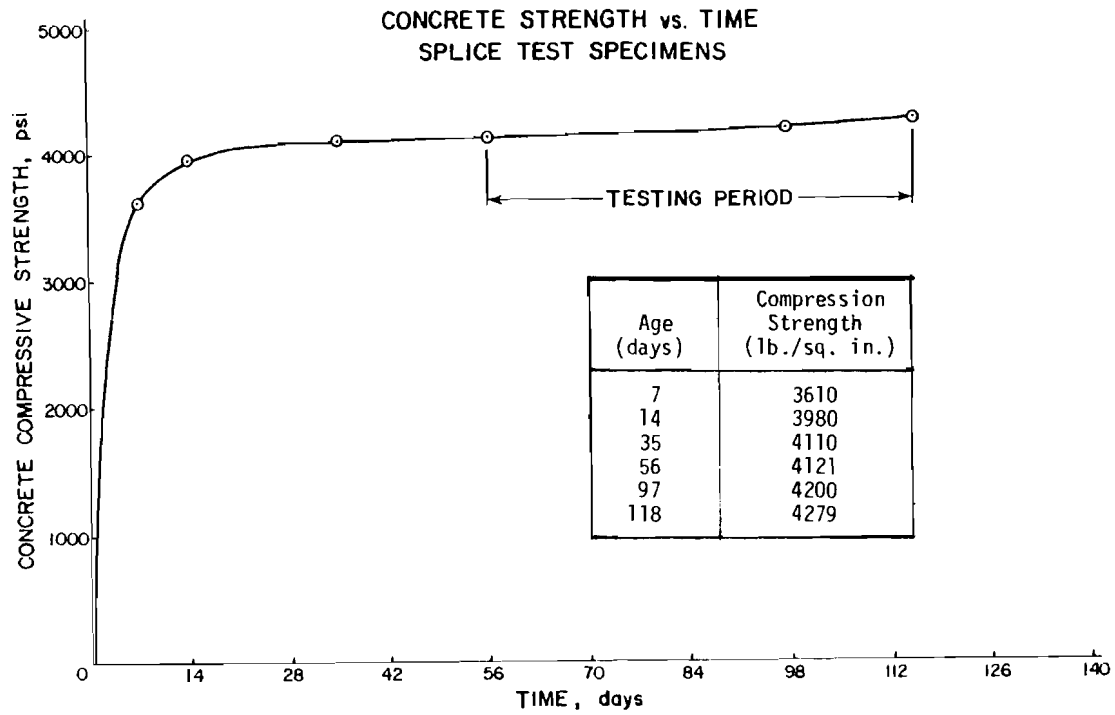
Concrete Mix Design for Horizontal/Vertical Test Specimens

Material	Batch Design			Full Size Batch lb./cu. yd.
	Volume cu. ft./sac	% Volume	Weight lb./sac	
Coarse Agg.	3.426	45.68	558.0	2008.6
Water	.836	11.14	52.2	187.6
Cement	.485	6.48	94.0	338.4
Air	0.000	0.00	0.0	0.0
Fine Agg.	2.753	36.70	448.3	1613.7

Cement Factor = 3.6 sac/cu. yd.  
Water Factor = 6.28 gal./sac

Water/Cement Ratio (by weight) = .55  
Slump = 3-1/2 in.

Fig. B.7 Concrete data--Specimen D4



Concrete Mix Design for Splice Test Specimens

Material	Batch Design			Full Size Batch lb./cu. yd.
	Volume cu. ft./sac	% Volume	Weight lb./sac	
Coarse Agg.	2.975	44.7	484.9	1963.7
Water	.811	12.2	50.6	205.1
Cement	.486	7.3	94.0	381.0
Air	2.391	0.0	0.0	0.0
Fine Agg.		35.8	389.5	1578.6

Cement Factor = 4.05 sac/cu. yd.  
Water Factor = 6.10 gal./sac

Water/Cement (by weight) = .54  
Slump = 5.5 in.

Fig. B.8 Concrete data--Specimens S1 and S2

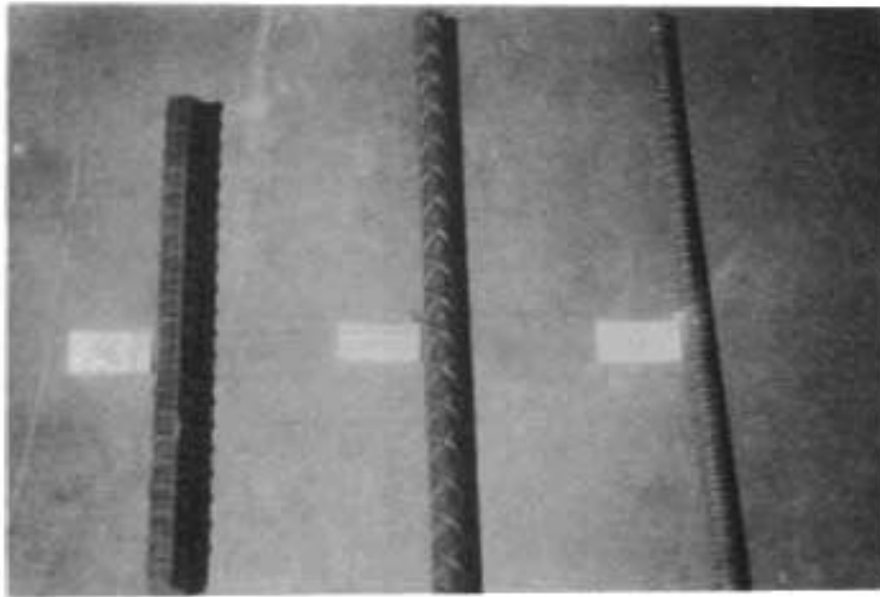


Fig. B.9 Deformation patterns of bars used in the investigation

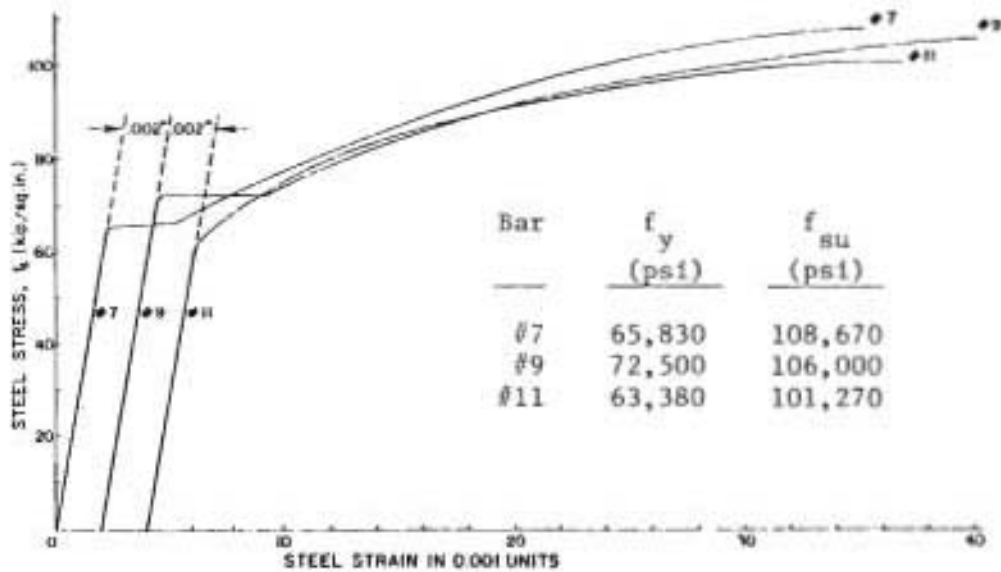


Fig. B.10 Stress-strain relationship for bars used in the study

TABLE B.6 DEFORMED BAR DESIGNATION NUMBERS, NOMINAL WEIGHTS, NOMINAL DIMENSIONS AND DEFORMATION CHARACTERISTICS

Bar designation no.*	Nominal weight lb./ft.	Nominal Dimensions**			Deformation Characteristics, in.				
		d <sub>b</sub> in.	a <sub>b</sub> sq. in.	Perimeter in.	Average Spacing		Average Height		Maximum <sup>+</sup> gap
					Maximum <sup>+</sup>	Measured	Minimum <sup>+</sup>	Measured	
3	0.376	0.375	0.11	1.178	0.262		0.015		0.143
7	2.044	0.875	0.60	2.749	0.612	0.595	0.044	0.048	0.334
9	3.400	1.128	1.00	3.544	0.790	0.718	0.056	0.067	0.431
11	5.313	1.410	1.56	4.430	0.987	0.956	0.071	0.075	0.540

\* Bar numbers are based on the number of eights of an inch included in the nominal diameter of the bars.

\*\* The nominal dimensions of a deformed bar are equivalent to those of a plain bar having the same weight per foot as the deformed bar.

<sup>+</sup> A.S.T.M. specifications.